VISUALISING LATENT FINGERMARKS WITH PURE ORGANIC PERSISTENT LUMINESCENT MATERIALS

by

Ryan Parmenter

A THESIS

Submitted to the Faculty of Sciences at The University of Kent

In Fulfilment of the Requirement for the degree of

MSC CHEMISTRY

University of Kent

SEPTEMBER 2020

School of Physical Sciences, Ingram Building, University of Kent, Canterbury, Kent, CT2 7NH, United Kingdom

Total word count : 22954

ACKNOWLEDGEMENTS

Table of Contents

LIST OF TABLES

LIST OF FIGURES

LIST OF ABBREVIATIONS

(3-Bromopropyl)triphenylphosphonium bromide (TPP)

(3-Bromopropyl)triphenylphosphonium bromide doped with N,N-dimethylaniline (TPP:DMA)

1,3-Propanediylbis(Triphenylphosphonium) Dibromide (PTP)

2,4,6-Tri(4-Pyridyl)-1,3,5-Triazine (4-TPT)

2,4,6-Tri(4-Pyridyl)-1,3,5-Triazine doped with N,N-dimethylaniline (4-TPT:DMA)

Centre for Applied Science and Technology (CAST)

Electromagnetic Spectrum (EMS)

Emission (Em)

Excitation (Ex)

High-Performance Liquid Chromatography (HPLC)

High-Performance Liquid Chromatography-Mass Spectroscopy (HPLC-MS)

Infrared (IR)

International Fingerprint Research Group (IFRG)

Intersystem Crossing (ISC)

Liquid-Chromatography Mass Spectrometry (LCMS)

Long Persistent Luminescence (LPL)

Long-Lasting Phosphorescence	(LLP)
Metal-Organic Framework	(MOF)
N, N-Dimethylaniline	(DMA)
Organic Long-Persistence Luminescence	(OLPL)
Organic Persistent Luminescent Materials	(PLMs)
Parts Per Million	(ppm)
Persistent Luminescence	(PL)
Proton Nuclear Magnetic Resonance	(^{1}H-NMR)
Scanning Electron Microscopy	(SEM)
Scanning Electron Microscopy with Energy Dispersive X-Rays	(SEM-EDX)
The Home Office	(THO)
Ultraviolet	(UV)
Ultraviolet Light-Emitting Device	(UV LED)
X-Ray Powder Diffraction	(XRD)

ABSTRACT

This past decade, organic persistent luminescent materials have gained considerable research interest and have been utilised by a diverse range of scientific disciplines. Here in this research, two organic persistent luminescent materials have been investigated, optimised, and prepared as fingerprint powders. Both powders were used as latent fingermark developers, following Phase 1 and 2 trials established by the International Fingerprint Research Group.

The first organic persistent luminescent material, (3-Bromopropyl)triphenylphosphonium bromide, was selected from a recent publication and it's photoluminescent properties were optimised. The second material investigated was 2,4,6-tri(4-pyridyl)-1,3,5-triazine. To the best of our knowledge, this is the first report which claims to have achieved a persistent luminescence in 2,4,6-tri(4-pyridyl)-1,3,5-triazine, without the need of inorganic doping systems.

Phase 2 trials identified both powdered materials to effectively develop latent fingermarks on non-porous surfaces, with (3-bromopropyl)triphenylphosphonium, performing slightly better out of the two. In summary, this study has identified the use of alternate organic persistent luminescent materials to be used as fingermark developers, and, with further investigations, may promise effective, low-cost alternatives to the persistent luminescent fingerprint powders currently on the market.

CHAPTER 1.   INTRODUCTION

1.1 Fingermarks

The skin of human fingers, hands and feet all exhibit intricate patterns formed through friction ridges and furrows, termed, friction ridge skin.[1] Skin is the largest organ of the body. It provides the first line of defence to infections and the mechanism for our sense of touch. It is generally accepted that friction ridge skin enhances grip on the hands and feet.[2] Research suggests that friction ridge skin begins to develop around the tenth week of gestation.[3] The primary ridges, serving as templates for future surface patterns, are well pronounced by the sixteenth week, with unique patterns fully established by the third trimester of foetal development.

The friction ridge skin on our fingertips generates different shaped patterns described as arches, loops, and whorls. The current consensus is that each finger has a unique arrangement of friction ridge skin which varies between every individual.[4] As the patterns are unique and remain unchanged throughout our lives, barring permanent damage (i.e. scarring), they are considered to be the best reference for personal identification and are a well-established class of evidence in criminal investigations.[5,6] Two terms are used to indicate the manner on which the impression was generated: fingerprints and fingermarks.

Fingerprints are reference impressions taken from the fingertips of an individual. These are obtained with their cooperation and under controlled conditions, using either an inking process or an optical device. Because of their pristine acquisition conditions, the fingerprints are near perfect representations of the friction ridge skin.[7]

A fingermark, on the other hand, is an impression left unknowingly by an individual through contact-transfer involving friction ridge skin of the fingers. Three types of fingermarks can be generated through contact-transfer: patent, plastic and latent.

Patent fingermarks are impression marks which are generated when a coloured substance i.e. blood, grease, ink, dirt, etc. is present on the fingertips and transfers upon contact with a surface. These marks contain visible ridge detail and are directly photographed for subsequent comparison in-person identification.

Plastic fingermarks are three-dimensional impressions of friction ridge skin that are generated when a fingertip has contact with a malleable solid i.e., fresh paint, wax, soap, tar, etc. Similarly, the distinct ridge pattern is visible to the naked eye and can usually be directly photographed using oblique lighting for subsequent comparison and identification.

Of the three types, latent fingermarks are the most common type of mark a person will leave. Latent marks are composed of transparent secretions which collect on the surface of friction ridge skin. The latent residues are transferred upon contact with a surface and are typically invisible to the eye requiring development. The composition of these secretions is a mixture of substances either produced and secreted by the epidermal glands or through extrinsic contaminants.[8] These compounds either exude from pores onto the friction ridges or are transferred to the friction ridges through contact transfer.[9]

Unlike fingerprints, the uncontrolled nature of deposition results in fingermarks with varying quality (e.g. in the worst-case scenarios, smudged, overlapped and partial prints).[5] Fingermarks are essential to criminal investigations as they constitute the partial representation of a person(s) fingerprint. Consequently, numerous efficient techniques have been developed and refined over the last few decades to detect latent fingermarks on various substrates.[7]

There is a range of development processes, which successfully enhance the appearance of a latent fingermark, substrate, or both. Using a developer will increase the contrast of ridge detail and enable an examiner to effectively distinguish characteristic patterns contained within the ridge detail. The visualisation processes are classed as being optical, chemical or physical.[10,11]

Optical processes expose the fingermark to a variety of light sources, at different angles, to reveal raised or indented ridge patterns. Different wavelengths can be investigated with a variety of filters to increase the contrast between the fingermark and the underlying substrate.

Chemical processes use chemical reactions to visualise latent fingermarks. Different chemicals can be applied to target the specific constituents in fingermarks (i.e., eccrine, apocrine, or sebaceous materials), resulting in a colour change. The now visible fingermark detail is photographed and the image is used to perform comparisons to fingerprints.

Physical developers are powders consisting of fine particles. When applied to a latent fingermark, the powders physically adhere to the latent deposits, enabling visualisation.[12] Different coloured powders are available to investigators and the colour is selected, to achieve the best contrast between the fingermark and the underlying surface.

Numerous development techniques exist which aid in fingermark visualisation; however, challenges remain due to the large and varied nature of fingermarks. Every individual fingermark will inherently possess a range of factors and variables that limit developer effectiveness.

These limitations arise from a range of variables which include the substrate colour and nature (e.g., porous, semi-porous and non-porous), donor characteristics (e.g., diet, age, gender), deposition conditions (e.g., deposition pressure and contact duration), environmental conditions (direct exposure to sun/heat or stored away), and the presence of extrinsic contaminants.[13,14]

Whilst research continues to investigate new and more efficient methods, those currently used are often under refinement to improve visualisation, better health and safety aspects, minimise costs and enable portability.[15] In the United Kingdom, The Home Office has undertaken extensive research, to improve efficiency and operational aspects of fingermark development processes according to the surface of deposition and likely environmental conditions. The resulting operational guidance is reported in *The Fingermark Visualisation Manual*, which is adopted by the 43 police forces in the country to assist in effective fingermark development.[11]

1.2 Powders for Visualising Latent Fingermarks

Powder developers have enabled the largest number of fingermark identifications worldwide.[9] In the United Kingdom, approximately 50% of the 50,000 fingermark identifications per annum arise from fingermarks developed using some form of powder developer.[9] Therefore, it is evident that even the smallest of proportional improvements in powder technology, achieved through research, has the potential to provide significant operational benefits, demonstrating the importance of continuing research in this area.

The main application of powders is the development of fingermarks on smooth non-porous substrates at crime scenes. The furrows between friction ridge skin are devoid of latent residue, therefore, the powder adheres to the latent residue generated from fiction ridges and is brushed off the furrows,[10] enhancing the ridge patterns and enabling the mark to be visualised. The speed, ease and effectiveness of the technique make powders well-suited to high volume crime applications.

Research to date has yielded four types of powder, namely: granular, metal flake, magnetic, or luminescent powder. The type of powder used should be selected according to the nature of the surface and the environmental conditions (i.e., if the surface is wet or dry), choosing both a class of powder which works well for that surface type and a powder colour that gives a good contrast against the background.

The developed mark is imaged to acquire a digital copy and if necessary, can be physically recovered using a lifting method. The lifted fingermarks can then be placed in isolation from a potentially distracting background to enhance visualisation.

The Home Office UK is responsible for ensuring that forensic processes are governed by strict standards that are continually updated. Although developed fingermarks can be lifted using adhesive mediums, they should first be developed to a standard which would enable personal identification to be performed using a photograph alone without the need to lift and recover the developed fingermark. *'The Fingermark Visualisation Manual',* declares "*it cannot be guaranteed that all of the ridge detail is transferred to the lift"*.[11] Therefore, it is in the best interest to the investigation for fingermarks to be developed for maximum contrast without lifting, so they can be photographed *'in-situ'* and compared to reference fingerprints.[9]

Powders can be used to develop latent marks on all smooth non-porous surfaces The only factor which needs considering is the colour compatibility between the surface and powder developer, aiming for the maximum achievable contrast.[10] This is achieved by using a developer colour that compliments the substrate colour.

Scientists estimate that humans can distinguish up to 10 million colours,[16] therefore, achieving an optimum contrast can be challenging. Luminescent materials can be incorporated with fingermark developer powders to improve the contrast offered by traditional powders and under most circumstances, luminescent powders have been shown to provide the best possible contrast.[9]

When an opaque object is exposed to white light, certain wavelengths of light are absorbed by the object and the wavelengths that are reflected are detected by our eyes. This same mechanism occurs when using non-luminescent powders to develop a latent fingermark. The reflected wavelengths of light enable us to visualise the coloured powder of the developed fingermark. Luminescent powders work differently, as these powders absorb and emit light, instead of reflecting it. The visual effect of light being emitted is that of an enhanced brightness with respect to the reflected light, therefore, luminescent powders offer greater visibility and contrast, compared to traditional non-luminescent powders.

1.3 Luminescence

Luminescence is a term used to explain the phenomena that occur when a substance emits light in response to an external stimulus. Luminescence encompasses a range of different processes as shown schematically in **Figure 1.1**.
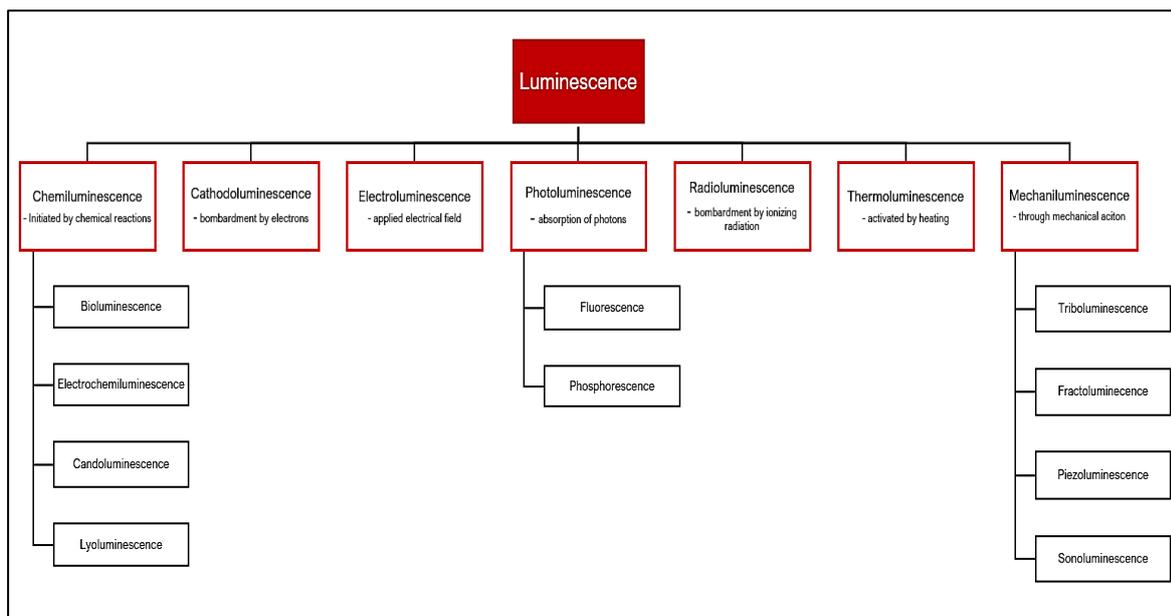
Figure 1.1: *Schematic representation of the types of luminescence and their energy sources.*

A hot body that emits radiation solely because of its high temperature is said to exhibit incandescence. All other forms of light emission are called luminescence.[17] Luminescence can be found in molecules with potential electronic energy excited state levels compatible with absorption and emission levels within the visible, ultra-violet (UV) and infrared range of the electromagnetic spectrum (EMS).[9]

Before irradiation, the electron(s) in these molecules will occupy a low energy ground state. When irradiated by the light of an appropriate wavelength, energy in the form of photons is absorbed by the electron. The energy from the absorbed photon is converted to kinetic vibrational energy, subsequently resulting in the electron being promoted to a higher energy state. When the source of excitation is removed, the excited electron relaxes back down to its ground state, in turn, releasing the energy in the form of a photon.

As some of the energy was used to excite the electron, the photon emitted during relaxation is of lower energy of a longer wavelength. During excitation, the photon absorbed by the electron is of higher energy and shorter wavelength. During relaxation, the photon emitted from the electron is of lower energy and a longer wavelength, this is due to some energy being converted and used as kinetic vibrational energy. The

difference between the absorbed and emitted energy is known as the Stokes' shift. Typically, the high excitation energy is delivered from the UV region of the electromagnetic spectrum (**Figure 1.2**).

The energy absorbed by the electron is a higher value than the energy emitted by the electron during relaxation. This is because some energy is spent promoting the electron to a higher energy state, therefore, the energy loss is emitted at a longer wavelength, often within the visible spectrum range of the EMS. This shift in wavelength energies is called red-shifting.
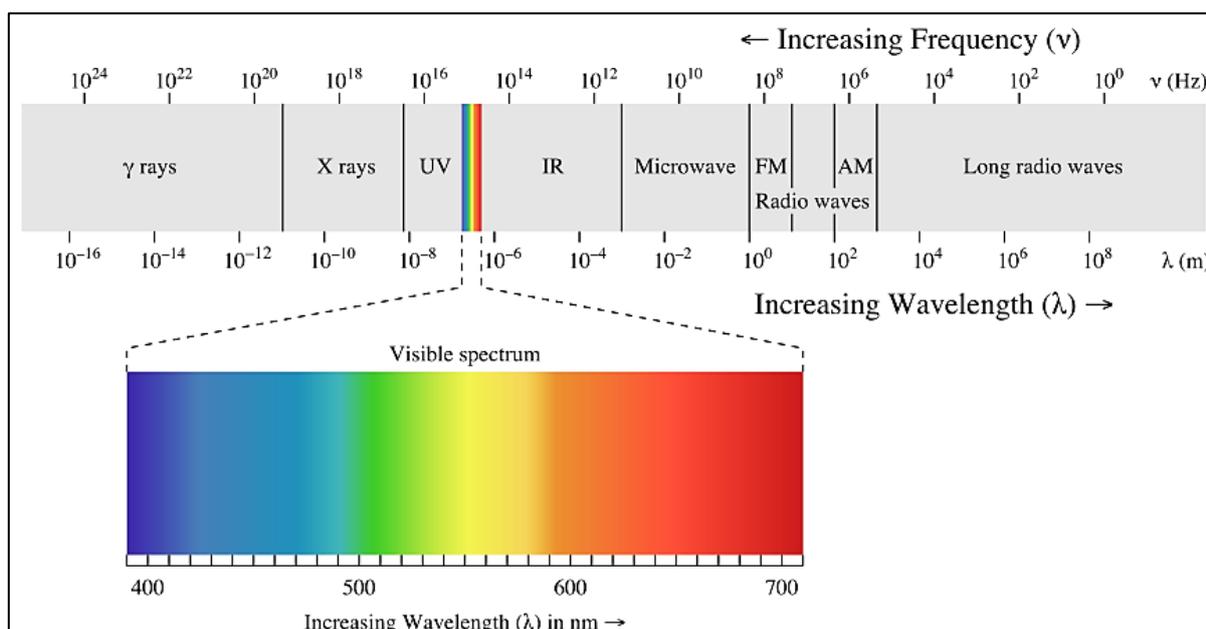
Figure 1.2: *Schematic representation of the electromagnetic spectrum[18]*

In some molecules, there may be several excited states to which electrons can be promoted, and several ground states to which they can return, therefore, the absorption and emission wavelengths can occur over a large portion of the electromagnetic spectrum.[9] A typical emission and absorption spectrum, with the corresponding excited states, are shown in **Figure 1.3**.
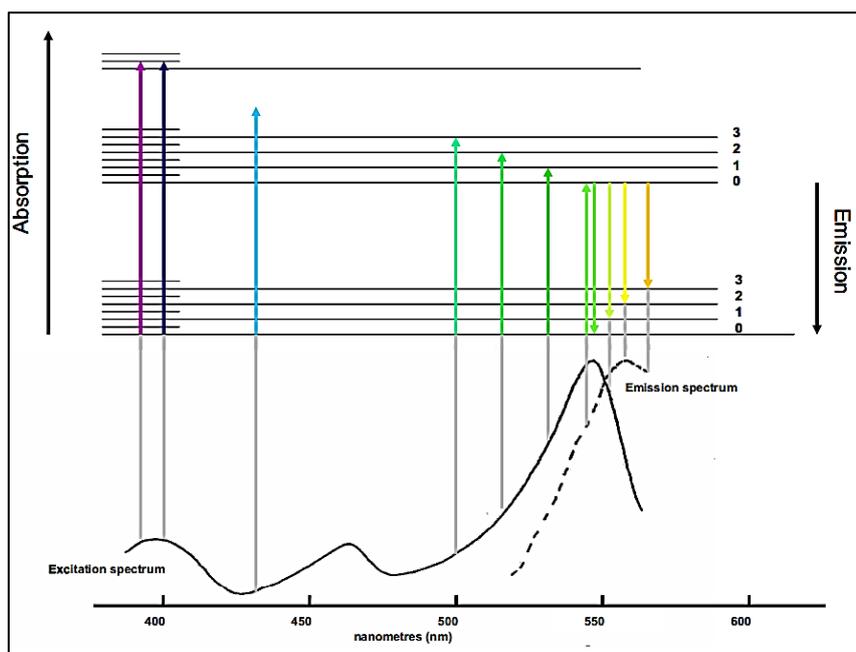
Figure 1.3 *Representation of excitation/emission spectra of a chemical with corresponding transitions between excited and ground states.[9]*

Photoluminescence governs two categories: fluorescence and phosphorescence. Both terms are used to describe the specific length of time it takes for an excited electron to reoccupy its ground energy state, this is also known as the material(s) decay lifetime. The assignment of the luminescence bands as fluorescence or phosphorescence is primarily determined via luminescence lifetime measurements.[19]

Fluorescence decays rapidly upon photon irradiation.[20] The lifetime measurements occur between the nano- to microsecond range, on average lasting around 1×10^{-9} - 1×10^{-6} s. Fluorescent materials are widely used as fingerprint powders, for the development of latent fingermarks on smooth, non-porous surfaces and some semi-porous surfaces.[21,22] Fluorescent powders are also applied to some chemically developed fingermarks, to further enhance ridge detail. The main benefits associated with fluorescent powders is that a large variety of colours are available, thus, allowing a colour to be chosen that will provide the optimal contrast of ridge detail against the substrate material.

With a brush, the powder is lightly dusted onto latent ridge detail and the developed fingermark is exposed to the light of a high energy wavelength (often UV). Fluorescence occurs and the filtered light emitted from the material is recorded. The mechanism of fluorescence is shown (**Figure 1.4**).
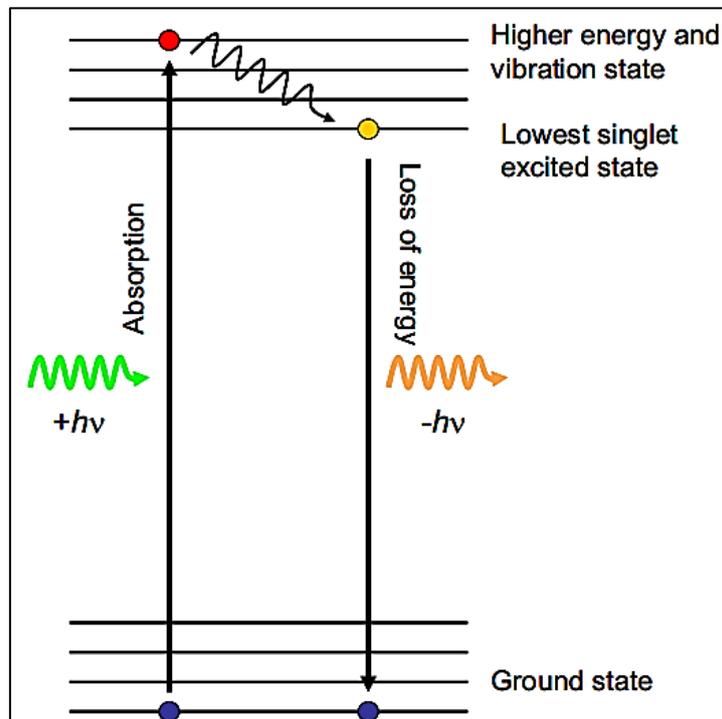
Figure 1.4: *Schematic diagram showing the mechanism by which fluorescence occurs.[9] The energy of an electronic transition is calculated using the equation $E_T = h\nu = \frac{hc}{\lambda}$ where h is Planck's constant, c is the velocity of light, v is frequency, and λ is the wavelength.*

Although fluorescent powders provide a great contrast to visualise latent ridge detail, a major limitation arises from the application to multi-coloured and/or patterned backgrounds, as these surfaces also fluorescence when irradiated, thus preventing visualisation of the fingermark, as shown in **Figure 1.5**.
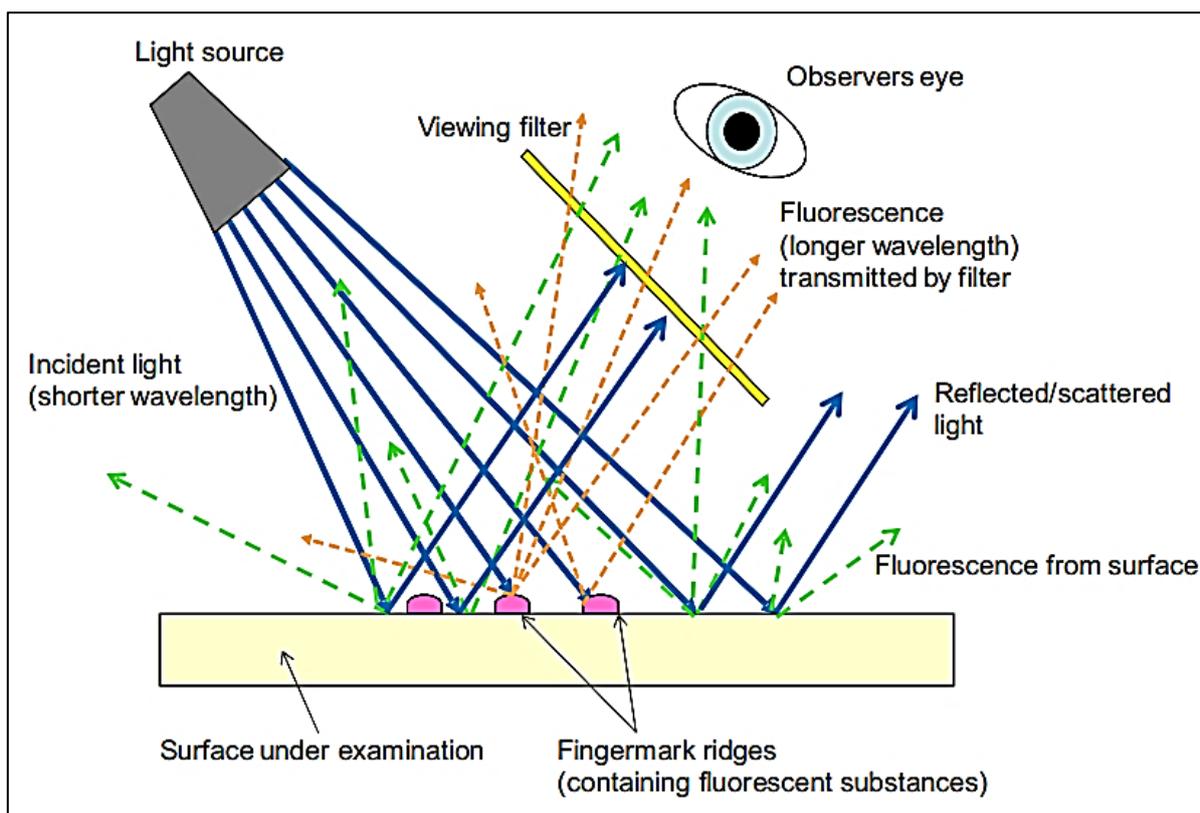
Figure 1.5: *Schematic representation of viewing fluorescent fingermark ridges on a substrate also containing a fluorescent species which results in fluoresce for both the substrate (depicted by the green arrows) and fingermark (depicted by the orange arrow) resulting in difficulties in discriminating the mark.*[9]

Phosphorescent materials have been proposed as an effective means to address multicoloured surfaces. Unlike fluorescence, phosphorescence has longer decay lifetimes or experience longer periods of relaxation after excitation occurs. Upon absorption of a photon, the singlet ground state (S_0) of a phosphorescent material is promoted to a much higher triplet state (T_1), or between any two energy levels that differ in their respective spin states. Upon relaxation, energy is released and often emitted as visible light. During relaxation, the electron experiences intersystem crossing (ISC) between additional states, extending the duration over which relaxation is experienced. This further extends observed emission for an average of 1×10^{-3} s. Phosphorescent emission is usually measured in milliseconds, however, certain materials show extended emission timescales which can range from milliseconds up to hours (as discussed in more detail in the next section).[20]

1.4 Persistent Luminescence

Long-Lasting Phosphorescence (LLP), Long Persistent Luminescence (LPL) or Persistent Luminescence (PL) characterise materials that, when excited with high energy radiation, continue to emit light that can be observed for seconds to hours after the removal of the excitation source.[23]

For LPL, the energy passes through an intermediate state which is discussed in further detail on the next page. **Figure 1.6** displays a schematic comparison of the different energy states between fluorescent, phosphorescent and PL materials. The emission decay profiles of phosphorescence and PL on logarithmic plots are compared (**Figure 1.7**).
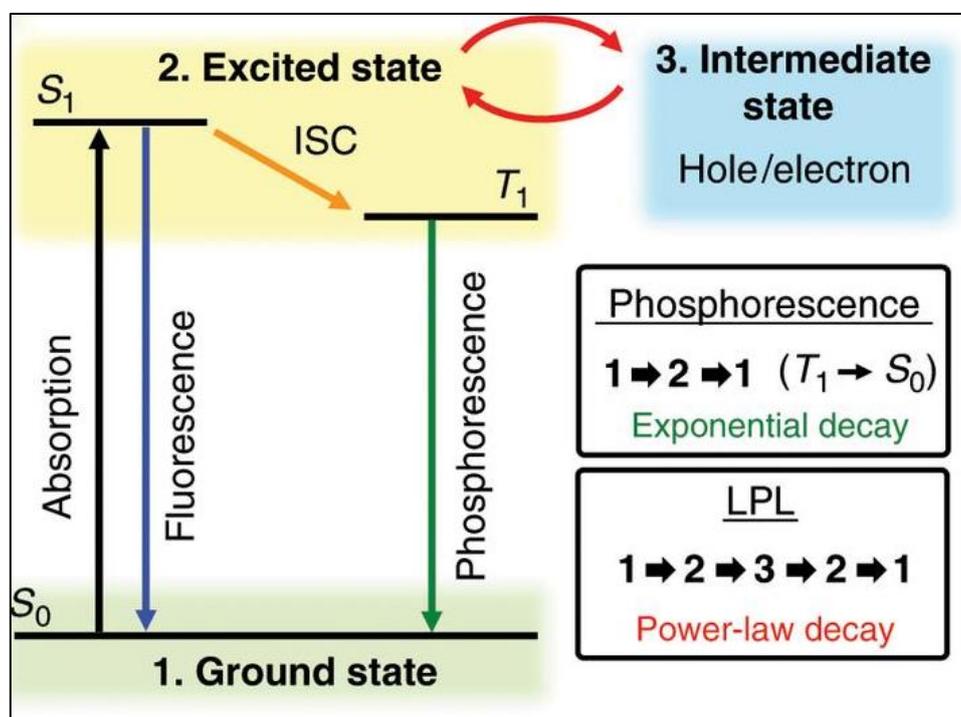
Figure 1.6: *Schematic diagram of fluorescence (1 → 2 → 1), phosphorescence (1 → 2 → ISC → 1) and PL (1 → 2 → ISC → 3 → 2 → 1).*[24]
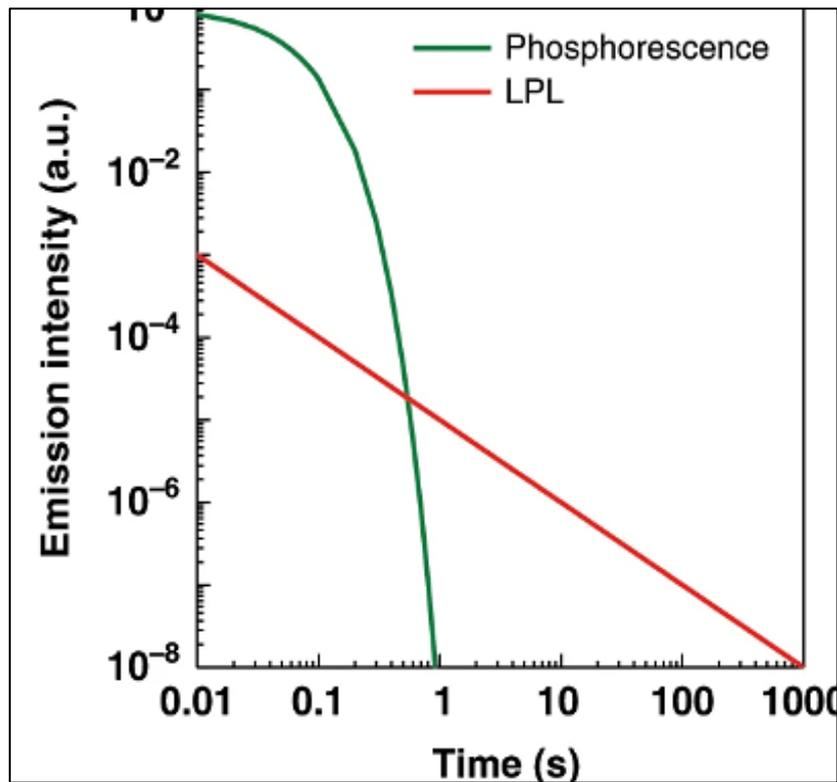
Figure 1.7: *The emission decay profiles of phosphorescence and LPL on logarithmic plots. Phosphorescence follows an exponential decay and LPL a power-law decay.*[24]

Non-radiative intermediate states in PLM's use a trap-assisted recombination mechanism, consisting of an emission centre and trap centre. Herein, an electron becomes *'trapped'* by an energy level within the bandgap, induced by the presence of foreign atoms and/or structural defects. Emission centres mostly consist of lanthanide ions and trap centres are generated by impurities and/or co-dopants. Both are found within the bandgap.[25]

During excitation, charge carriers become captured by traps and the energy is stored within the conduction band. After excitation has ceased, charge carriers are liberated and return to an empty valence band, yielding the long-lived luminescence.

1.4.1 Persistent Luminescence: Inorganic Materials

Most research into persistent luminescence has focused on using inorganic materials. Discovered in 1953, the first PLM was zinc sulphide (ZnS) doped with copper (Cu) and this was generally considered to be the best PLM on the market for four decades.[26]

This opinion changed in 1996, with Matsuzawa *et al* reported the production of a material luminescence ten times longer and brighter than anything else at the time.[27] The material was achieved by introducing dysprosium(III) and europium(II) ions into strontium aluminate. This work demonstrated that persistent luminescence could be achieved via an inorganic host co-doped with rare earth elements.

Due to the many possible combinations of inorganic host co-doped donor systems available, this publication prompted lots of interest, which led to the discovery of new host donor systems, with varying intensities, durations and emission colours.[28,29,30,31,32] Furthermore, this research provided greater insight and understanding of the mechanisms involved with PLM's. A range of dopant concentrations is investigated to identify the optimal concentration that results in the highest emission intensity and the longest duration of LPL. The inorganic persistent luminescent systems known to date use molar doping concentrations which typically range between 0.1-10%.[33,27,34,35,36]

Moreover, these materials have proven to be beneficial when incorporated into fingermark developers, more specifically, when applied to fingermarks on multi-coloured, fluorescent surfaces. This is because removal of the source of excitation terminates any emissions produced by the fluorescent surface, whereas PLM's continue to emit light. The delayed/extended emissions provide enough time for the investigator to take a photograph, which is used for comparison/identification purposes.

Though research has identified host-donor systems and explained persistent luminescent mechanisms, there are many limitations still present, suppressing large scale use of the rare-earth-doped materials. These are mainly due to the costly nature of rare earth materials, limited availability, complex synthesis, high energy fabrication processes ($\geq$1000 °C) and insolubility.[37,25,38] Recent developments in organic PLM's may propose a solution to these limitations and provide an alternative to current systems using inorganic PLM's.[39]

1.4.2 Persistent Luminescence: Organic Materials

To overcome the drawbacks of inorganic persistent luminescent systems, several types of organic PLM's have been investigated. Owing to the short-lived singlet exciton for fluorescence, it is a greater challenge to achieve a PL in pure organic molecules.[39] They often produce a low luminescent intensity and photostability, rendering organic systems unsuitable for high-sensitivity detection.[40]

As progress and understanding have developed for inorganic systems, it was proposed that if charge carriers could be stored within rare earth and heavy metals to achieve a persistent luminescence, organic molecules could theoretically do the same.[41]

An *et al* proposed that triplet excited states could be stabilised by strong coupling in H-aggregated structures.[42] This principle identified a variety of organic molecules with ultra-long second luminescent properties, subsequently, stabilising the excited triplet excitations due to manipulation of the intermolecular interactions increased the persistent luminescent lifetime from milliseconds to seconds.[43]

Inspired by the role of inorganic trap species, Kabe and Adachi hypothesized a novel strategy to obtain a persistent luminescence in organic systems.[41] Gradual coalescing a strong electron donor and a strong electron acceptor, the two radical anions and cations produced a stable radical cation with high triplet energy. The environment provided conditions to generate exciplex emission, achieving an LPL system capable of emitting for up to an hour.[41]

Förster energy transfer is a mechanism of fluorescence resonance energy transfer involving a donor fluorophore in an excited electronic state, which has the potential to transfer its excitation energy to a nearby acceptor chromophore in a non-radiative fashion through long-range dipole-dipole interactions.[17] The generated exciplexes transfer energy to the emitter dopants via Förster energy transfer, with emitter dopants acting as electron trapping sites, further improving the intensity and emission duration.[44,45,41,46]

Persistent luminescent materials have this additional intermediate state where transfer states and charge separation subsequently result in the slow recombination of initially generated excitons. To achieve this transfer state, centres must be able to trap the excited electrons of a phosphorescent material. To do this, electron donors are incorporated into the host material.

Incorporating an electron-donating molecule into the structure of an electron acceptor results in the formation of electron trapping sites within the host structure. Charge transfers excited states form between the host and donor material during photoexcitation. Removal of the excitation source results in donor molecule electrons to diffuse into the surrounding host molecules, forming stable charge-separated states. Gradual recombination generates charge-transfer excited states, producing an emission that can be observed for an extended period (**Figure 1.8**).[47]
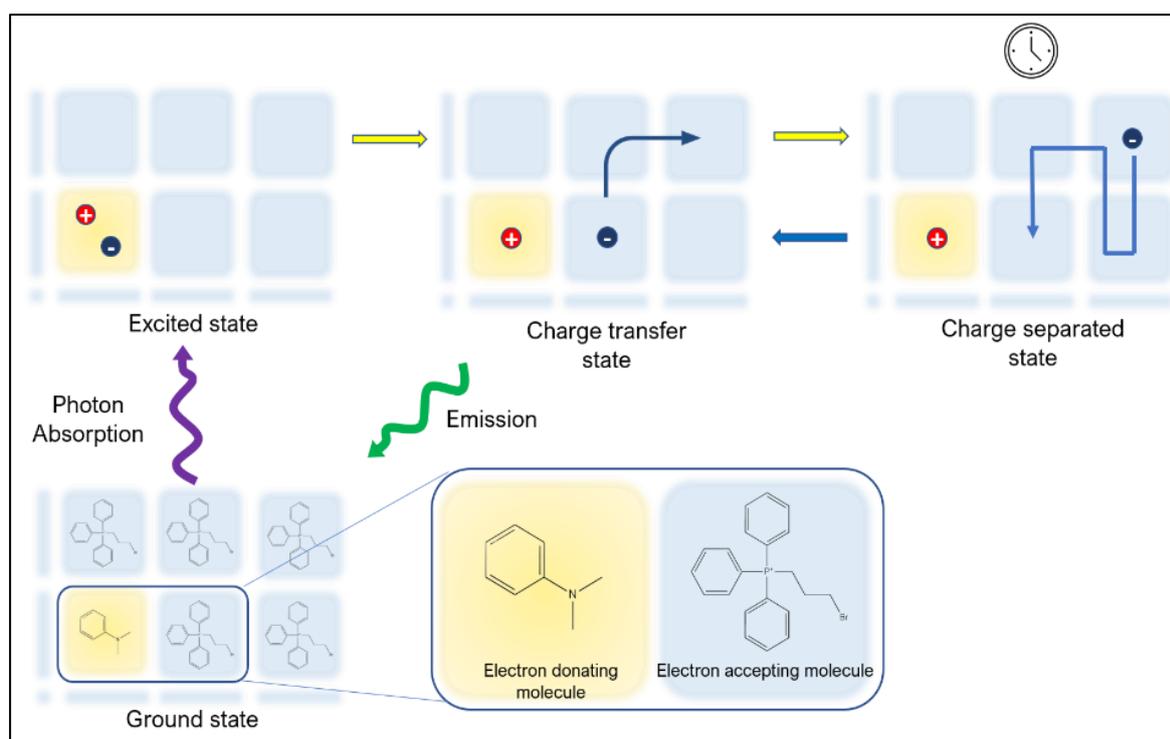
Figure 1.8: Schematic diagram illustrating the incorporation of the electron-donating molecule into the structure of an electron-acceptor. Changer transfer states occur during photoexcitation. Removal of the excitation source results in donor molecule electrons to diffuse into surrounding host molecules, forming stable charge-separated states.

Protection of the excited state is required to ensure high efficiency of excited radical species. Purely organic phosphor bromine salts have been reported that are capable of emitting intense green emission that is detectible for up to 7 hours.[48]

The cationic nature of the phosphonium core is an ideal acceptor for the electron of the photoinduced charge transfer process. Furthermore, being surrounded by other cationic phosphoniums, the excited radical can migrate to multiple cores before finally recombining with the electron-donating radical resulting in the observed emission. Pure organic doped nanomaterials are relatively new, therefore they have yet to be investigated as fingermark developers.

1.5 Nanoparticles

Nanoparticles are currently the dominant research focus over a range of scientific fields, especially that of fingermark powders in Forensic Science.

A nanomaterial is a material which has a morphology smaller than 100 nm in at least one dimension. Similarly, nanoparticles constitute a category of nanomaterials that are nanoscale in all three dimensions. In contrast, nanostructures are nanoscale structures which are on the surface of materials (not necessarily nanomaterials).[49] An expanding number of research groups have replaced conventional powders with rare-earth-doped nanomaterials.[50]

The nano-sized particles promise higher resolution of ridge detail, enabling very weak latent fingermarks to be visualised.[51] Optical properties, specifically related to luminescence, offer a strong advantage in terms of contrast and the chemical versatility through surface modifications provide an increased selectivity.[12]

Although nanoparticles have been identified as effective fingermark developers, they are rarely used within casework.[50] This is likely due to the increased levels of toxicity which arise from the materials physical properties.[52] As the smaller sizes provide the opportunity for increased uptake and interaction with biological tissues.[53] In addition to this, the shape of the nanomaterial can significantly increase the toxicity.[54]

1.6   Desirable Properties of Latent Powder Developers

Aside from substrate compatibility and colour, certain chemical and physical characteristics can increase adhesion to latent residues. This attraction is believed to be affected by a variety of factors, namely, the shape, size, surface chemistry and the electrostatic charge of the powdered particle, as well as, preferential adhesion to a particular component of a latent fingermark (e.g. lipid fraction) and a lower adhesion to the substrate.[12]

Different powder's have been analysed and differentiated by scanning electron microscopes (SEM). Powders can either be a collection of smaller spherically shaped particles (granular) or larger flat flakes. Although a powders effectiveness is very surface specific, flake powders generally outperform granular ones on smooth surfaces owing to their larger surface area which increases contact with latent residues.[12,55]

Effective commercial powders rely on two factors for effective adhesion and visualisation: pigments and binders. The pigment is the minor component which contains the properties enabling the visualisation of latent detail. The binder is the major component which adheres to the fingermark. The pigment and binder particles work together to adhere to the latent residue, yielding a developed and visible fingermark.

Some typical formulations of the different classifications of powders are mentioned below, however, only a representative sample of a specific type of powder is provided per class of powders. It is also important to mention that similar products may vary on the formulation depending on the manufacturer and source of materials.

Carbon powder is a black granular powder comprised of amorphous elemental carbon. The particles are smooth and irregular shaped ranging between 5-10 µm in size. The white powder is a combination of particles, an example being magnesium silicate flakes (20 – 100 µm), mixed with titanium dioxide pigment (<1 µm). The small granules coat the surface of the flakes, suggesting the larger flakes act as a carrier for the smaller granules.

Metal flake powders are achieved by ball-milling larger metallic particles.[56] The popular aluminium powder consists of smooth aluminium particles with irregular edges, ranging between 1 - 12 µm in diameter and 0.5 µm in thickness.

Magnetic powders are typically composed of large magnetic particles that act as carriers for smaller nonmagnetic colourants (e.g. carbon black powder, bronze flakes, aluminium flakes, fluorescent powder, etc.) A common formulation of black magnetic powder contains elemental iron (20-200 µm) and smaller particles of iron oxide (3-12 µm).

Luminescent powders can be either granular or magnetic and are available in a range of emission colours.[56] Typical formulations include small fluorescent dyes mixed with larger organic carrier materials such as those mentioned above.

As the particle sizes range between common powders, a question arises as to whether a certain particle size is more advantageous. A recent study investigated different sized formulations of iron oxide magnetic powder, obtained through ball-milling and sieving.[57] The sizes ranged between 33 – 82 µm for the different formulations, subsequently, each formulation was applied as fingermark developers. It was found that the batch containing 57-67 µm sized particles were most effective at fingermark visualisation. It was also noted that as the porosity of substrates increased, formulations containing smaller particles exhibited poorer visibility as they became trapped within the substrate pores resulting in greater background development.

Similarly, an earlier study investigated silica nanoparticles and identified fingermarks of the highest quality to be obtained using nanoparticles between 45-63 µm in size.[58] The powders were applied using '*standard commercial brushes*' which included a squirrel hairbrush and a Zephyr brush. There is no explanation for the use of two different brush types other than both being commonly used by forensic scientists and no indication as to which performed better in the study.

The surface chemistry effects on fingermark development have also been investigated.[59,60] Flake powders without stearic acid coatings were less effective at developing fingermarks, as opposed to those with stearic acid coating. Further investigations identified 70 μm sized particles to be most effective at developing high-quality fingermarks. These studies report similar ranges, suggesting the desired particle size for fingermark powders to be in the range of 50-70 μm.

The effectiveness of powder is not just dependant on the limiting variables mentioned previously. The operator skill and means of application are equally important. Moreover, UK police forces were asked to participate in a survey to identify which powders they used most, and their application method.[55] Survey responses identified aluminium powder to be most popular, with a variety of application methods including, glass and polyester Zephyr, feather, and squirrel hair brushes. Using this data, The Home Office (THO) Centre for Applied Science and Technology (CAST), conducted extensive laboratory trials to identify which applicator was most effective at developing marks using aluminium powder. For each applicator, 10,000 fingermarks were developed and assessed.[9]

The results concluded that the glass fibre, Zephyr-style brushes produced the optimum development and contrast for ridge detail. The glass fibres retained and released the powder very well, enabling a gradual build-up of the adhering particles. In contrast, squirrel hair/mop style brushes performed significantly worse when used with aluminium powder, instead, these are found to be more effective when used with granular powders.

Subsequently, THO investigated the effectiveness of aluminium powder on a range of substrates.[9] Surveys identified the four most common surfaces which aluminium powder was applied to as, glass, uPVC, painted wood, and painted metal, in all 12,640 latent fingermarks were developed and graded. This work concluded that glass fibre/ Zephyr style brushes again provided optimum results.

It is widely believed that fluorescent powders work best with slightly thicker, animal hairbrushes, however, there is currently no research to substantiate this. Even so, the results of this investigation would have identified brushes to use for fluorescent powders made of inorganic materials. As there is currently no research to indicate which brush is best used for the application of organic doped luminescent materials, the powders will first be investigated and imaged using SEM-EDX (scanning electron microscopy with energy dispersive X-rays). This will identify the shape(s) (i.e. flake, granular), and size(s) of the material, thus, indicating the most suitable brush for the material.

1.7 Aims

In this research, two organic long-persistence luminescent (OLPL) materials have been investigated as fingermark developers. The first material, (3-bromopropyl)triphenylphosphonium (TPP), is a bromine-phosphonium salt that can be synthesised by refluxing triphenylphosphine and 1,3-dibromopropane in acetonitrile (**Figure 1.9**).[48] The persistent luminescent emission is achieved through the presence of the dopant: N,N-dimethylaniline (DMA), during the recrystallisation. It is believed DMA is trapped within the crystal lattice, resulting in the doped system.
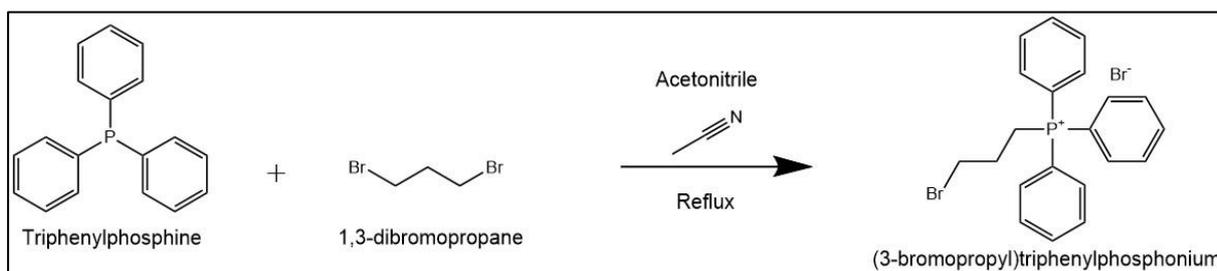
Figure 1.9: Chemical Synthesis of (3-Bromopropyl)triphenylphosphonium bromide

The second material, 2,4,6-tri(4-pyridyl)-1,3,5-triazine (4-TPT), is a neutral, rigid, tripodal organic molecule.[61] Under high pressures and in the presence of a strong base, 4-cyanopyridine reacts to produce the 4-TPT molecule (**Figure 1.10**).
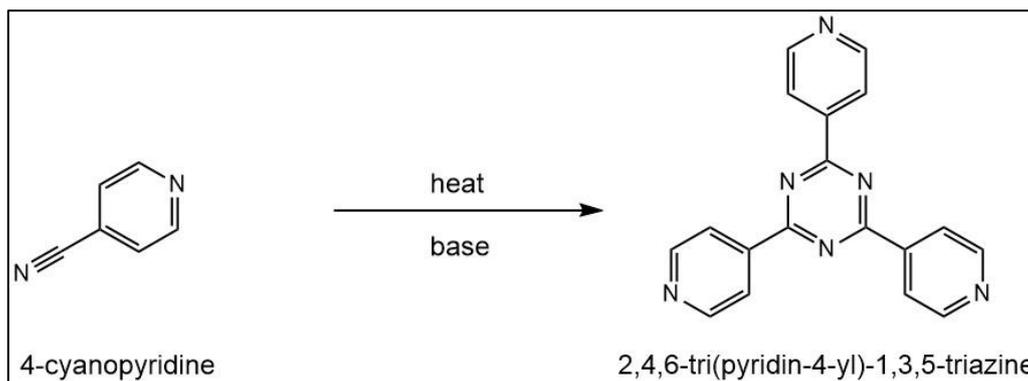
Figure 1.10: *Chemical Synthesis of 2,4,6-tri(4-pyridyl)-1,3,5-triazine*

The rigidity and trigonal geometry of 4-TPT can lead to the formation of nanosized cages and porous frameworks enclosing cavities, chambers, and channels.[62] The addition of electron donor (DMA) during the synthesis, enables trapping of the DMA dopant within these nanosized cages, here, the electron-donating capability of the dopant results in the 4-TPT material exhibiting photoluminescent properties with increased intensity and extended duration compared with the undoped material. Currently, all published literature which has claimed to produce a persistent luminescence in the 4-TPT material has achieved these via metal-organic frameworks. To the best of the author's knowledge, this thesis represents the first observation of persistent luminescence derived from 4-TPT, without inclusion within a metal-organic framework (MOF).

A scientific explanation and understanding of the mechanisms within organic persistent luminescent systems have developed very recently. Organic PLM's have only been of recent interest due to advances that have increased the emission duration. Although further research is required to confirm the mechanism, the well-understood and thorough investigations for inorganic PLM's are believed to be very similar to the organic mechanisms.

Due to the recent advances and developments on organic persistent luminescent materials, their emissive properties may prove beneficial to crime scene investigators as latent fingermark developers. As the powders in wide-spread use are comprised of inorganic formulations, this research will investigate and assess the suitability of developing latent fingermarks using organic PLM's.

This research further explores the persistent luminescence of the two organic materials: (3-Bromopropyl)triphenylphosphonium bromide (TPP) and 2,4,6-tri-4-pyridyl-1,3,5-triazine (4-TPT). Different strategies and factors were investigated to obtain an emissive material that has been optimised for emission intensity. The optimised materials were then prepared as fingermark powders and applied to latent fingermarks according to the guidelines established by the International Fingerprint Research Group.[63]

To investigate the effect of dopant concentration on the two materials investigated in this work, recrystallisation of TPP and the synthesis of 4-TPT were performed under identical conditions, however different concentrations of DMA were tested to determine the optimal doping concentration. This work explores both material optimisation (Chapter 3) and a fingerprint performance study of these materials (Chapter 4).

CHAPTER 2.   EXPERIMENTAL

The powders used for the development of latent fingermarks were synthesised and optimised for desirable luminescent properties, the experimental methods section of this thesis is divided into two separate parts; chemical synthesis, characterisation, and optimisation (section 2,1), followed by a study assessing the ability of the powders to visualise latent fingermarks.

2.1   (3-Bromopropyl)triphenylphosphonium bromide

2.1.1   Materials

Triphenylphosphine ($C_{18}H_{15}P$), 1,3-dibromopropane ($C_3H_6Br_2$), celite (SiO_2), acetonitrile (C_2H_3N), N,N-dimethylaniline ($C_8H_{11}N$), dichloromethane ($CHCl_2$), ethyl acetate ($C_4H_8O_2$), and diethyl ether ($C_4H_{10}O$) were obtained from Sigma-Aldrich as commercial products of analytical grade and used without further purification.

2.1.2   Synthesis

The synthetic route used an adapted methodology from published literature,[48] to increase the yield of the synthesised material.

Triphenylphosphine (4 g, 15.25 mmol), 1,3-dibromopropane (15 mL, 147.11 mmol) and acetonitrile (240 mL) were added to a round bottom flask. The reaction mixture was heated to 95 °C and maintained at reflux for 24 hours. The solvent was removed under vacuum affording a crude white solid (3.39 g, 85%).

2.1.3   Recrystallisation

The crude product was introduced to a flask containing dichloromethane (50 mL) and the solution was warmed to 30 °C. Additional dichloromethane was added to the warming solution until the product was fully dissolved. The solution was filtered through celite into a receiving flask and a buffer layer of dichloromethane with ethyl acetate (1:1) was added in equal volume, followed by a layer of ethyl acetate in equal volume. The flask was sealed and allowed to stand for a few days, affording two types of

crystals, (3-Bromopropyl)triphenylphosphonium bromide (granular plates, 3.29 g, 82%) and 1,3-propanediylbis(triphenylphosphonium) dibromide (thin needles, 0.31 g, 8%).

The undesired needles were manually sorted, enabling the desired (3-Bromopropyl)triphenylphosphonium bromide crystals to be isolated. The desired product was then washed with warm ethyl acetate (3 x 5 mL). The recrystallisation was repeated to afford (3-Bromopropyl)triphenylphosphonium bromide as transparent blocky crystals (2.90 g, 72%).

TPP: Mp 226-229 °C, ^{1}H-NMR (400 MHz, chloroform-d) δ 7.87 – 7.77 (m, 9H), 7.70 (m, 6H), 4.15 – 4.07 (m, 2H), 3.86 (td, J = 6.2, 1.6 Hz, 2H), 2.27 – 2.18 (m, 2H).

2.1.4 Doping of (3-Bromopropyl)triphenylphosphonium bromide

2.1.4.1 Layered Diffusion

(3-Bromopropyl)triphenylphosphonium (0.2 g, mmol) was gently stirred in a warming solution of dichloromethane (30 °C, 10 mL) until dissolved. To obtain a doping concentration of 1:20, N,N-dimethylaniline (1.09 mL) was introduced to the solution. Stirring was continued for one minute. The stirrer bar was then removed, and the solution was recrystallised via double-layer diffusion, which included a buffer layer of dichloromethane and ethyl acetate (1:1, 10 mL), followed by a final layer of ethyl acetate (10 mL). The vial was sealed and set aside for five days, forming green transparent doped (3-Bromopropyl)triphenylphosphonium bromide crystals (TPP:DMA) (0.17 g, 85%).

2.1.4.2 Vapour Diffusion

(3-Bromopropyl)triphenylphosphonium bromide (0.2 g) was gently stirred in a warming solution of dichloromethane (30 °C, 10 mL) until dissolved. N,N-dimethylaniline (1.09 mL) was introduced to the solution and stirring continued for one minute. The stirrer bar was removed, and the smaller vial holding the solute was placed into the middle of a larger vessel containing diethyl ether (20 mL). The larger vessel was sealed and set aside for five days, forming green transparent doped (3-Bromopropyl)triphenylphosphonium bromide crystals (TPP:DMA) (0.17 g, 85%).

2.1.5 Powder Preparation

The crystals obtained in the crystallisations were isolated using a spatula and placed aside for 1 hour, giving time for the excess solvent to evaporate. Then, the crystals were gently and manually ground by hand for using an agate pestle and mortar, until a powder had formed (20-30 seconds). The powders were further air-dried for 24 hr before instrumental analysis.

2.2 2,4,6-tri(4-pyridyl)-1,3,5-triazine (4-TPT)

2.2.1 Material

4-cyanopyridine ($C_6H_4N_2$), 18-crown-6 ($C_{12}H_{24}O_6$), potassium hydroxide (KOH), N,N-dimethylaniline ($C_8H_{11}N$), mesitylene (C_9H_{12}), sodium hydroxide (NaOH) and pyridine (C_5H_5N) were obtained from Sigma-Aldrich as commercial products of analytical grade and used without further purification.

2.2.2 Synthesis

4-cyanopyridine (0.5 g, 4.8 mmol), 18-crown-6 (0.05 g, 0.19 mmol), potassium hydroxide (12.5 mg, mmol) and mesitylene (0.25 mL) were added to a charged round bottom flask. The flask was purged using nitrogen and sealed with a rubber septum. The mixture was heated to 200 ºC and stirred under nitrogen for 4 hours. The colour changed from transparent brown to an opaque brown/red within a short time.

With gentle stirring, the flask was raised from the hot plate and pyridine (3 mL) was introduced to the flask. This yielded a fine crystalline material which was filtered into a Büchner funnel and washed with additional pyridine (2 x 3 mL). The material was dried under vacuum, yielding 2,4,6-tri(4-pyridyl)-1,3,5-triazine (4-TPT) as a yellow crystalline solid (0.32 g, 63%)

^{1}H-NMR (400 MHz, chloroform-d) δ 8.96 (d, J = 5.9 Hz, 6H), 8.59 (d, J = 6.0 Hz, 6H). (Mp: 372-374 °C).

2.2.3 Doping 2,4,6-tri(4-pyridyl)-1,3,5-triazine

The synthesis procedure was prepared as described in section 2.2.2, with the addition of N,N-dimethylaniline (20 μL). The flask was purged using nitrogen and sealed using a rubber septum. The mixture was heated to 200 °C and stirred under nitrogen for 4 hours. The colour changed from transparent brown to an opaque brown/red within a short time.

With gentle stirring, the flask was slightly raised from the hot plate and pyridine (3 mL) was introduced to the flask. This yielded a fine crystal compound which was filtered into a Büchner funnel and washed with additional pyridine (2 x 3 mL). The material was dried under vacuum, yielding doped 2,4,6-tri(4-pyridyl)-1,3,5-triazine (4-TPT:DMA) as a white crystalline solid (0.36 g, 71%).

2.3 Characterisation

2.3.1 Fluorimetry

A materials' photoluminescent properties can be measured using a Fluorometer. The sample is mounted inside the instrument and a beam of light at a specific wavelength or range of wavelengths is passed through a monochromator and directed towards the sample. The light emitted from the sample is detected by a transducer and converted to an electrical signal which is interpreted onto a digital spectrum. A fluorometer can be used to measure the excitation (Ex) and emission (Em) spectra of a sample. The photoluminescent measurements were recorded at room temperature using a Cary Eclipse Fluorescence Spectrophotometer by Agilent Technologies using the solid sample holder accessory. Spectral data were interpreted using the Cary Eclipse software. Further details of the excitation and emission parameters are provided in Chapter 3 in the relevant figure captions.

2.3.2 Proton Nuclear Magnetic Resonance Spectroscopy

Proton Nuclear Magnetic Resonance (^{1}H-NMR) Spectroscopy measures the energy required to change the alignment of NMR active nuclei (^{1}H). The sample is placed into a magnetic field and the radio wave frequency is applied to the sample, then increased over a range. The intramolecular magnetic fields around an atom within a molecule will absorb radio waves at frequencies, which are characteristic to the environment which the proton is in. The field strength and resonance frequencies are measured in parts per million (ppm) and displayed on a spectrograph, serving as a *'fingerprint'* for the configuration of hydrogens within the sample being measured.[64] An example ^{1}H-NMR spectrum of ethanol is shown in the supplementary information file (appendix A).

^{1}H-NMR spectra were recorded at 298 K on a Jeol ECS-400 spectrometers with the chemical shifts ($δ$) reported in parts per million (ppm) and referenced to deuterated chloroform ($CDCl_3$). The spectral data were analysed using the software MestReNova (version 12).

2.3.3 Scanning Electron Microscopy with Energy Dispersive X-rays

Scanning Electron Microscopy (SEM) with Energy Dispersive X-rays (EDX) is an instrument which examines a specimen to yield information on the topography, chemical composition and crystallographic information of the sample being investigated.

A sample is placed into a vacuum and an electron source is pointed towards the sample. Secondary electrons are produced when the incident electron beam excites electrons in the sample, losing some of its energy in the process. The excited electron moves towards the surface of the sample, if the energy is sufficient, the surface of the sample is excited, producing secondary electrons. Additionally, when the incident electron beam strikes the sample surface, some of the electrons are scattered and are referred to as backscattered electrons. Both types of electrons are detected and provide an image of the sample. Secondary electron imaging is surface sensitive and provides a greater optical resolution, whereas backscattered electrons are sensitive to the atomic mass of the nuclei they are scattered from. When elemental mass increases, the number of backscattered electrons produced increase, thus, appearing brighter on the image.

Energy-dispersive X-ray analysis includes an X-ray detector in the SEM instrument. The electron beam causes a state of excitation for electrons in the sample. Upon relaxation, electrons emit characteristic X-rays. These X-rays are received by a detector and provide elemental information about the sample.

SEM images were recorded on a Hitachi S3400-N SEM in the School of Physical Sciences at the University of Kent. This was used to record the morphology of TPP:DMA and 4-TPT:DMA. The system was equipped with Oxford Instruments EDX systems, running INCA software (version 7).

2.3.4 X-ray Diffraction

X-ray diffraction is an instrument which provides information on the ordered arrangement of atoms by analysing the bond lengths and angles within a solid. The X-ray crystallographer determines the spacing and arrangement of atoms which can be defined by Bragg's law. Bragg's law for a given set of lattice planes with an inter-plane distance of *d*, the condition for diffraction (peak) to occur can be simply written as:

Equation 2.1

$$n\lambda = 2d \sin \theta$$

In this equation, the variable *d* is the distance between atomic layers in a crystal, lambda (λ) is the wavelength of the incident X-ray beam, and *n* is an integer representing the order of the diffraction peak.

In simple structures, the peaks in an X-ray diffraction pattern are directly related to the atomic distances through (**Equation 2.1**) as illustrated (**Figure 2.1**). X-ray diffraction (XRD) instruments, particularly single-crystal instruments, include a low-temperature system for cooling the crystal sample, reducing the thermal motion of atoms, thus, improving the resolution of the experiment.
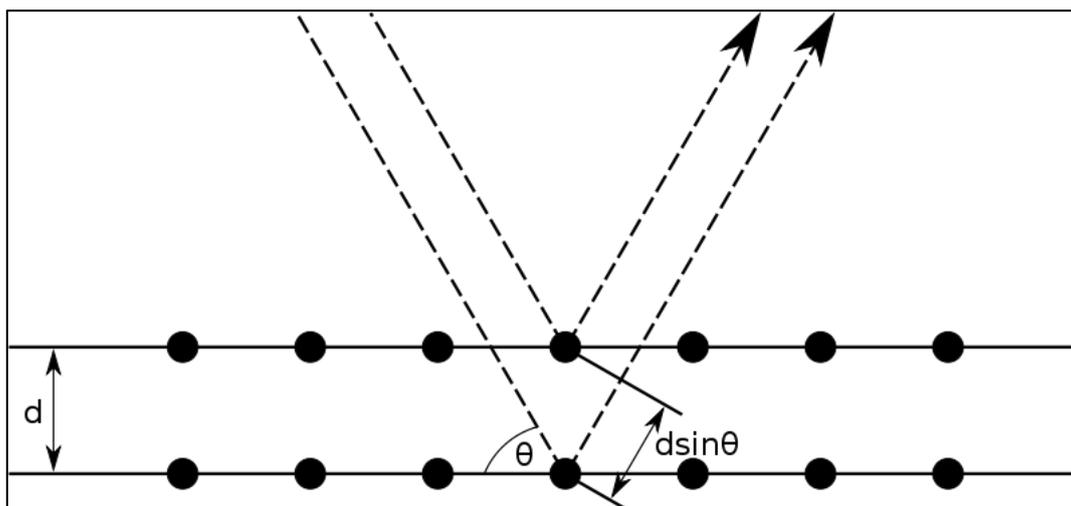
Figure 2.1: *Schematic illustration of Bragg's Law showing an incident X-ray beam interacting with the atoms arranged periodically. The spheres represent the placement of atoms and Bragg's Law illustrates that a set of parallel planes in the crystal produce a diffraction pattern when diffracting an X-ray beam of wavelength λ upon the planes at angle θ and are reflected at the same angle.*

2.3.5 Powder X-ray Diffraction (XRD)

Powder X-ray Diffraction (PXRD) is an analytical technique primarily used for phase identification of a crystalline material and can provide information on unit cell dimensions. Powder XRD looks at a large sample of polycrystalline materials and provides information about the phase (polymorph) and crystallinity of the material, the pattern is considered as the *"fingerprint"* of the material. The diffractometer consists of an X-ray source, a goniometer, and a detector. X-rays are directed toward the crystal sample and the atoms within the crystalline material will cause the incoming X-rays to diffract in a pattern characteristic of the structure. X-ray photons scattered at the given angle are detected, and the intensity is plotted against the angle of diffraction which is displayed as a pattern. The positions of the atoms in the crystal can then be determined along with their bonding.

Powdered X-ray diffraction patterns were collected using the Rigaku Miniflex 600 (Cu Kα, λ = 1.5406 Å) over a 2θ range from 5 - 70 degrees with a step size of 0.02 degrees and a count time of 1 second/step. Software CrystalDiffract (version 6) was used to interpret the diffraction patterns.

2.3.6 Single-Crystal X-ray Diffraction

Single-crystal X-ray Diffraction allows absolute structure determination. With single-crystal XRD data, the exact atomic positions can be observed, and thus bond lengths and angles can be determined. The diffractometer contains a monochromator crystal to select specific X-ray wavelengths and a collimator that focuses a narrow incident   X-ray beam on to the sample.

Single-crystal XRD data were recorded on a Rigaku SuperNova single-crystal X-ray diffraction instrument at temperatures of 120 K and 230 K. The crystals were mounted on a wire loop using epoxy and data collected in all geometries. Data were interpreted using SHELX software.

2.3.7 High-Performance Liquid Chromatography with Mass Spectrometry

High-performance liquid chromatography-mass spectrometry (HPLC-MS) is an analytical technique used to separate, identify, and quantify each component within a mixture. A solvent containing the sample is passed through a column which has been filled with an absorbent solid material such as silica. Each component of the sample will react differently, with the stationary phase, causing the components to separate and exit the column at different intervals. The retention factors are recorded and displayed on a chromatogram.

HPLC-MS data were obtained on a Thermo Scientific MSQ Plus LC-MS system using a Phenomenex Luna 5 μm 150 x 4.6 mm column set at 40 °C. Mobile Phase A = H_2O + 0.1% v/v formic acid, B = MeOH + 0.1% v/v formic acid, with a flow rate fixed at 1.5 mL/min. Mobile Phase gradient 2% B to 100% over 8 minutes, 100% B for 2.5 minutes with a total run time of 13 minutes. Analyte ions were produced using Electrospray Ionisation Mass Spectrometry in positive mode (ESI +ve) a mass range of 100 – 2000 Da and a scan time of 1.0 second with a cone voltage of + 7 V and a probe temperature set at 350 °C. The samples (TPP 2 mg, TPP:DMA 2.2 mg, DMA 2 mg) were dissolved in 1.5 mL MeOH + 5% H_2O and 1 μL was injected. The absorption wavelength was set at 254 nm. The Chromatic Data System (CDS software) used was Thermo Chromeleon (version 7.2).

CHAPTER 3. SYNTHESIS, OPTIMISATION AND CHARACTERISATION OF ORGANIC PHOTOLUMINESCENT MATERIALS

3.1 (3-Bromopropyl)triphenylphosphonium bromide

3.1.1 Synthesis optimisation

The first synthesis of TPP was performed using the same conditions as the published report.[48] In contrast with the reference report, column chromatography was performed following the dissolution of the product and filtration through celite. Recrystallisation was performed affording two types of crystals: blocks (**Figure 3.1a**) and needles (**Figure 3.1b**).

a   b
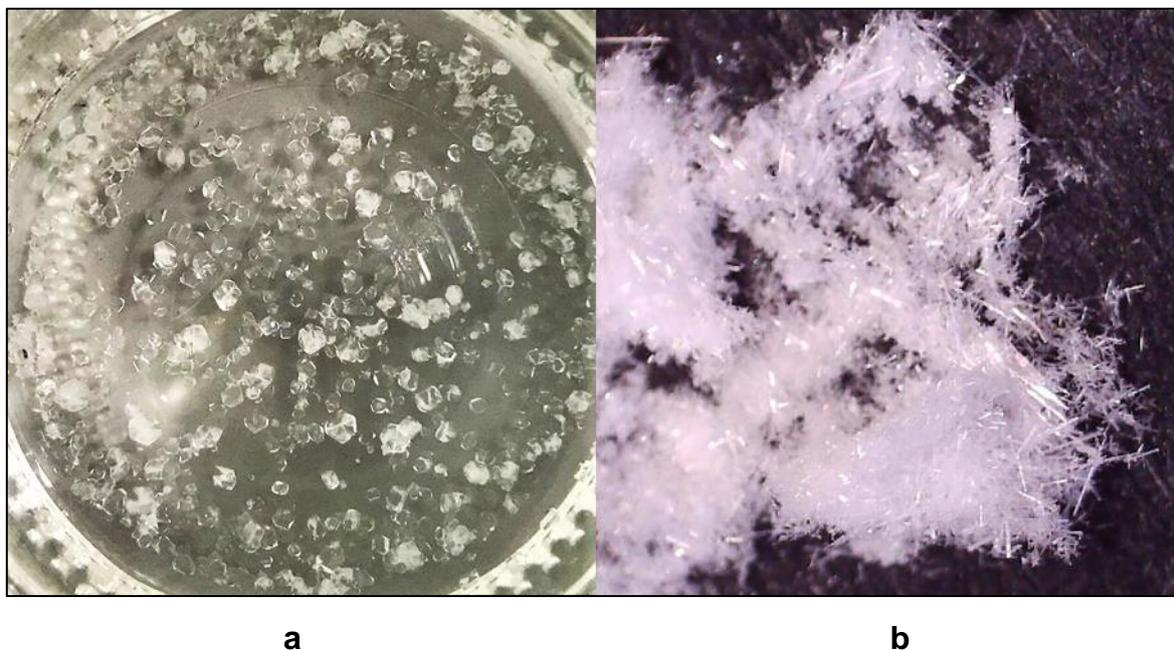
Figure 3.1: *The two types of crystals recovered from the layered diffusion recrystallisation of the synthesised material.* **3a** *displays the desired (3-Bromopropyl)triphenylphosphonium bromide blocky shaped crystals that formed during the second recrystallisation (layered diffusion) of the synthesised material.* **3b** *displays the undesired 1,3-propanediylbis(triphenylphosphonium) dibromide needle-shaped crystals that were recovered from the first recrystallisation.*

Single crystal data were obtained for both types of crystals. Results identified the blocky shaped crystals to be the desired product; (3-Bromopropyl)triphenylphosphonium (TPP) (**Figure 3.2**). And the needle-shaped crystals the be the less desired by-product; 1,3-propanediylbis (triphenylphosphonium) dibromide (PTP) (**Figure 3.3**). PTP likely forms when the Bromo alkane undergoes further reaction, replacing the Bromo group with a carbon-carbon bond attaching an additional triphenylphosphonium to yield triphenyl(propyl)phosphonium.
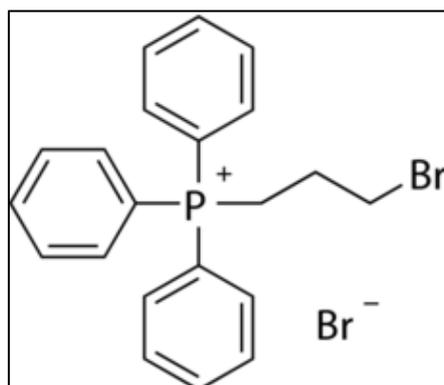
Figure 3.2: *The chemical structure of the desired product (3-Bromopropyl)triphenylphosphonium bromide obtained upon recrystallisation.*
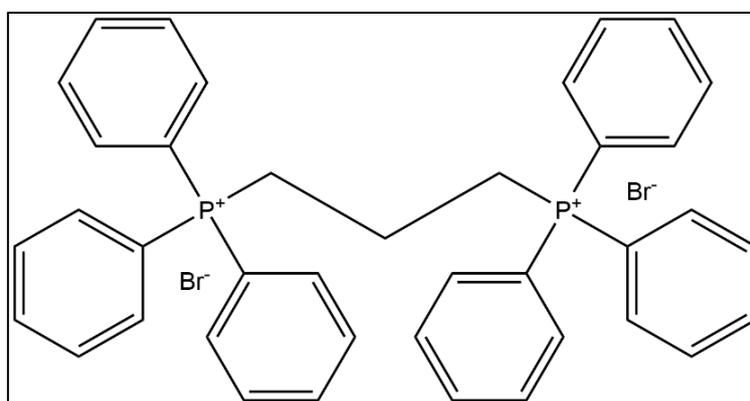
Figure 3.3: *The chemical structure of the undesired product 1,3-propanediylbis(triphenylphosphonium) dibromide obtained upon recrystallisation.*

The afforded yields were 51.9%: TPP (30.3%) and PTP (21.6%). The published synthetic route was modified by adding excess 1,3-dibromopropane to the reaction mixture. This increased the afforded yield to 90%: TPP (82%) and PTP (8%). The addition of reactant 1,3-dibromopropane in excess increased the recovered mass of the desired TPP product as this increased the chances of the desired (1,3-bromopropyl) material to form during the synthesis.

3.1.2 Doping

The published work that identified the first organic persistent luminescence in TPP claimed a key factor of the organic persistent luminescent duration to be the concentration of DMA trapped inside the crystals.[48] There are two photoluminescent properties of a persistent luminescent material, the emission intensity, and the emission duration. Given the particular use of these materials, the emission intensity was favoured over the luminescent duration because the duration only needs to extend to a time that enables a photograph to be taken (< 3 s). Therefore, rather than investigating the effect of dopant concentration on emission duration, this research focusses on the effects that changing doping concentration has on the emission intensity.

The variables that maximise the concentration of dopant trapped within recrystallised organic materials are yet to be established, therefore, investigations were made to optimise the photoluminescent properties of the doped (3-Bromopropyl)triphenylphosphonium bromide crystals using two methods of crystallisation: layered diffusion and vapour diffusion, to identify whether a particular system performed better at maximising the concentration of dopant trapped within the crystal.

3.1.3 Optimisation

Layered diffusion is a standard method of crystallisation whereby a saturated solution of the organic material was prepared by dissolving TPP in dichloromethane, a good solvent of high density. This solution is transferred to a vial, and an equal volume of ethyl acetate, a solvent with lower TPP solubility and less density, is carefully introduced to form a separate layer above it. This vial is sealed for a few days, during which, the two layers slowly diffuse into one another, resulting in the formation of crystals at the interlayer of the diffusing solvents. Similarly, doped crystals can be obtained by introducing dopant into the TPP solution, followed by the introduction of the second layer as above. It is believed that as the crystals form at the interlayer, the presence of dopant impurities become trapped within the forming crystal lattices.

Similarly, vapour diffusion is the crystallisation process whereby crystals form as a result of the diffusion of solvent vapours. Seven vials that contain an identical mass of TPP were prepared in dichloromethane. These vials were placed into a larger vessel which contains diethyl ether. The larger vessel was sealed, and the gas phase of the volatile poor solvent diffuses into the vial containing the solute. Eventually, over saturation of the dissolved product occurs, forming crystals. Similar to layered diffusion, the dopant is introduced to the vial containing the dissolved TPP material. Again, it is hoped that the presence of dopant impurities become trapped as the crystal forms.

To investigate the effects of dopant concentration on the photoluminescent properties, a series of identical crystallisation's were performed by both methods of crystallisation described above. Different molar concentrations of DMA were introduced to crystallisations, the chosen mole ratio of TPP to DMA investigated in this study included: 1:1. 1:2, 1:5, 1:10, 1:20, 1:30 and 1:40. Additional concentrations greater than 1:40 were investigated, however, the large concentration of dopant resulted in the precipitation of the dissolved TPP material. This precipitant was isolated and the photoluminescent properties were investigated, however, the persistent luminescent properties were absent.

With the investigated ratios described above, seven separate vials containing identical amounts of TPP were dissolved in identical volumes of dichloromethane. The increasing molar concentrations of DMA have introduced accordingly, and crystallisations were performed. The TPP:DMA crystals were recovered, and the

photoluminescent of these samples were explored in the solid-state, at room temperature. Photoluminescent emission values for layered diffusion (**Figure 3.4**) and vapour diffusion (**Figure 3.5**) are displayed indicated in the figure.
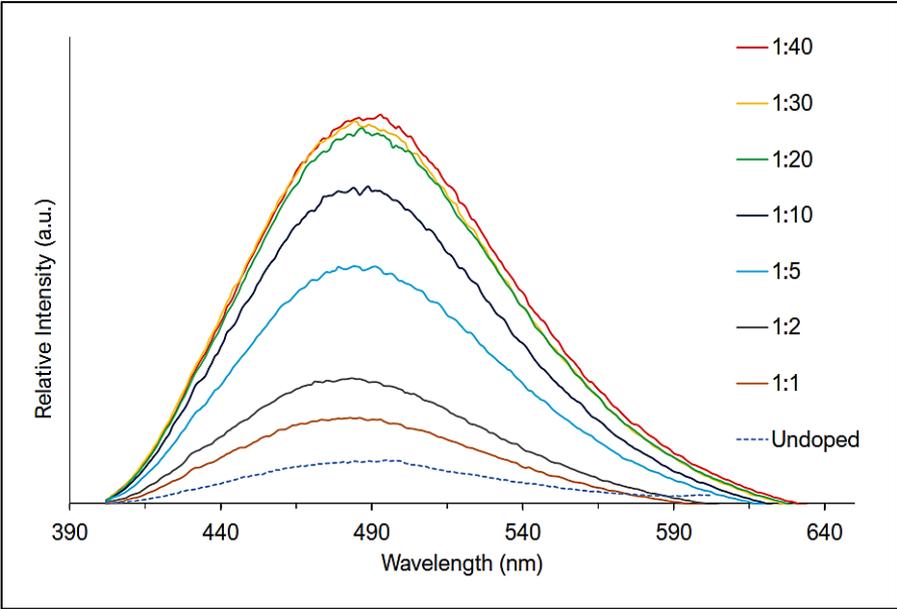
Figure 3.4: *Emission spectra of the doped crystalline powders recrystallised through* ***layered diffusion****. The intensity values are normalised and measured as crystalline powders at room temperature. λex = 315 nm*
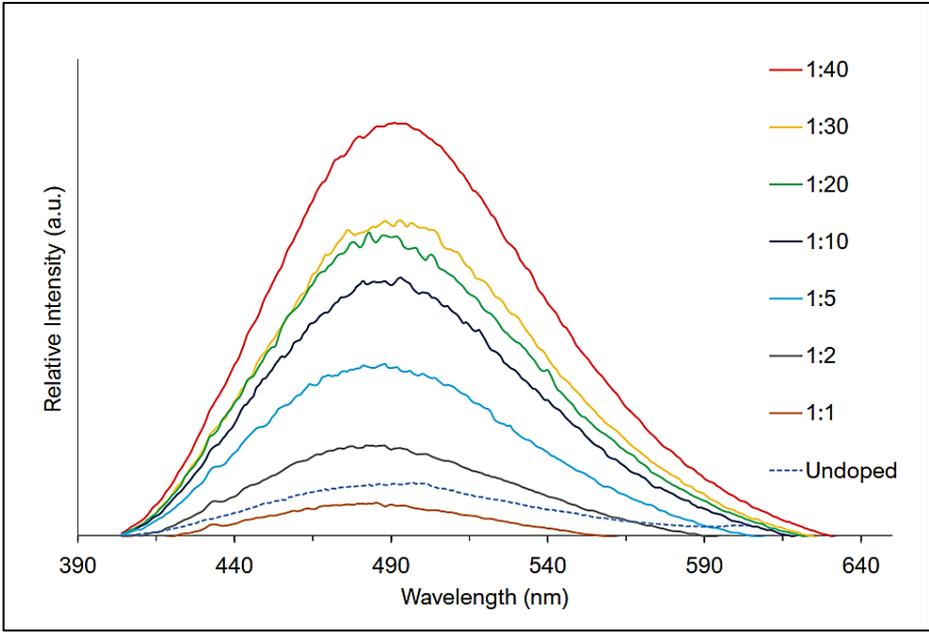
Figure 3.5: *Emission spectra of the doped crystalline powders recrystallised through* ***vapour diffusion****. The intensity values are normalised and measured as crystalline powders at room temperature. λex = 315 nm*

The Max. emission intensities displayed for each of the doping concentrations via both methods of recrystallisation are shown in **Figure 3.6**, with the numerical values reported in **Table 3.1**.
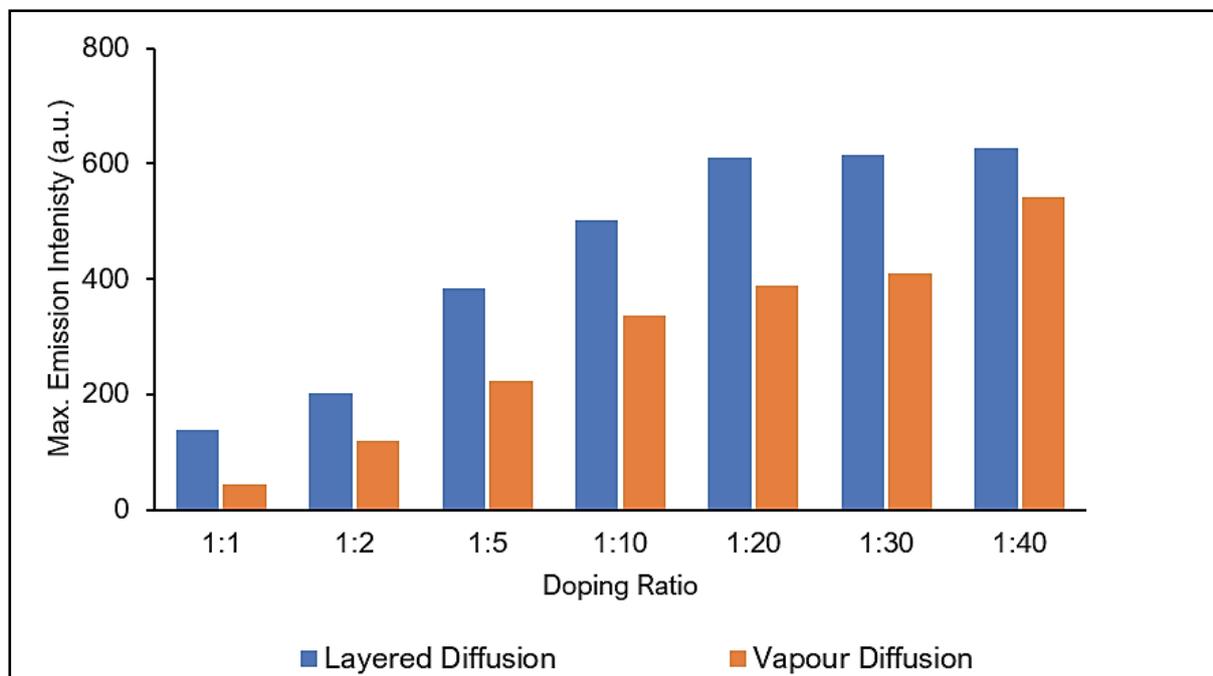
Figure 3.6: *Highest emission intensity values achieved from doped crystals obtained through layered diffusion (blue) and vapour diffusion (orange). The intensity values for both types of crystallisation were obtained using the same fluorometer parameters and measured as crystalline powders at room temperature. λex = 315 nm*

Table 3.1: *Highest emission intensity values achieved from doped crystals obtained through layered diffusion and vapour diffusion. The intensity values for both types of crystallisation were obtained as arbitrary units, using the same fluorometer parameters and measured as crystalline powders at room temperature. λex = 315 nm*

	Doping Ratio (TPP:DMA)						
	1:1	1:2	1:5	1:10	1:20	1:30	1:40
Layered Diffusion	139	202	384	502	609	615	627
Vapour Diffusion	43	118	223	337	389	410	543

Very little difference is observed for the maximum emission intensities achieved via layered diffusion at 1:20, 1:30 and 1:40 mole ratios. Indicating that a saturated solution can be obtained through the addition of dopant at a mole ratio 1:20. Layered diffusion appeared to reach a maximum doping factor at the 1:20 doping ratio. Vapour diffusion could continue to increase, to reach a similar maximum, however, the addition of higher DMA doping ratios would precipitate the TPP in dichloromethane suggesting that vapour diffusion results in a lower saturation concentration. The alternative to this would be to identify better-suited solvents of lower volatility and higher boiling points to perhaps further increase dopant concentrations.

As a result, layered diffusion was identified as the better type of recrystallisation to use for increasing the concentration of dopant trapped within the crystal lattices within these experiments. A possible explanation as to why layered diffusion performed better than recrystallisation may be due to the differences in solvent densities. Solvent density is a key factor for layered diffusion to occur requiring a solvent in which TPP is less soluble and which has a lower density.[65] In this case, the preferred solvent, dichloromethane, has a density of 1.33 g/mL whereas the alternative, ethyl acetate, has a density of only 0.9 g/mL. N,N-dimethylaniline has a density of 0.96 g/mL, therefore, sits at the interlayer of the two diffusing solvents. In layered diffusion, crystals form at the interlayer, therefore, N,N-dimethylaniline would be found in larger concentrations at the interlayer within this diffusing system, increasing the probability of DMA being present within the crystals.

As the crystals obtained through vapour diffusion had not achieved emission intensities as large as layered diffusion, vapour diffusion was considered to be the less favoured method to use when doping organic materials, however, this can only be stated for the specific parameters used in this study. There are currently no indications regarding the factors that affect doping concentration; it is likely to be a combination of many factors. The surface contact area of the dissolved TPP solution available to diethyl ether is potentially an important factor affecting the diffusion rate and requires further investigation. These results may vary depending on the solvents used in the system, as well as temperature effects and solvent volumes, all require further investigation to identify if/how these factors affect the photoluminescent properties and doping concentrations of the recovered material.

The synthesised products were exposed to a handheld ultraviolet light-emitting device (UV LED) (UltraFire 501B 365 nm). Through visual observation and qualitative analysis of luminescent emission, the luminescence of the crystals which formed in higher dopant concentrations were noticeably more intense upon UV exposure (**Figure 3.7**). This observation correlates with results obtained in the fluorimetry study.
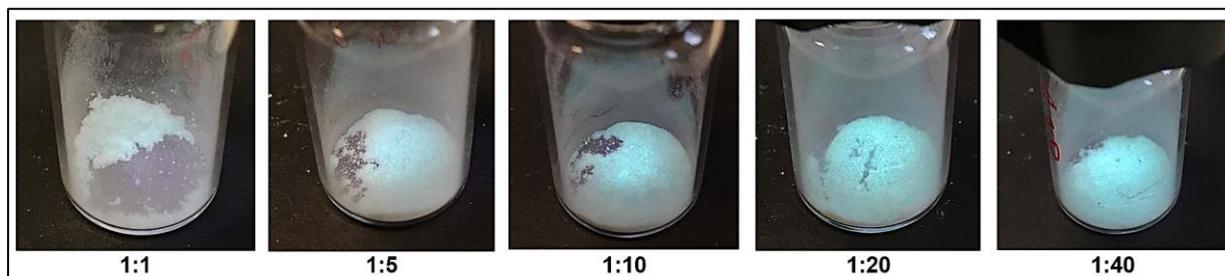
Figure 3.7: Powdered (3-bromopropyl)triphenylphosphonium crystals doped with different concentrations of N,N-dimethylaniline and recrystallised via layered diffusion. DMA molar doping ratios increase from left to right, the lowest 1:1 and the largest 1:40. The images have been taken using an iPhone 7 whilst the powders are exposed to a handheld UV LED.

The term *'dopant'* suggests that DMA is doped (trapped) within the host material. If this was the case, it could be assumed/explained that the fluorimetry results correlate to the concentration of dopant within the material. The more dopant encased within the material, the greater the emission intensity, until a maximum is reached. To confirm the presence of dopant and quantify the concentration, ^{1}H-NMR spectra were obtained.

Figure 3.8 displays the ^{1}H-NMR spectrum of undoped (3-Bromopropyl)triphenylphosphonium bromide, which is consistent with the expected spectrum of the structure, as evidenced by the reference spectrum (Appendix B). The multiplet at 7.87-7.77 ppm is attributed to nine protons in total, three are in a CH environment on the 3,4,5 position for each benzene ring. The multiplet at 7.75-7.65 ppm is attributed to six protons in total, two are in a CH environment on the 2,6 position for each benzene ring. Due to differences in chemical equivalence, there are three separate CH_2 environments. The multiplet at 4.15-4.07 ppm is the two protons on the carbon attached to the bromine atom. The triple doublet at 3.86 ppm is the two protons on the carbon attached to the phosphor atom. The multiplet at 2.27-2.18 ppm is the two protons on the carbon in the centre of the propyl group.

Figure 3.9 displays the ^{1}H-NMR spectrum of (3-Bromopropyl)triphenylphosphonium bromide and N,N-dimethylaniline. Similarly, TPP signals are observed and the different proton environments are labelled on the spectrum A-E. The additional signals observed and labelled F-H, are consistent with the expected spectrum of DMA, as evidenced by the reference spectrum (Appendix C). The spectrum obtained from the mixed sample shows evidence of both expected phases, indicating what should be expected in the spectrum of TPP:DMA. For N,N-dimethylaniline, there are two CH environments, the double doublet at 7.35-7.33 ppm is attributed to the two protons in the 3,5 position of the benzene ring and the singlet at 6.84 ppm is attributed to the three protons in the 2,4,6 position of the benzene ring. There is one CH_2 environment, and the two CH_3 on the structure, are the high-intensity signals at 3.03 ppm, attributed to six its protons.

Figure 3.10 displays the ^{1}H-NMR spectrum of the doped TPP:DMA material, obtained using the doping ratio of 1:20 and recrystallised by layered diffusion. This spectrum display evidence of (3-Bromopropyl)triphenylphosphonium bromide structure, however, there is no evidence of DMA in the spectrum. The spectrum obtained for the mixed sample shows that signals belonging to DMA would be expected between 7.38,7.36 ppm and 3.05 ppm, however, these are not observed in this spectrum.

Figure 3.11 expands the regions in the ^{1}H-NMR spectrum of TPP:DMA, where signals belonging to DMA should be observed. The expanded regions may potentially display trace signals belonging to DMA at 7.38-7.36 ppm. However, the absence of the strongest signal at 3.05 ppm does not support these detections.
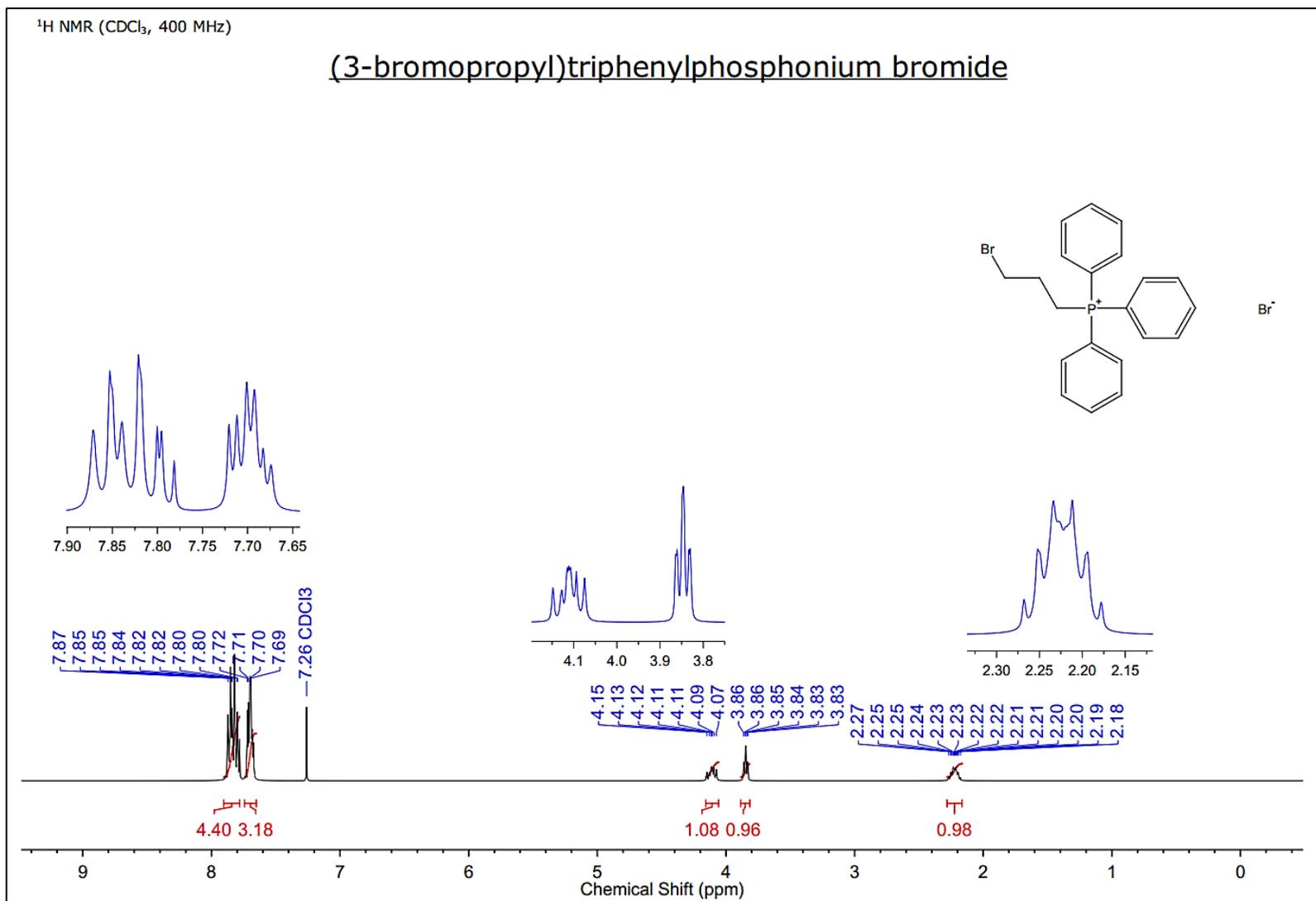
Figure 3.8: ^{1}H-NMR spectra of (3-Bromopropyl)triphenylphosphonium bromide in CDCl$_3$.
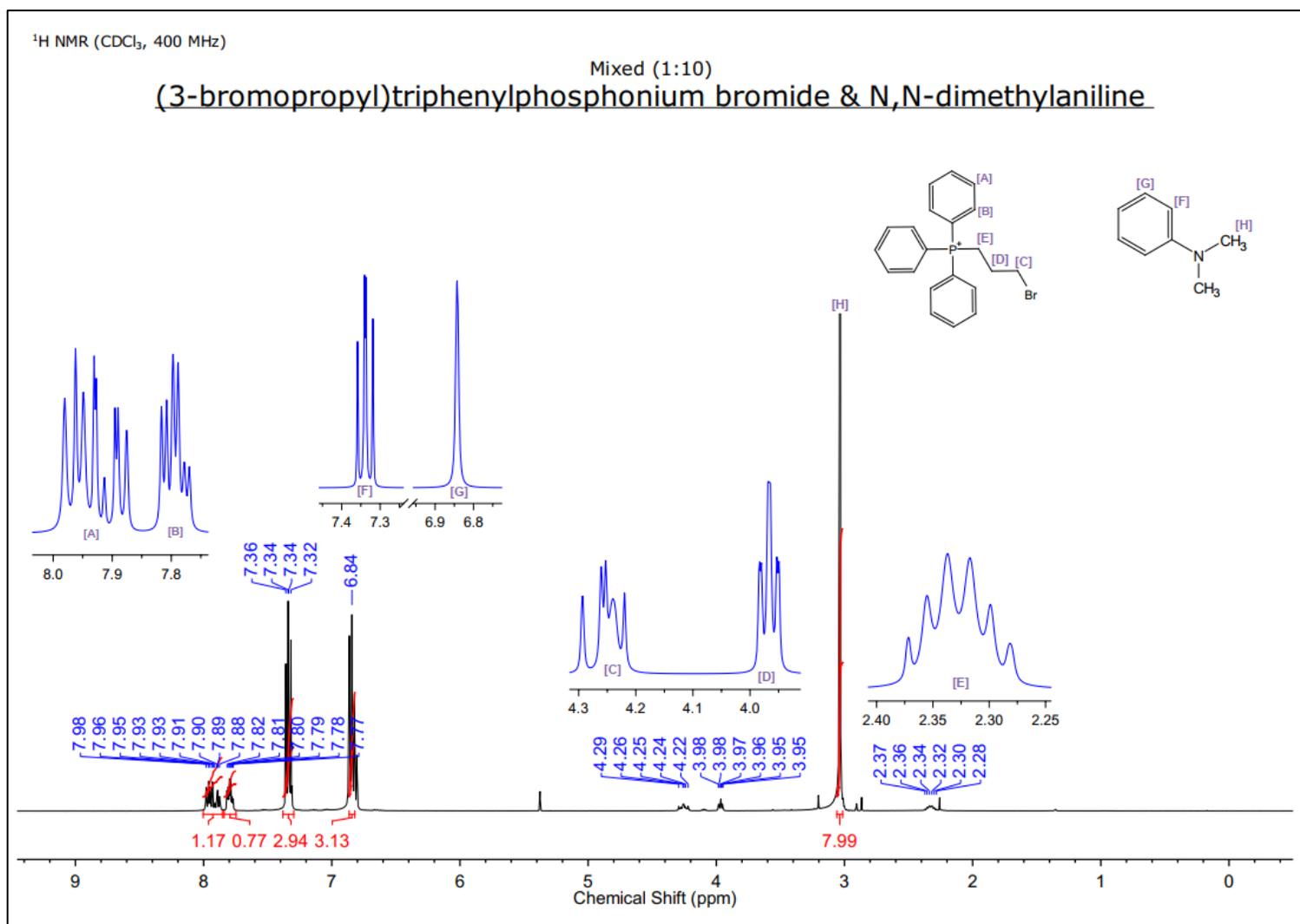
Figure 3.9: The ¹H-NMR spectrum of a mixed sample containing (3-Bromopropyl)triphenylphosphonium bromide (A-E) and N,N-dimethylaniline (F-H).
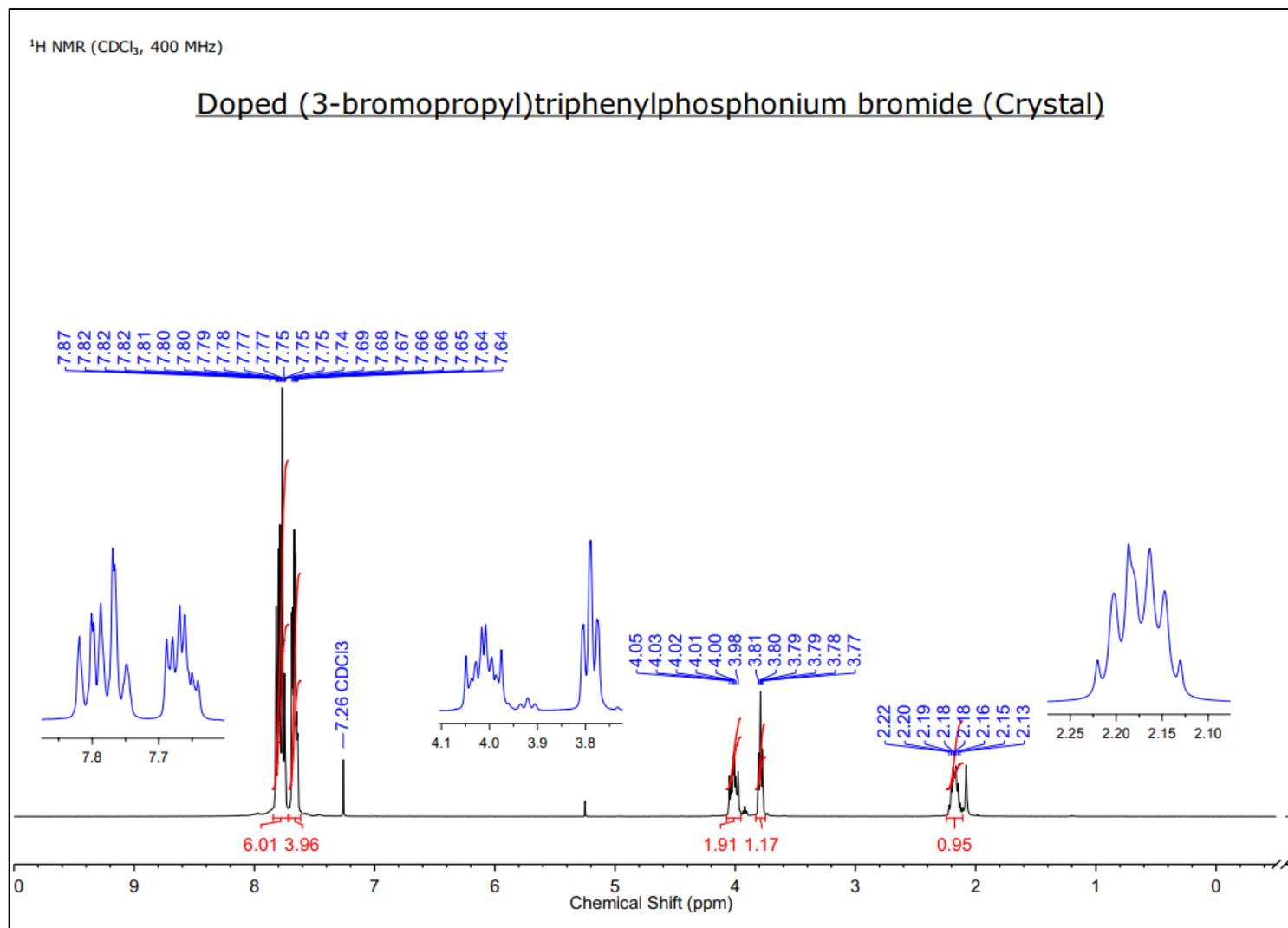
Figure 3.10: *The ¹H-NMR spectrum of (3-Bromopropyl)triphenylphosphonium bromide doped with DMA (1:20) and recrystallised through layered diffusion.*
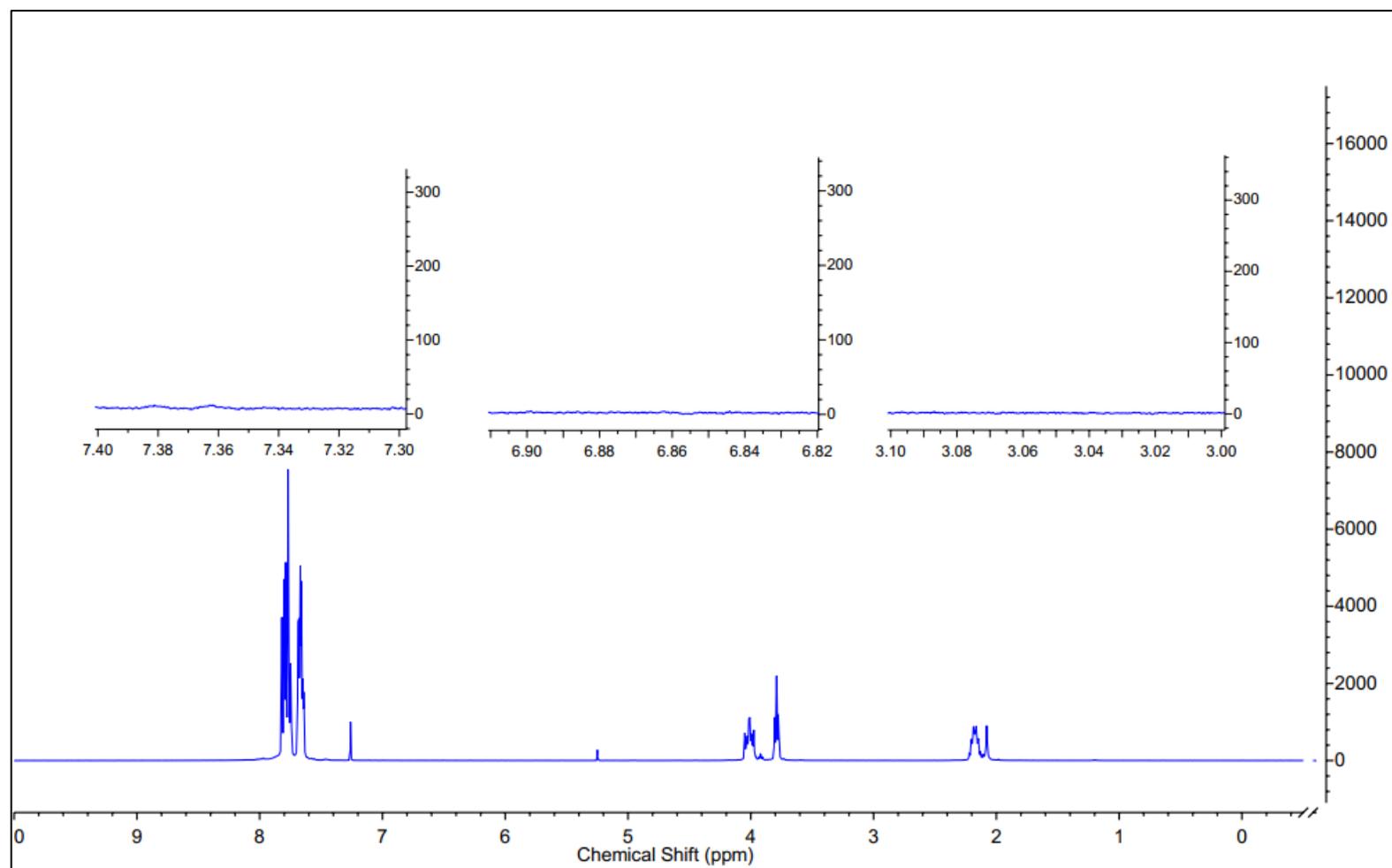
Figure 3.11: *Expanded regions where the dopant (DMA) signals should be observed in the ^{1}H-NMR spectrum of (3-Bromopropyl)triphenylphosphonium bromide doped with DMA (1:20) and recrystallised via layered diffusion. No signals can be seen, either due to no dopant being present within the sample or, the technique is not sensitive enough. Potentially, trace signals belonging to DMA may be seen observed at 7.38,7.36 ppm, however, the lack of the strongest signal at 3.05 ppm contradicts this.*

Although a large quantity (25 mg) of optimal doped TPP:DMA crystals had been used, DMA could not be identified in the ^{1}H-NMR spectrum of the *'doped'* material. Possible reasons for this are detailed in the following paragraphs.

Firstly, it is possible that the concentration of DMA within TPP:DMA is extremely low and ^{1}H-NMR spectroscopy is not sensitive enough to detect the low concentrations of DMA in the sample.

Serial dilutions of DMA in $CDCl_3$ were prepared for ^{1}H-NMR analysis, to identify the concentration limit of detection of DMA (**Figure 3.12**). The aromatic regions are observed between 7.5-6.5 ppm, as well as the singlet derived from the CH_3 signal at 3 ppm, in the ^{1}H-NMR spectrum containing 1% DMA in $CDCl_3$. As the dilution increases, the aromatic regions are not observed, however, the CH_3 signal at 3 ppm is displayed in the ^{1}H-NMR spectrum containing 0.1% of DMA in $CDCl_3$. This signal can still be observed but is of considerably low intensity in the ^{1}H-NMR spectrum containing 0.05% of DMA in $CDCl_3$. This signal is no longer observed in the spectrum containing 0.01% of DMA in $CDCl_3$. Suggesting for this instrument, that the concentration limit of detection of DMA in $CDCl_3$ is between 0.01-0.05%. this occurrence additionally suggests that the concentration of DMA in TPP:DMA, is between, or below this detection limit.
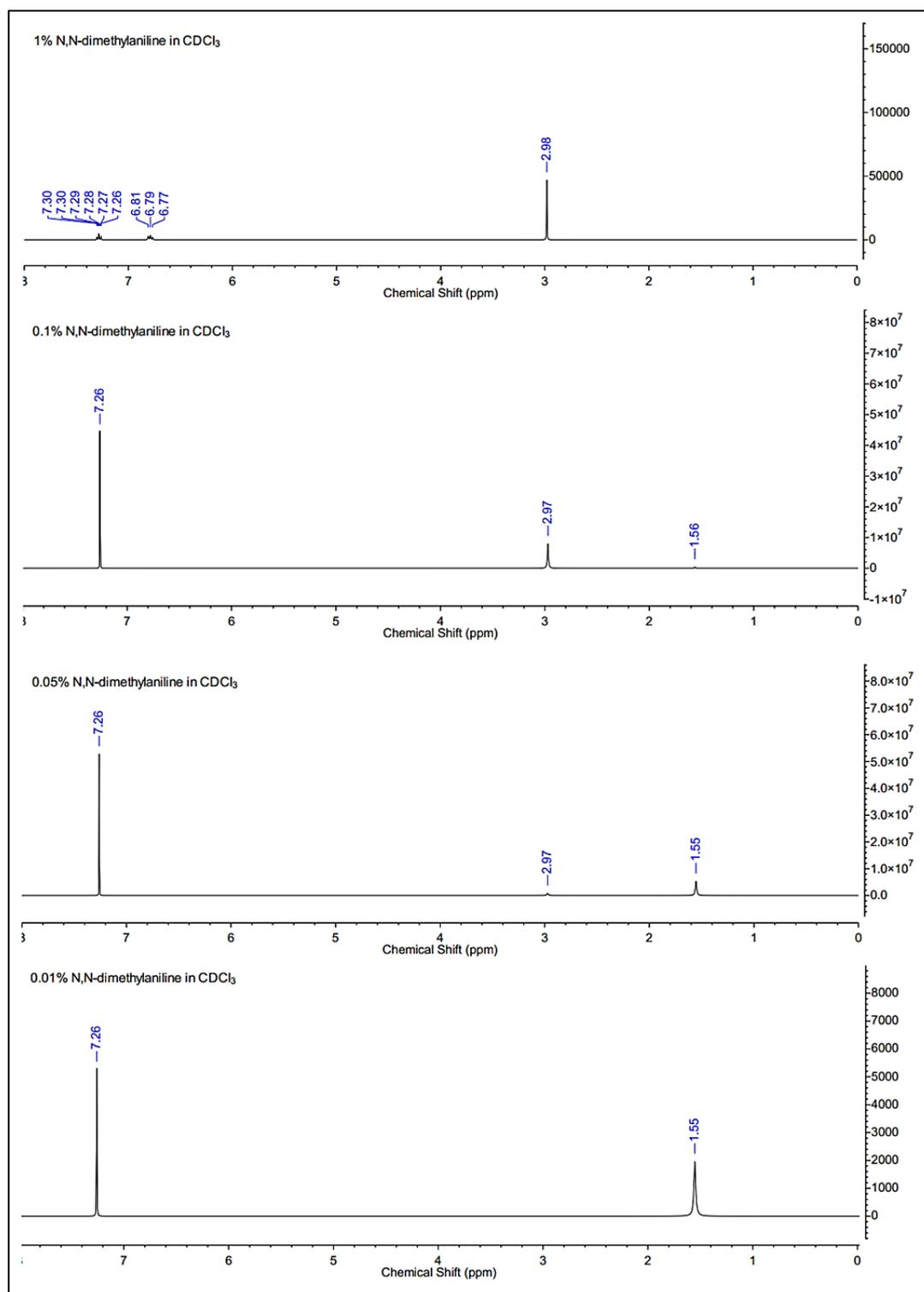
Figure 3.12: *^{1}H-NMR serial dilution spectrums of N,N-dimethylaniline in deuterated chloroform (CDCl$_3$) which is assigned to the peak observed at 7.26 ppm. 1% is effective to detect the DMA signals, with the multiplets owing to the aromatic ring being observed (6.5-7.5 ppm) and the proton signal derived from CH$_3$ (2.98 ppm). 0.1% aromatic regions have disappeared, however, the CH$_3$ signal can still be observed. 0.05% trace-signal for the CH$_3$ is observed. 0.01% no evidence for the presence of DMA is observed. The signal observed in the spectra at 1.55 ppm is assigned to water, due to the hygroscopic nature of CDCl$_3$.*

The second possible explanation is that DMA is not being doped into the material at all. Although the organic doping mechanisms for persistent luminescent materials suggest DMA is being doped into TPP during recrystallisation, this needs to be confirmed using a different analytical technique. High-performance Liquid Chromatography with Mass Spectrometry (HPLC-MS) is a particularly useful technique for detecting and quantifying trace-level compounds in a material. As it is a possibility that ^{1}H-NMR spectroscopy lacks in sensitivity for the detection of trace DMA concentrations, HPLC-MS was used to complement these findings. The HPLC chromatograms for TPP, DMA and TPP:DMA is shown (**Figure 3.13**) followed by the mass spectrums (**Figure 3.14**).
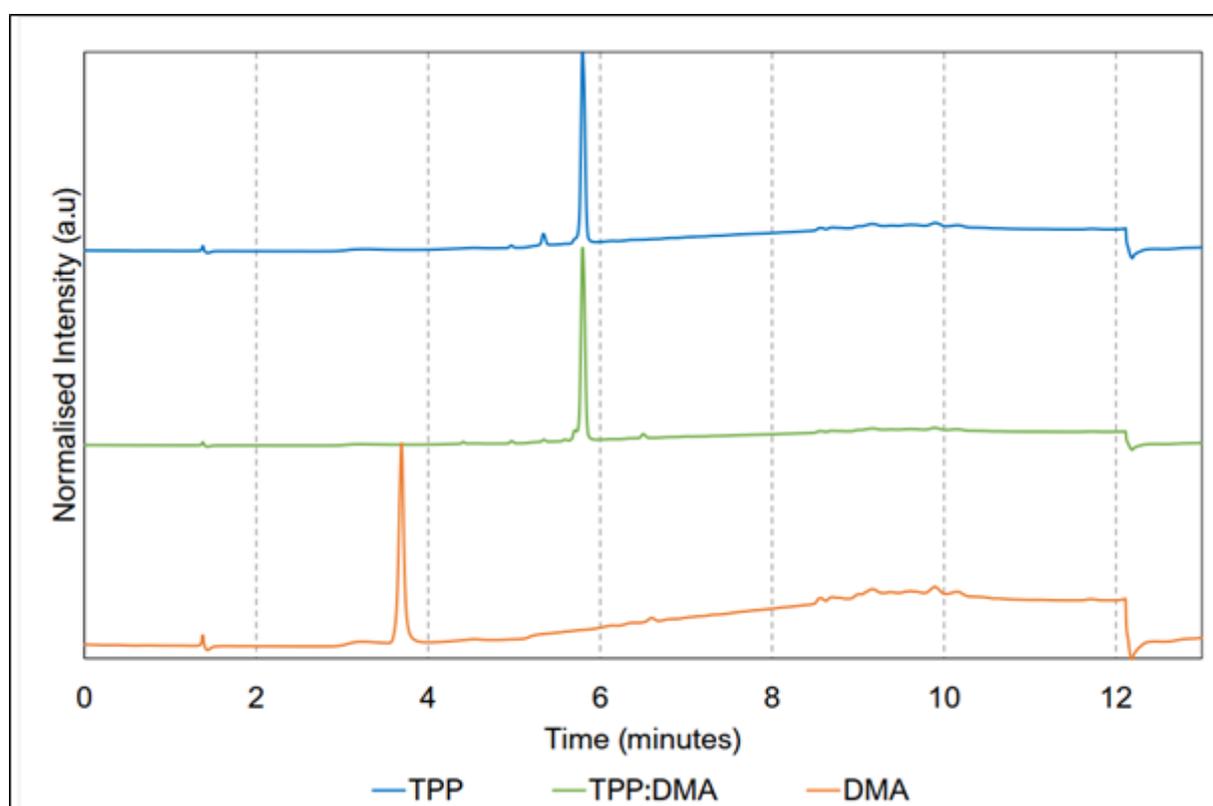
Figure 3.13: *HPLC chromatograms obtained for undoped TPP (a) TPP:DMA (b) and DMA (c).*
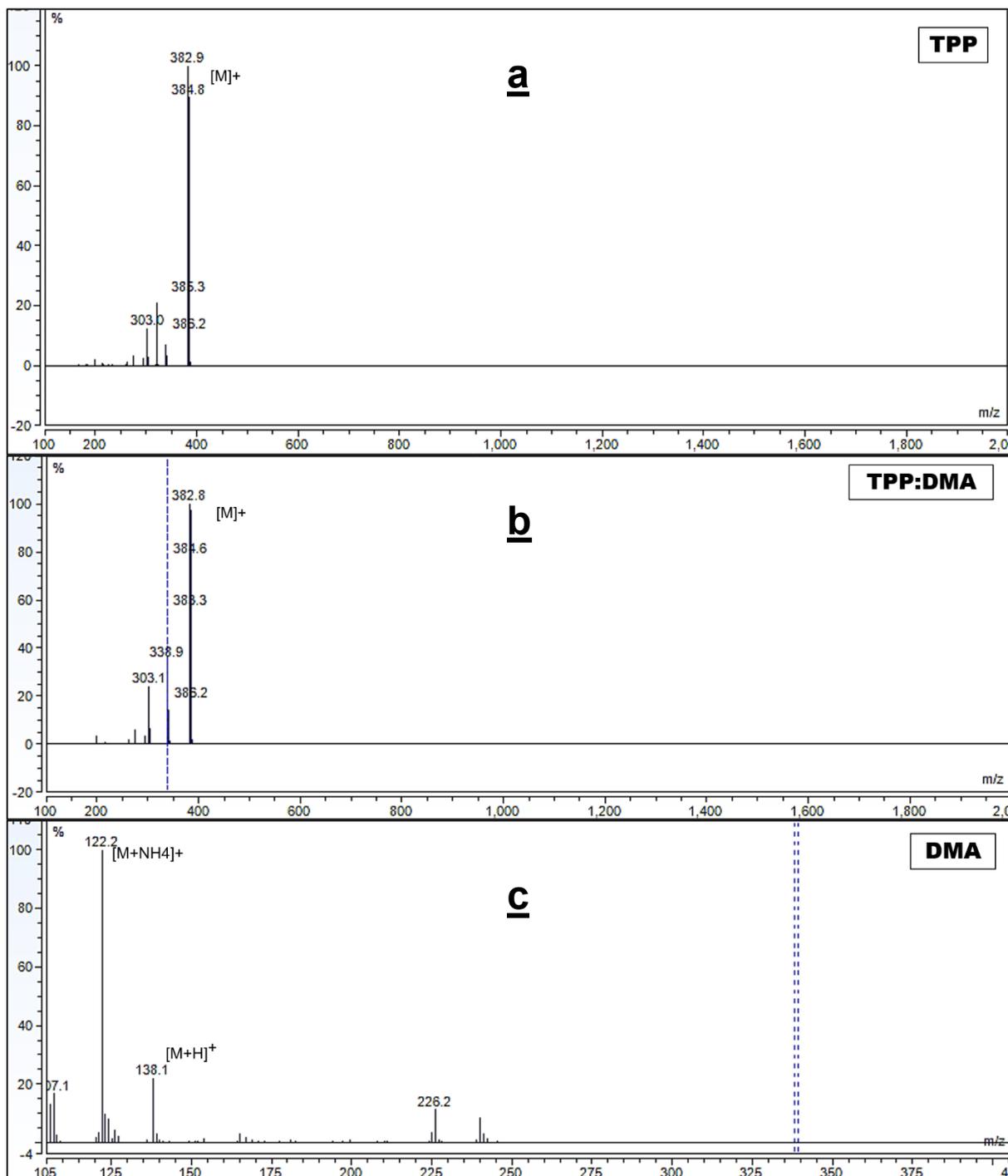
Figure 3.14: *Figure displaying the mass spectrums: (a) Mass spectrum of TPP. (b) Mass spectrum of TPP:DMA. (c) Mass spectrum of DMA.*

The chromatograms display that DMA has a retention time of 3.7 minutes, whereas the TPP derivative has a retention time of 5.8 minutes. If there was any DMA present in the *'doped'* sample, it would also have a retention time of 3.7 minutes. The method used provides an improved resolution compared to the published literature,[48] whilst retaining the same selectivity (2.0 minutes difference in the retention time between the two different materials). In this method, the order of elution is also reversed compared to the literature method and the DMA elutes before the TPP derivative.

The Mass spectra in TPP:DMA are consistent with the expected fragments of TPP and confirm the retention times for that material, however, the low-intensity peak observed at 6.3 minutes (**Figure 3.14 b**) relates to a compound *m/z* of 410 Da; therefore, it does not appear to be related to DMA. The conclusion is that there is no DMA in the doped sample, based upon both the UV-chromatogram and the mass spec data.

The spectrum obtained for the mixed sample shows DMA signals should be observed between 7.38,7.36 ppm and 3.05 ppm, however, these are not observed in this spectrum. This finding is extremely interesting and unexpected given that the LPL behaviour is observed in the *'doped'* sample. Increasing the moles of dopant during the recrystallisation affects the luminescent intensity and duration, however, the presence of dopant cannot be detected in any of the *'doped'* materials.

Research indicates that Hydrochloric Acid (HCl) can quench fluorescence intensity.[66,67] With this in mind, a likely hypothesis is DMA removes residual traces of HCl which would otherwise be trapped within the lattices during crystallisation. Increasing the concentration of DMA, removes larger amounts of residual HCl until a maximum is reached (in this case 1:40), affording TPP:DMA crystals of increased photoluminescent emission intensities and durations.

An additional observation is that extended grinding of TPP:DMA crystals caused the green colour to fade, resulting in a reduction of luminescent intensity. Luminescent properties and SEM-EDX imaging was used to understand the effect of particle size on luminescent intensity. A single batch of doped TPP:DMA was ground to obtain three different sizes: large, medium, and small. (**Figure 3.15**, **Figure 3.16**, **Figure 3.17**).
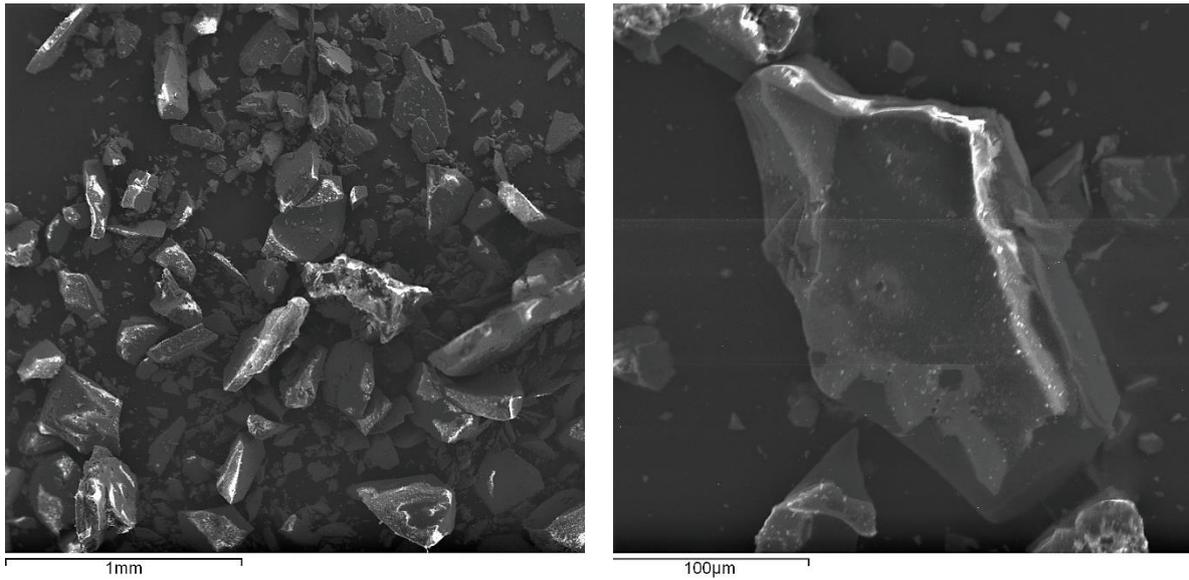
Figure 3.15: SEM images showing TPP:DMA ground to a **large** powder 1 mm (left) and 100 μm (right). The average particle size was measured to be 450 μm.
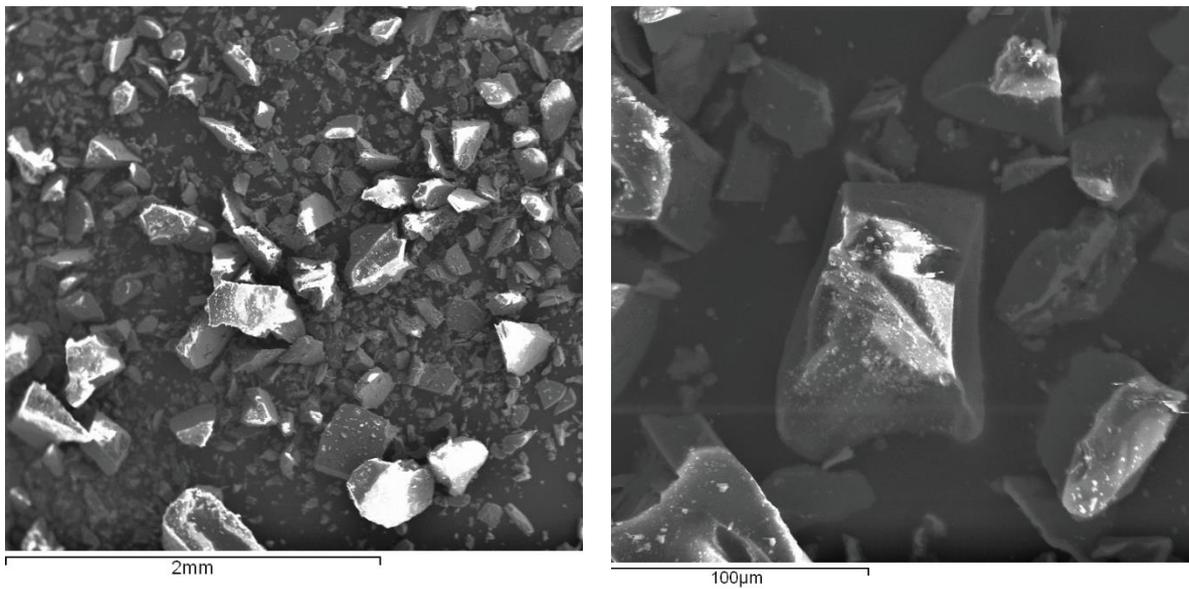
Figure 3.16: SEM images showing TPP:DMA ground to a **medium** powder 2 mm (left) and 100 μm (right). The average particle size was measured to be 204 μm.
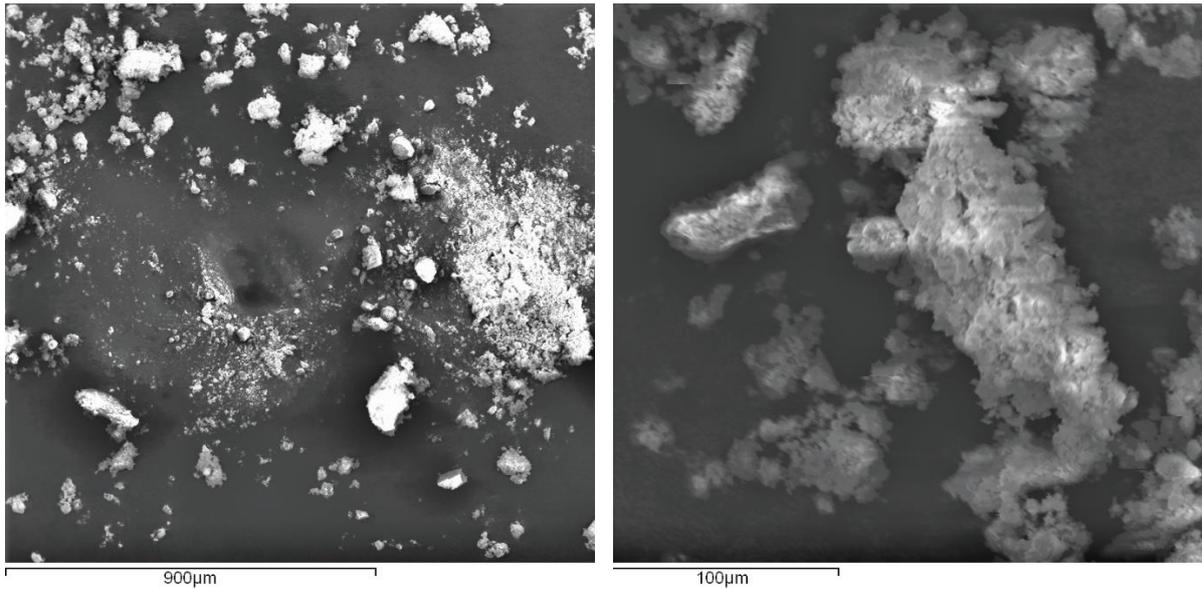
Figure 3.17: *SEM images showing TPP:DMA ground to a **small** powder 900 µm (left) and 100 µm (right). The average particle size was measured to be 94 µm.*

The average particle size for large, medium and small powders were measured to be 450 µm, 205 µm and 94 µm, respectively. Luminescent spectra for each of these samples were obtained (**Figure 3.18**)
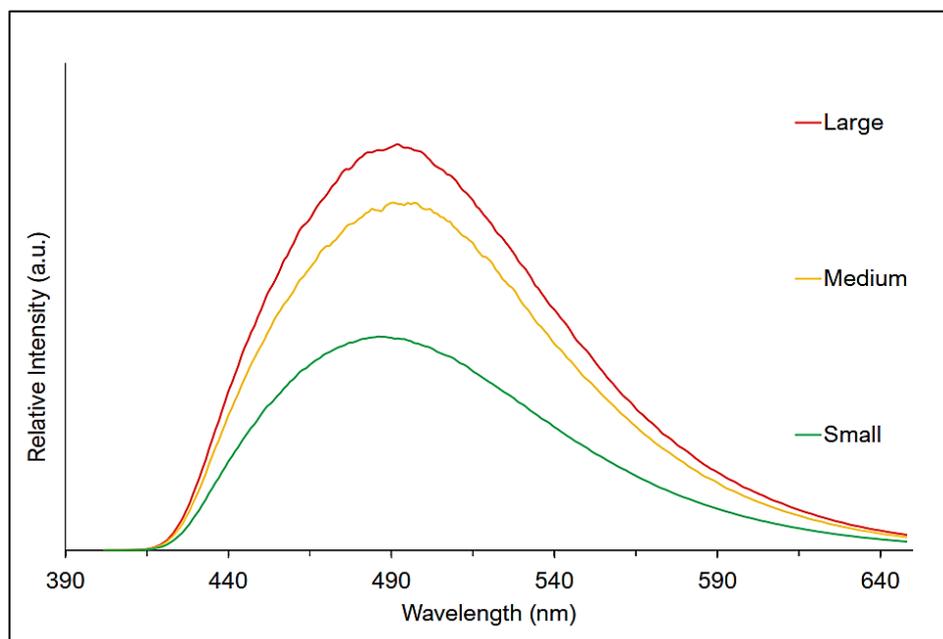
Figure 3.18 *Emission intensities for the same batch of TPP:DMA ground by hand to produce different crystalline sizes: large, medium, and small. The intensity values are normalised and measured as crystalline powders at room temperature. λex = 315 nm*

66

The results display that as TPP:DMA is ground into smaller sizes, the intensity of fluorescent emission decreases. If the *'doping'* theory had been valid, the reasonable assumption is crystalline layers of TPP act as a barrier, in effect, *'trapping'* the dopant and preventing its release. When the crystal is ground to smaller sizes, the crystalline barriers are broken, and the dopant is liberated.

The reduction in intensity suggests a lower electron density in the surrounding host atoms, however, the HPLC-MS and ^{1}H-NMR results contradict this theory as dopant had not been detected. In contrast, the reduction in particle size may increase the surface area exposed to oxygen in the atmosphere, inferring oxygen-induced quenching.

The evidence provided through fluorimetry and SEM-EDX imaging identified a correlation between particle size and fluorescent intensity. The next step was to verify the single-phase nature of the undoped (3-Bromopropyl)triphenylphosphonium bromide material and the optimal doped TPP:DMA material. Additionally, as the size was found to affect fluorescent intensity, two different sizes of TPP:DMA were prepared; fine and coarse (**Figure 3.19**).
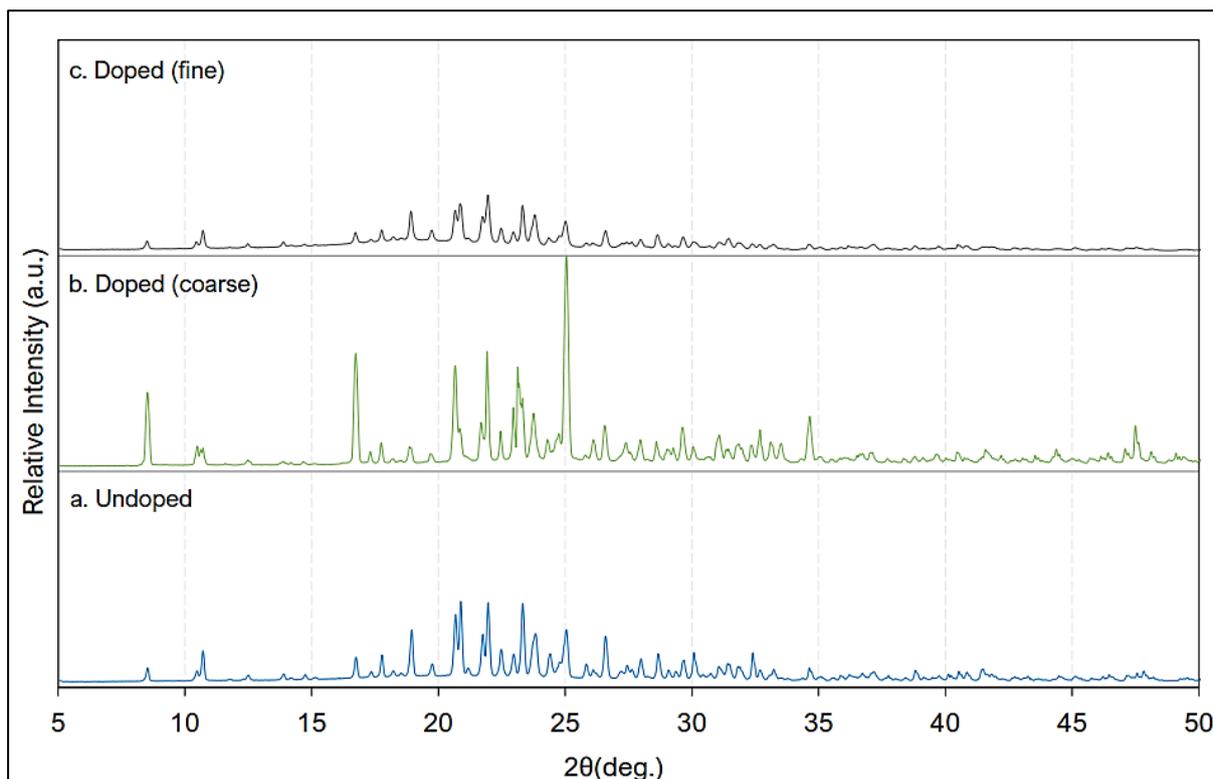
Figure 3.19 *X-ray diffraction patterns of TPP crystalline powders. (a) Undoped TPP. (b) Doped TPP (1:20) crystals ground to a coarse powder. (c) Doped TPP (1:20) crystals ground to a fine powder.*

Whilst at glance, there appear to be differences in the intensities in the XRD patterns, these changes are most likely the result of preferred orientation. Preferred orientation occurs because of alignment in the preferred way of the crystallites within crystals making up the structure. The structure looks anisotropic, meaning that there is a very limited range of possibilities for preferred stacking within the crystals. As the finely ground powder of the doped material remains fairly course, resulting in changes in the diffraction pattern, therefore, the next step is to compare the diffraction patterns of the experimental XRD pattern to the actual predicted pattern (**Figure 3.20**).
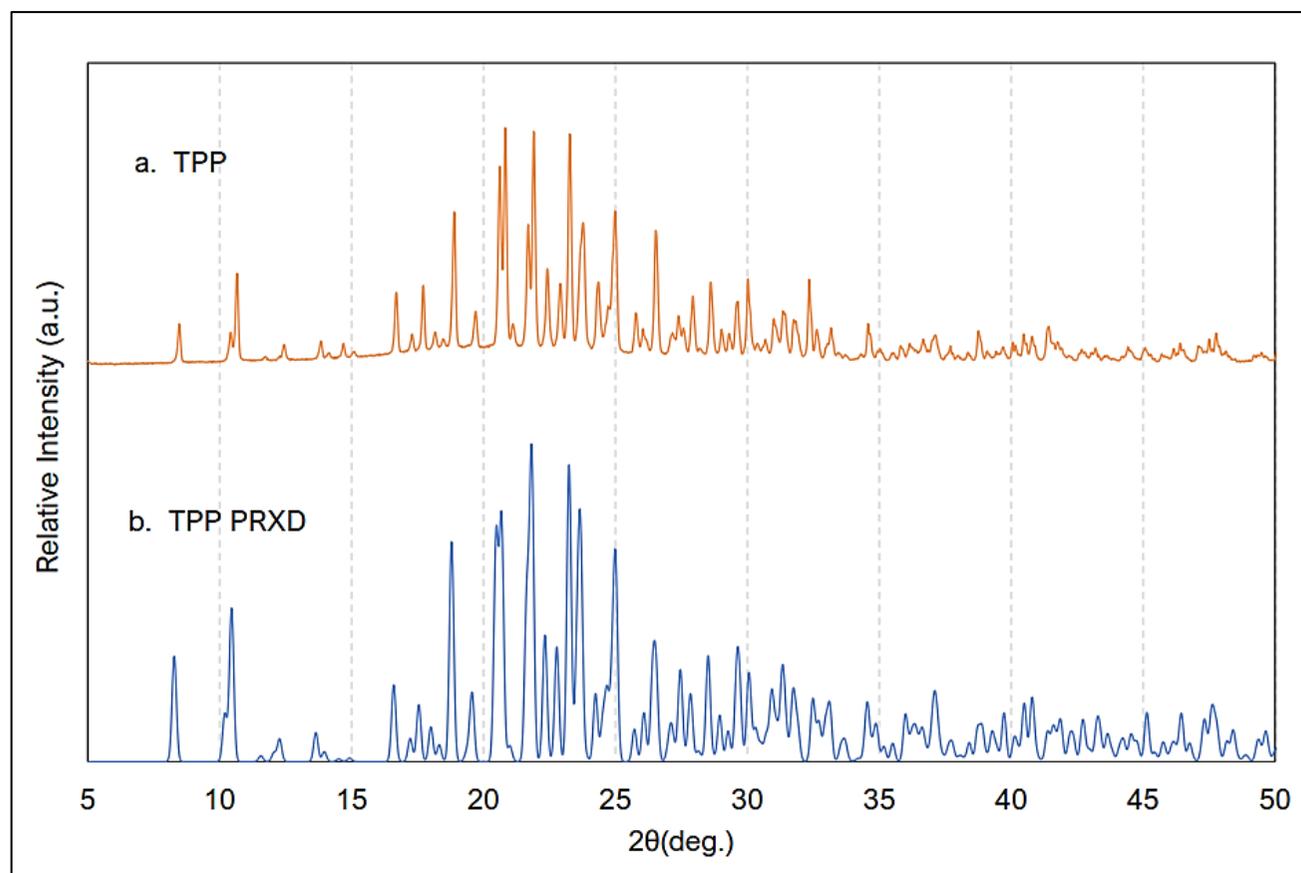
Figure 3.20: *XRD patterns (a) Synthesised TPP. (b) The predicted pattern obtained from TPP crystal data.*

A comparison of the experimental and predicted patterns displays peaks at the same points along the axis. This is a good indication that the experimental XRD patterns and peaks in the undoped material are a single phase, and the intensity differences observed in the doped (coarse) and doped (fine) TPP:DMA XRD patterns are due to preferred orientation. Single-crystal XRD data collected for the doped TPP:DMA sample at 120 K and 320 K both confirmed the structure to be identical to the undoped sample with no evidence for DMA consistent with the ^{1}H-NMR and HPLC-MS results discussed above. Furthermore, these results confirm the suggestion that changes seen in the powder XRD data arise because of the preferred orientation of the crystallites.

3.1.4 Visible Persistent Luminescence

The doped TPP:DMA materials being used in this study have been reported in a recent publication.[48] The UV excitation results taken from this study suggest that TTP:DMA exhibits a persistent luminescence which is maintained for hours after irradiation; however, these emissions are near-impossible to observe in our materials due to the emission intensity being too low. In this prior work, the material was placed into a

light-proof container and a digital camera was manually set to a long exposure (30-seconds) and large aperture to capture the emissions, which potentially, limits the use in a forensic context.

The author of this research has identified unreported persistent luminescent properties in the TPP:DMA material. The optimised TPP:DMA material obtained in the optimisation section (3.1.3) was recrystallised using layered diffusion method discussed (Chapter 2.1.3). This material labelled; TPP:DMA:R, when exposed to a low-powered handheld UV torch, emitted a visible intense green persistent luminescence, this was observed under natural laboratory conditions. This material (TPP:DMA:R) has different photoluminescent properties to TPP:DMA. As previously mentioned, the persistent luminescence of TPP:DMA can only be observed using a digital camera and altered f-stop/shutter settings, however, the persistent luminescent properties of TPP:DMA:R can be directly observed, even in bright conditions (**Figure 3.21**, Appendix D).

Figure 3.21: *Visible PL of TT:DMA:R. Images were taken from the video (Appendix D) of TPP:DMA:R that has been irradiated for 5 seconds using a handheld UV torch. The source of excitation is removed, and the green persistent luminescent emissions are observed for more than 2 s. The images were recorded using the camera app on an iPhone 7.*

The initial drive to recrystallise the optimised TPP:DMA material had been to completely remove the effects caused by DMA from the crystal. However, the initial blue phosphorescent TPP material was not formed during this process. Instead, a persistent luminescence of high intensity and fast decay had formed. The role of DMA in this system is not yet understood; if the organic doping theory was correct, TPP:DMA:R could have been doped with unremoved trace amounts of DMA, present in the recrystallising system. However, as the doping theory cannot be confirmed, further investigation is required to understand how photoluminescent behaviour differs between TPP:DMA and TPP:DMA:R. The fluorometer was used to record the luminescent intensity and decay time for both materials. These measurements are plotted and compared (**Figure 3.22**).
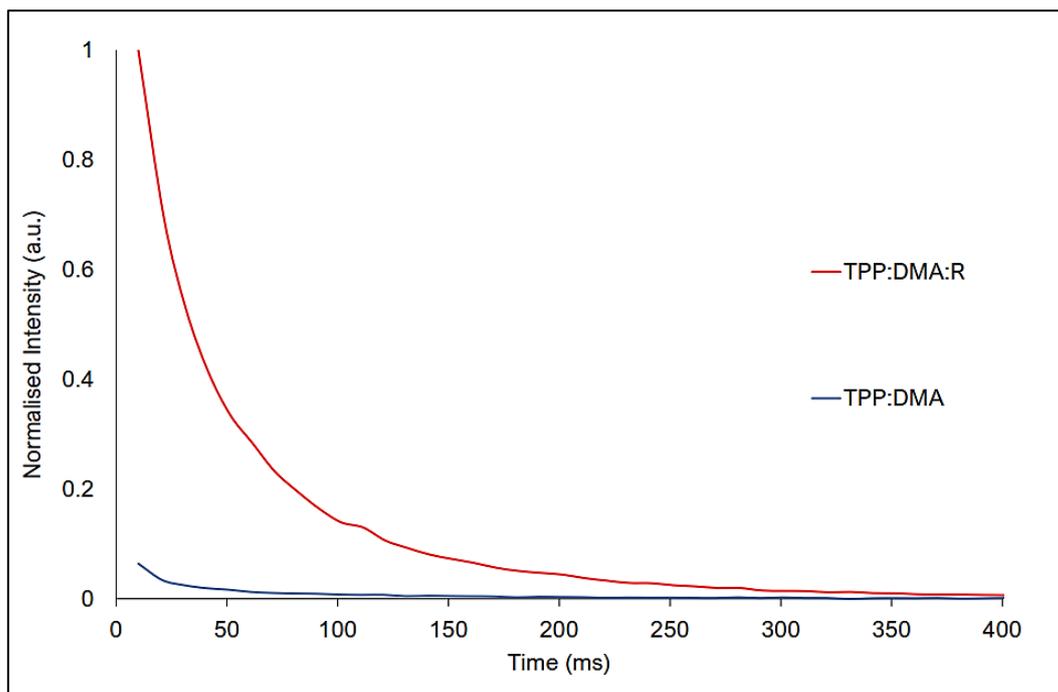
Figure 3.22: *The emission decay profiles of TPP:DMA (1:20) and TPP:DMA:R. The intensity values are normalised and measured as crystalline powders at room temperature. λ = 315 nm.*

3.2 2,4,6-tri(4-pyridyl)-1,3,5-triazine

3.2.1 Doping

2,4,6-tri(4-pyridyl)-1,3,5-triazine (4-TPT) was the next material to be investigated in this research. 4-TPT behaves as an electron acceptor ligand due to the presence of a triazine ring. The formation of nanosized cages and porous frameworks enclosing cavities during the synthesis provides an opportunity to encapsulate electron-rich guests which then promote donor-acceptor interactions with the electron-deficient 4-TPT material.

To investigate the effects of dopant concentration on the photoluminescent properties of 4-TPT, a series of identical experiments were conducted wherein the concentration of an introduced dopant was varied. A particular emphasis was placed on the method for obtaining a doping ratio. This is because the yield of the synthesis must be '*presumed*', as the exact molar ratio upon the addition of the dopant is unknown. Here, it is assumed that a 1 g reaction of 4-cyanopyridine would synthesise 1 g of 4-TPT (100% yield) giving that the reaction has 100% atom economy. Dopant was introduced to the reaction and the mole ratio was theorised against a 100% formation of 4-TPT.

The moles of 4-cyanopyridine to DMA investigated in this research were, 2:1, 4:1, 10:1, 15:1 and 20:1. A 1:1 molar ratio had also been investigated; however, the synthesised material did not exhibit a persistent luminescence or an intense emission.

The synthesised products were briefly exposed to a handheld UV LED (UltraFire 501B 365nm), to visually assess whether the doped synthesis had produced a material that exhibited persistent luminescent properties. Upon exposure to UV radiation (365 nm), all of the materials exhibited a blue emission which is darker and bolder when compared to the emissions of undoped 4-TPT; additionally, upon removal of the UV source, an intense white/yellow persistent luminescent/phosphorescent emission was displayed. This was observed for a few seconds, with some of the doped materials displaying brighter and longer emissions than others (**Figure 3.23** and Appendix E).
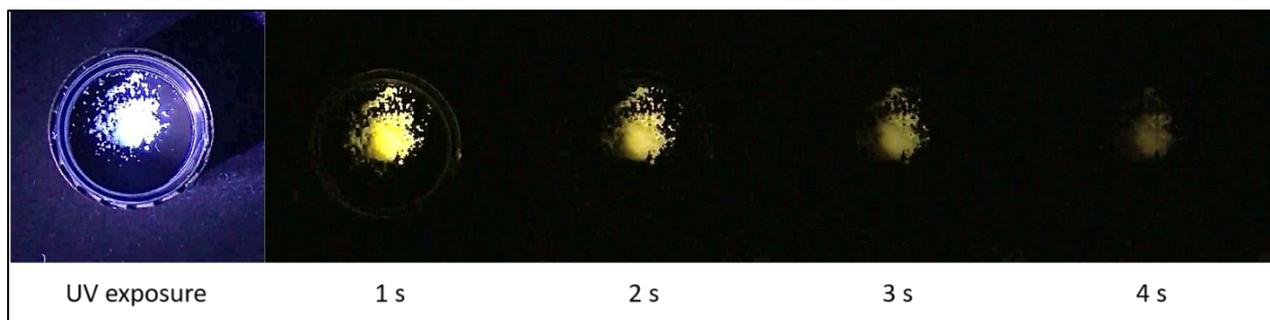
Figure 3.23: *Visible PL of 4-TPT:DMA. Images were taken from the video (Appendix E) of 4-TPT:DMA that has been irradiated for 5 seconds using a handheld UV torch. The source of excitation is removed, and the yellow persistent luminescent emissions are observed for more than 4 s. The images were recorded using the camera app on an iPhone 7.*

To identify the optimal mole ratio of dopant to include in the synthesis, solid-state luminescence data were obtained for each of the synthesised materials (**Figure 3.24**).
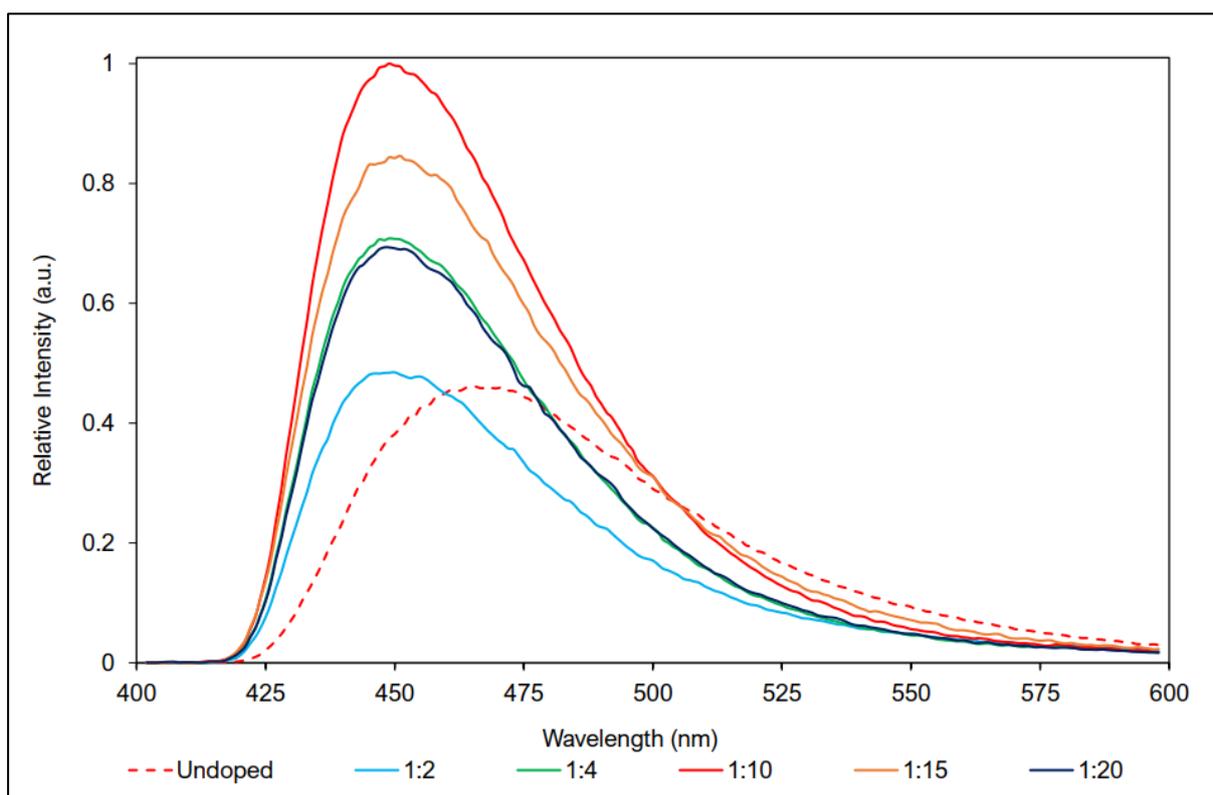
Figure 3.24: *Emission spectra of 4-TPT and 4-TPT:DMA at different doping values. The intensity values are normalised and measured as crystalline powders at room temperature. λex = 390 nm*

These results identified the optimal doping ratio to use in the synthesis to be 1:10. Unlike TPP:DMA, where the doping had reached a maximum, introducing concentrations of DMA greater than 1:10 decreased the luminescence intensity. This may be attributed to a change in the optimal conditions for the product to synthesise.

When using an excitation wavelength of 390 nm, 4-TPT emits a blue luminescence with a broad emission and maximum peak centred at 465 nm. The 4-TPT:DMA crystalline powder emits a blue luminescence of increased intensity that is slightly narrower than the broad emission peak of 4-TPT. Visibly, the colour of emission in 4-TPT:DMA is darker and bolder than 4-TPT. This can be attributed to the blue-shift of 15 nm, ascribed to the exciplex emission, arising from the exciplex formation between 4-TPT and DMA in 4-TPT:DMA.

Following these results, the same materials lifetime properties were investigated, to establish the effect of dopant concentration on the persistent luminescence. These lifetime measurements were recorded using the fluorimeter (**Figure 3.25**).
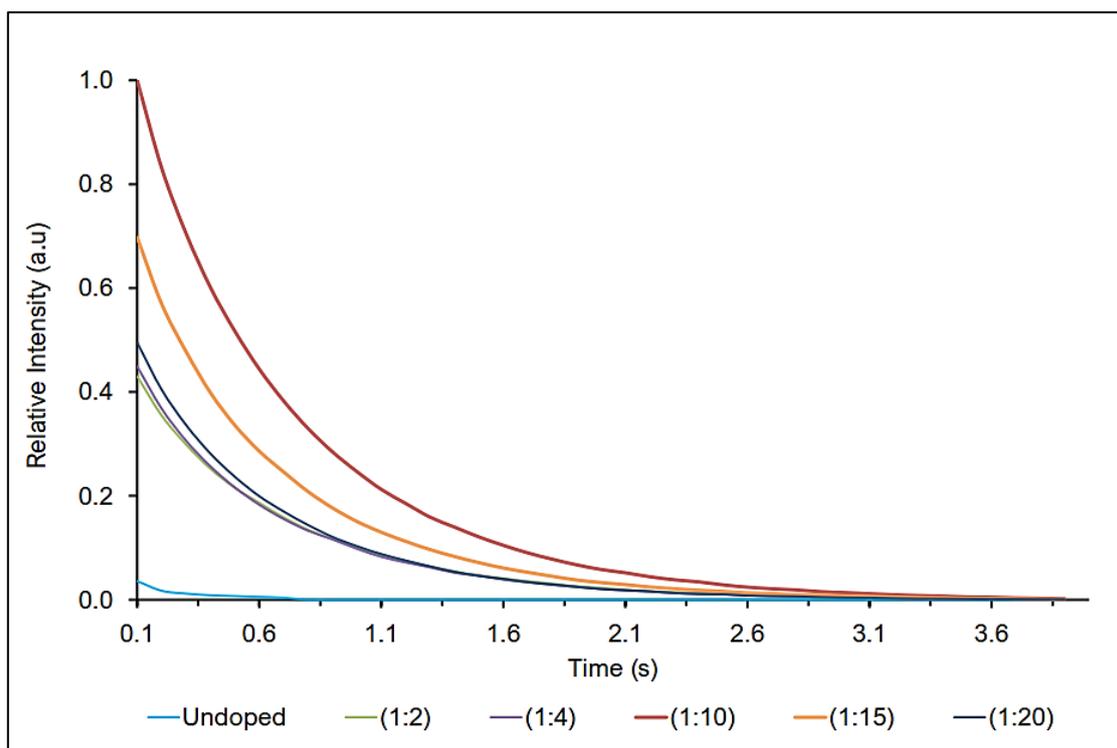
Figure 3.25: *Measurements of the luminescent decay for 4-TPT and 4-TPT:DMA at different doping concentrations. The intensity values are normalised and measured as crystalline powders at room temperature. λex = 365 nm.*

Although undoped 4-TPT exhibited intense fluorescent emission, similar to doped samples (1:4 and 1:20) upon irradiation, it appeared to have no white/yellow persistent luminescence, suggesting that the undoped sample decays rapidly (almost instantaneously) upon removal of the excitation source. To analyse and quantify the decay times, lifetime measurements for the undoped and various doped samples were recorded using the fluorometer.

To obtain the lifetime measurements, a sample was introduced to the solid-state holder and momentarily exposed to a known quantity of radiation (λex = 365 nm). The luminescent emissions emitted by the material were then recorded for the desired length of time (here 4 s). To record the lifetime after exposure to UV, an interval of 0.1 s bridged the gap between the material being irradiated, and the start of the measurement.

Within this pre-recording delay, the emission intensity of the undoped material, which exhibited a fluorescent intensity like 1:4 and 1:20 materials, had almost completely decayed. The luminescent data shown above demonstrates this material's great promise for improved emission intensities and lifetimes on doping especially when compared to more costly inorganic materials.

Following the identification of the optimised material, the next steps were to obtain excitation and emission spectra for 4-TPT and 4-TPT:DMA. Due to its persistent luminescent emission, phosphorescent data was also included for 4-TPT:DMA (**Figure 3.26**).
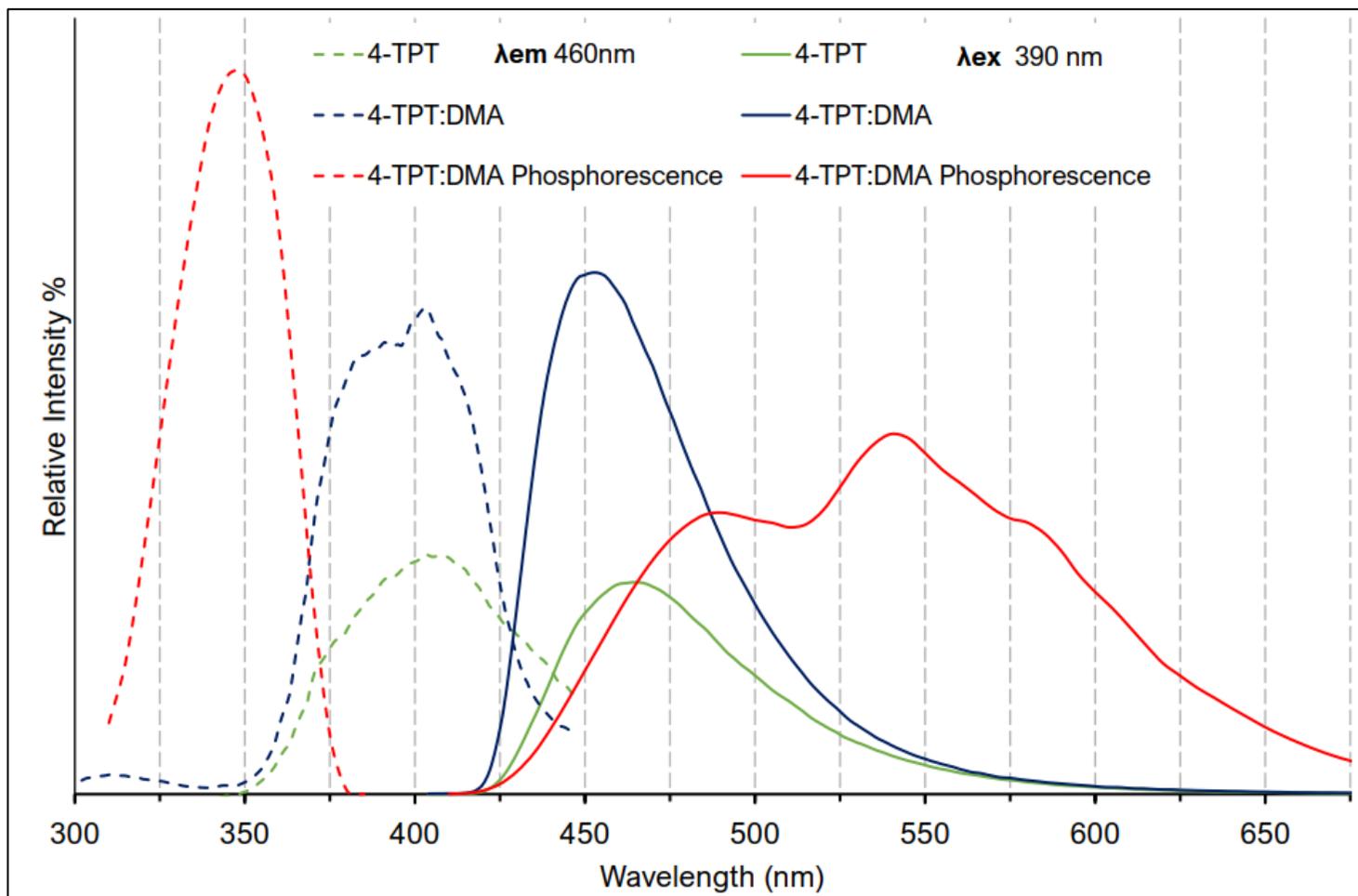
Figure 3.26: *Solid-state excited and emission spectra of 4-TPT and 4-TPT:DMA. The wavelength of **emission** was set at 460 nm and the solid-state sample was exposed to different wavelengths of excitation to identify the excitation wavelengths. These are represented as coloured dashes in the figure above. The wavelength of **excitation** was set at 390 nm and emission data was recorded over the range of 400-700 nm. These are represented as solid lines in the figure above. The intensity values are normalised and measured as crystalline powders at room temperature. λem = 460 nm. λex = 390 nm. Phosphorescent fluorometer parameters are shown in Appendix F.*

The broad phosphorescent emission results correlate to the visible yellow phosphorescence, observed in the material after the removal of UV radiation. The most intense peaks attributed to 4-TPT:DMA demonstrate why the doped material emits a luminescence of greater intensity.

To understand the particle shape and size of 4-TPT:DMA, the physical properties were investigated using SEM-EDX imaging (**Figure 3.27**). These images of 4-TPT:DMA display a variety of shape and sizes. Compared to TPP:DMA, 4-TPT:DMA appears to be uneven and irregular. This is most likely due to the material being taken directly from the synthesis, without performing recrystallisation. The average particle size of this material was identified to be 145 µm.
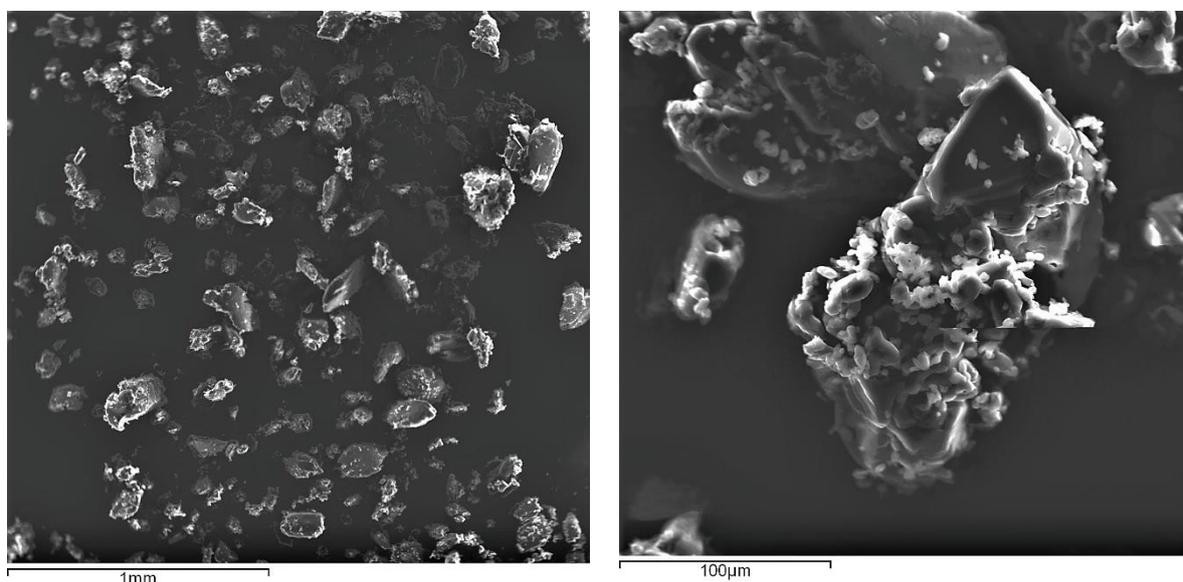
Figure 3.27: SEM-EDX image of 4-TPT:DMA (left) and magnified (right). These images are of the 4-TPT:DMA product recovered from the synthesis; therefore, no grinding had occurred. The average particle size was found to be 145 µm.

Moreover, shifting the focus towards doping, it could be assumed/explained that the fluorimetry results correlate to the concentration of dopant within the material. The more dopant encased within the material, the greater the emission intensity, until a maximum is reached. To confirm the presence of dopant and quantify the concentration, ^{1}H-NMR spectra were obtained.

Introducing DMA to the synthesis of 4-TPT has shown to affect the photoluminescent properties of the synthesised material. To determine whether this is due to the *'doping'* mechanisms, ^{1}H NMR spectra were recorded for 4-TPT and 4-TPT:DMA, to examine if DMA signals could be observed.

Figure 3.28 displays the ^{1}H-NMR spectra of 2,4,6-tri(4-pyridyl)-1,3,5-triazine, which is consistent with the expected spectrum of the structure, as evidenced by the reference spectrum (Appendix G). There are only two CH proton environments in the 4-TPT compound. The doublet at 8.96 ppm is attributed to six protons in total, in the 3,5 position of the 4-pyridyl derivative. The double doublet at 8.59 ppm is attributed to six protons in total, in the 2,6 positions of the 4-pyridyl derivative.

Figure 3.29 ^{1}H-NMR spectra of doped 2,4,6-tri(4-pyridyl)-1,3,5-triazine: with N,N-dimethylaniline. This spectrum displays evidence of 2,4,6-tri(4-pyridyl)-1,3,5-triazine, however, there is no evidence of DMA in the spectrum. The spectrum of N,N-dimethylaniline (Appendix C) indicates that we would expect to observe signals between 7.38,7.36 ppm and 3.05 ppm, however, these are not present in this spectrum.

Figure 3.30 ^{1}H-NMR spectra of doped 2,4,6-tri(4-pyridyl)-1,3,5-triazine: with N,N-dimethylaniline. The regions where the dopant (DMA) signals should be observed have been expanded. No peaks can be detected, either due to the dopant not being present or the traces being so minimal that it's below the threshold of detection.
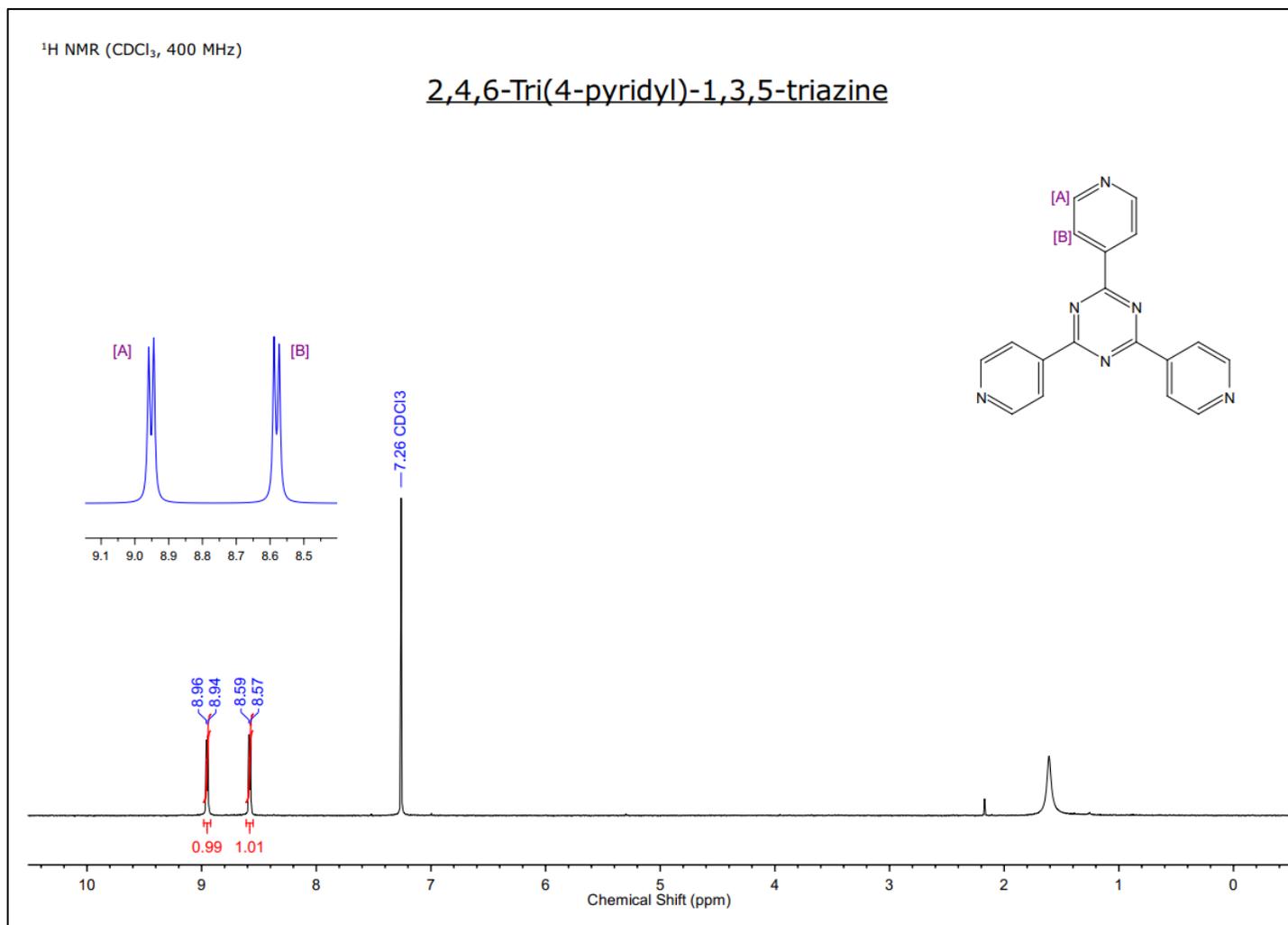
Figure 3.28: *¹H-NMR spectra of 2,4,6-tri(4-pyridyl)-1,3,5-triazine in CDCl₃. Characteristic aromatic resonances are shown in the inset (ranging from 8.5–9.0 ppm).*
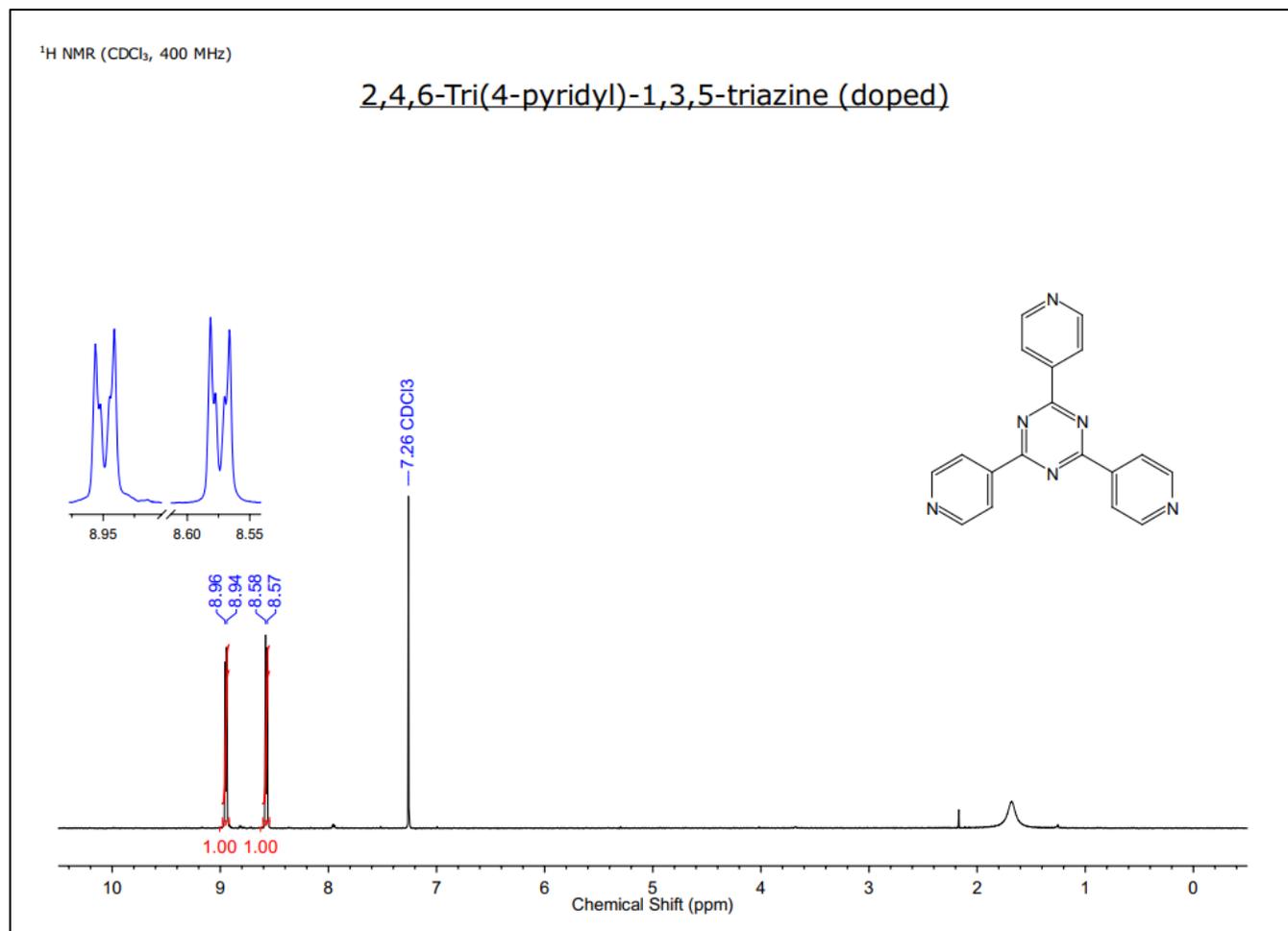
Figure 3.29: *^{1}H-NMR spectra of 2,4,6-tri(4-pyridyl)-1,3,5-triazine in CDCl$_3$. Characteristic aromatic resonances are shown in the inset (ranging from 8.5–9.0 ppm). Similar to TPP:DMA, DMA could not be detected in the ^{1}H-NMR spectra of the doped 4-TPT material. No signals are visible either due to the dopant not being present or the traces are below the threshold for detection.*
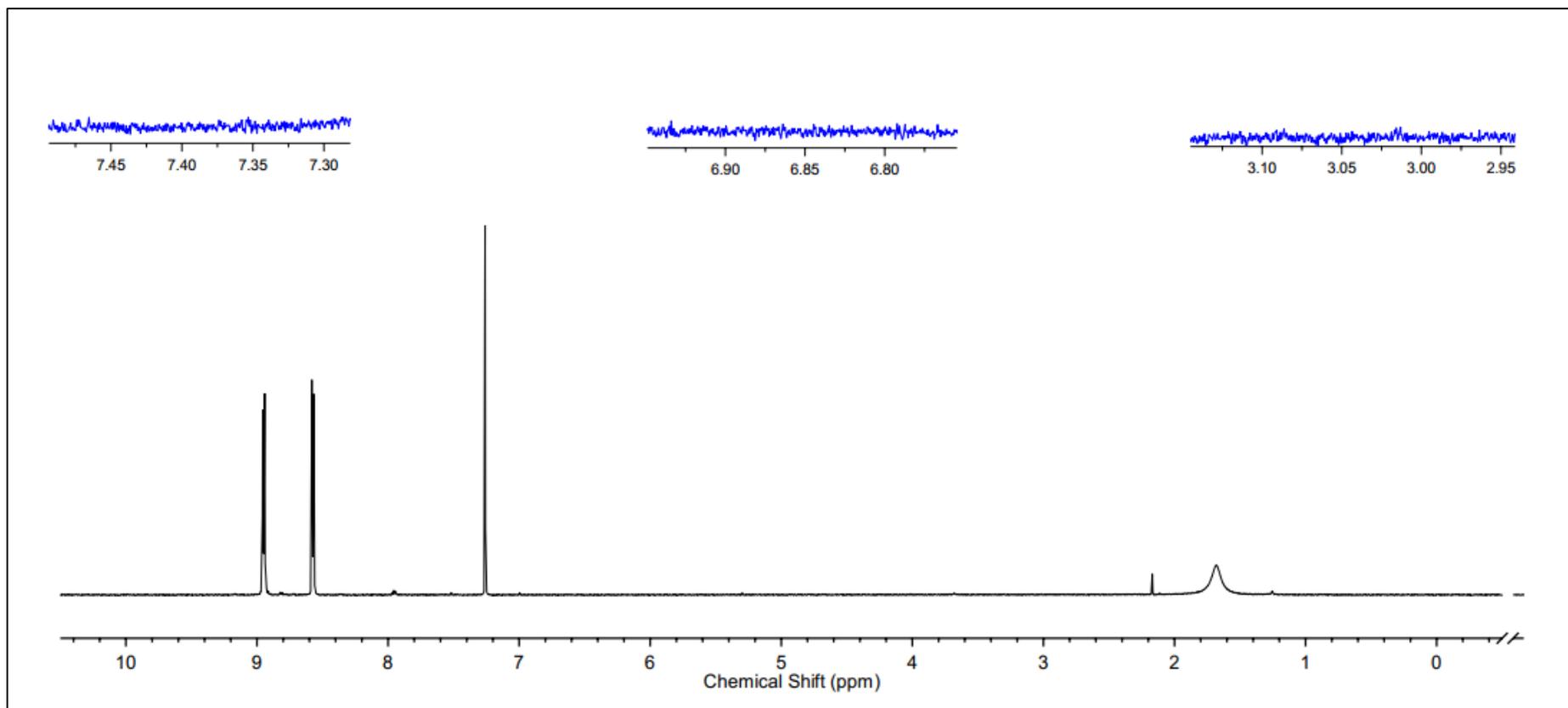
Figure 3.30: *Expanded regions where the dopant (DMA) signals should be observed in the ^{1}H-NMR spectrum of 2,4,6-tri(4-pyridyl)-1,3,5-triazine that has been doped with DMA. No signals are visible either due to the dopant not being present or due to the traces being so minimal that it cannot be detected.*

Similar to the ^{1}H-NMR result of TPP:DMA, the 4-TPT:DMA spectra did not display any presence of DMA in the initially believed *'doped'* material. Once again, it was hypothesised that this may be due to ^{1}H-NMR spectroscopy being a technique which lacks sensitivity to detect these trace signals of DMA. At this moment in time, it is unclear whether the mechanisms of *'doping'* are correct, and further investigations with using other analytical techniques are required to conclusively state if DMA is truly absent 4-TPT:DMA material.

As fluorimetry and SEM-EDX imaging identified a correlation between particle size and fluorescent intensity, the next step was to verify the single-phase nature of the undoped 4-TPT and doped 4-TPT:DMA materials. Additionally, as the size was found to affect fluorescent intensity, two different sizes of 4-TPT:DMA; a fine powder and coarse crystalline, were prepared and analysed using XRD (**Figure 3.31**), additionally, the diffraction patterns of the experimental XRD pattern were compared to the actual predicted pattern (**Figure 3.32**).
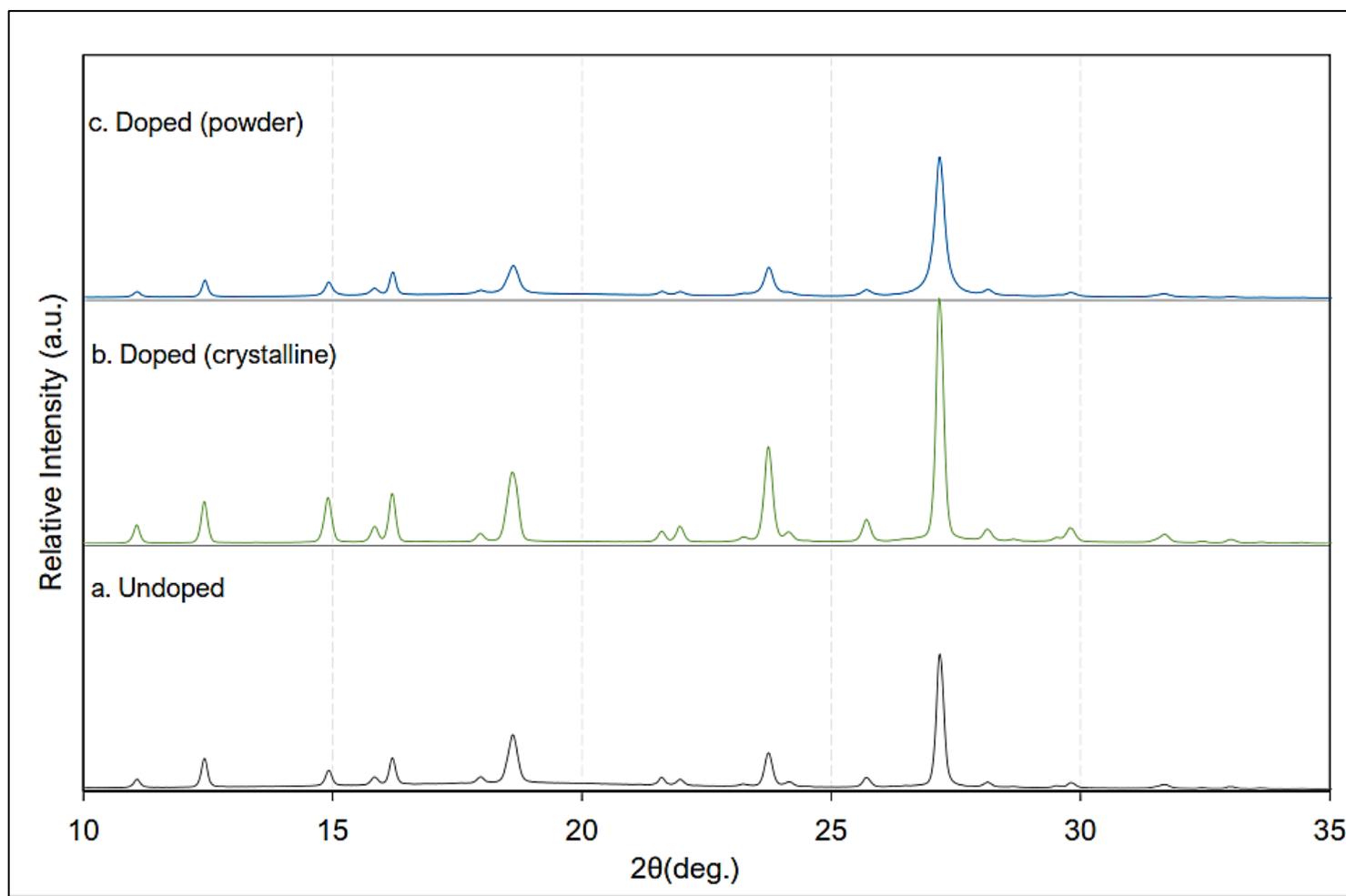
Figure 3.31: *X-ray diffraction patterns of 4-TPT crystalline powders. (a) Undoped. (b) Doped 4-TPT:DMA (1:10) crystals ground to a coarse powder. (c) Doped 4-TPT:DMA (1:10) crystals ground to a fine powder.*
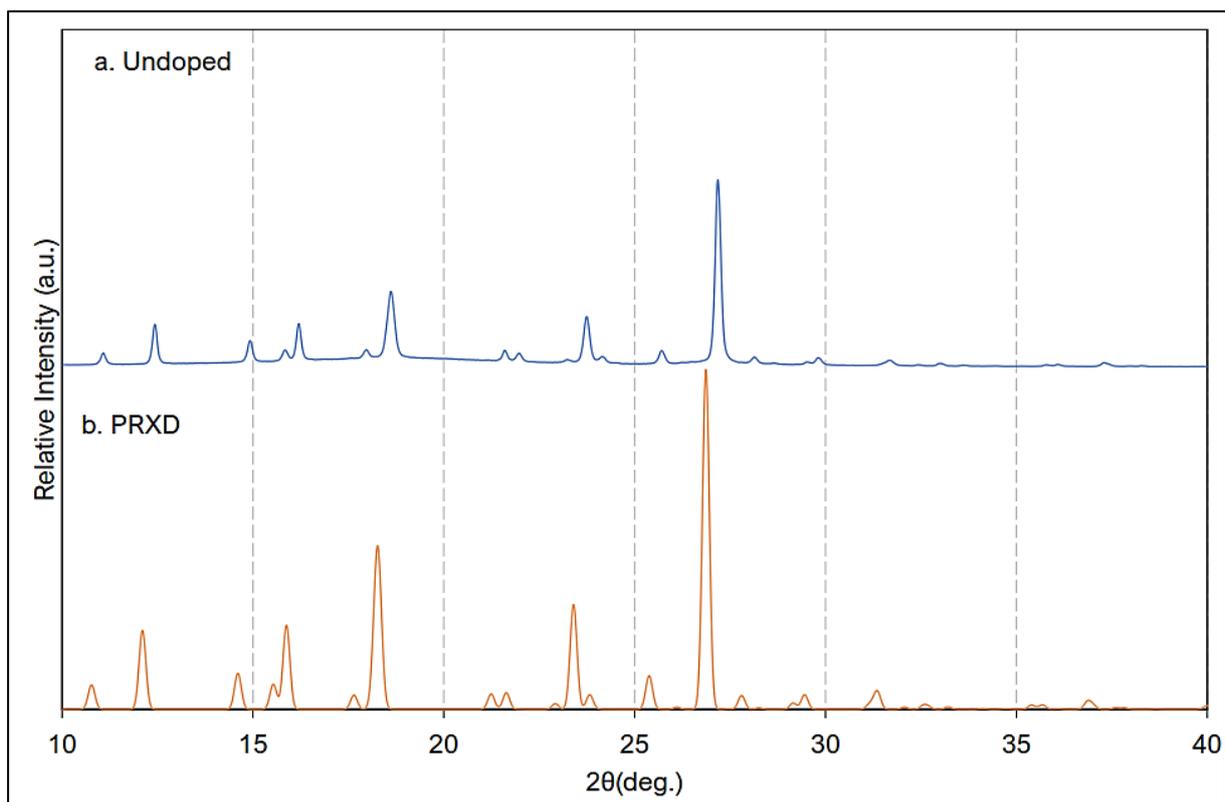
Figure 3.32: *XRD patterns for experimental undoped 4-TPT (a) and the predicted PXRD pattern obtained from the crystal data (b).*

Similarly, to TPP:DMA, comparing the peaks of 4-TPT:DMA (crystalline and powder) shows a reduction in the intensity of the finer powdered material. Single-crystal XRD data was obtained from the Cambridge Crystallographic Data Centre depository.[68] Spectral interpretation confirmed the structure to be identical to the experimental 4-TPT pattern. A comparison of the experimental and predicted patterns shows peaks at the same points along the axis. This is a good indication that the experimental XRD patterns and peaks in the undoped material are a single phase, and the intensity differences observed in the 4-TPT:DMA crystalline and powder are due to preferred orientation.

As mentioned previously, the preliminary work performed on 4-TPT:DMA yielded some promising results, however, it is unclear whether the hypothesised mechanisms of *'doping'* are correct, and further investigations with other analytical techniques are required to identify and understand the role of *'doping'* in this material.

85

3.3 Conclusion

In this chapter, methods to optimise the photoluminescent properties of materials TPP:DMA and 4-TPT:DMA were explored. The effect of dopant concentration and optimised dopant incorporation method(s) were investigated to afford an optimised material with excellent photoluminescent properties. The photoluminescent absorption and emission properties were recorded on the fluorometer.

Introducing DMA in the molar ratio of 1:20 – 1:40 (TPP:DMA) to the layered diffusion, afforded emission properties of similar intensities, suggesting that a maximum '*doping*' factor had been achieved. ^{1}H-NMR spectroscopy results discovered that the actual concentration of dopant was much lower than previously thought, as DMA was not detected.

Despite being a more sensitive technique than ^{1}H-NMR, LCMS also yielded no signal for DMA, despite being reported that *"a key factor of the OLPL duration is the amount of DMA trapped inside the TPP crystals"*.[48] The conclusions drawn from these results suggest that DMA is not *'trapped'* within crystals, thus, it is suggested that the reported reasons for organic persistent luminescence in TPP:DMA must be incorrect.

Moreover, a possible explanation for the changes in the physical appearance and photoluminescent properties of TPP:DMA, is that DMA may remove trace amounts of hydrochloric acid (HCl) from the crystallising system resulting in emission quenching.

Increasing the concentration of DMA to the layered diffusion re-crystallisations, removed greater amounts of residual HCl and formed crystals with higher luminescent intensities until a maximum was achieved. The fluorometer showed little difference in intensities for TPP:DMA crystals doped between ratios of 1:20 – 1:40, suggesting the residual HCl was sufficiently removed when a doping ratio of 1:20 or greater was introduced to the system.

TPP:DMA crystals were dissolved and re-crystallised via layered diffusion, in an attempt to obtain pure TPP crystals. This produced crystals with unreported luminescent properties, that exhibited an intense luminescent emission that could be observed for a few seconds.

A less detailed investigation had been performed on the 4-TPT:DMA material, as it had not been researched until nearer the end of this research. It is believed that the work reported here is the first to demonstrate the yellow phosphorescent emissions, observed in 4-TPT:DMA, using purely organic materials. Similarly, ^{1}H-NMR spectroscopy had been investigated for the undoped and doped material, to quantify the proton ratio between 4-TPT and DMA, however, this instrument was not sensitive enough to detect DMA. As such, the presence of DMA within the doped material is yet to be confirmed. It can only be inferred that the persistent luminescence is achieved through doping, however, given the findings above, this requires further investigations as the dopant may be reacting in the synthesis and not doping into the material at all. To achieve the optimised yellow phosphorescent material, the volume of DMA to include in the synthesis was identified as, for 10 moles of 4-cyanopyridine, 1 mole of N,N-dimethylaniline was introduced.

The optimised methods were employed to produce a large quantity for both materials, which were prepared as a powder and applied to fingermarks, following the guidelines published by the International Fingerprint Research Group and discussed in Chapter 4 of this thesis.[63]

CHAPTER 4.   EVALUATION OF ORGANIC PHOTOLUMINESCENT MATERIALS FOR THE DEVELOPMENT OF LATENT FINGERMARKS

The first material prepared as a powder is optimised TPP:DMA and the second material prepared as a powder is optimised 4-TPT:DMA. The objective of this study was to assess the suitability of these materials as latent fingermark developers. All work in this chapter was performed under Ethics approval from the University of Kent (Ref:0601920).

4.1   Study Guidelines for the Assessment of Fingermark Detection Techniques

Pilot investigations were performed according to the *Guidelines for the Assessment of Fingermark Detection Techniques,* published by the *International Fingerprint Research Group* (IFRG).[63] This document highlights best practices to undertake studies investigating the effectiveness of new materials to visualise latent fingermarks. Most of these factors emphasise the variability of fingermark composition, which includes the donor, substrate, environment, time, and method of application. Each of these factors has been considered individually and the rationale underpinning of the methodology used in this research is detailed and discussed in this chapter.

Phase 1 (Pilot Studies) involves initial pilot or proof-of-concept investigations of novel fingermark detection methods (reagents or techniques) or major modifications to existing methods. Phase 2 (Optimisation & Comparison) is a more detailed investigation and evaluation of a method. Phase 3 studies further validate the results of phase 1 & 2 studies with phase 4 implementing the material(s) into operational casework.

For a phase 1 study, initial proof of concept investigations focuses on the interaction of the powder particles to the different types of residues found in latent fingermarks (sebaceous/oils, eccrine/amino acids). This is to establish whether developer interaction occurs to a specific constituent of the latent residue. Studies can investigate this by applying the powder to '*groomed'* fingermarks, which are fingermarks enriched with one type of latent residue (i.e. sebaceous, eccrine, and apocrine). Several routes have been proposed as a means of obtaining groomed fingermarks, as detailed below.

Typically, eccrine marks are achieved by first thoroughly washing the hands, followed by wearing gloves for thirty minutes. After the gloves are removed the fingertip is contacted with a substrate to generate a fingermark. Sebaceous fingermarks are obtained by washing and drying of the hands, followed by rubbing of the fingertip across the forehead and/or nose, thereby transferring sebaceous material onto the finger, which is then deposited onto a substrate. Other routes use amino acid solutions and synthetic eccrine perspiration as analytical standards. Pots containing specific constituents found in latent residues are also available for purchase.[69]

Irrespective of the method used to obtain groomed marks, research has identified many flaws relating to their use in terms of validity.[70–72] Exemplar marks generated naturally are highly variable and may or may not contain all three types of deposits (sebaceous, eccrine, apocrine). Therefore, natural marks should be used wherever possible. It is recommended that any study investigating the validity of fingermark detection methods use ungroomed, "*natural*" marks, as this type of fingermark is more likely to mimic operational samples.

With that in mind, powders are believed to not target a specific constituent of latent residue, however, the same cannot be said for some of the other methods of fingermark development (i.e. chemical reactions). As fingermark powders are believed to adhere to latent residues through a combination of physical factors (as opposed to chemically targeting a specific substituent), this study did not include groomed marks. Instead, natural fingermarks were used that represent/mimic those typically encountered in operation.

Natural fingermarks are representative of fingermarks most likely to be encountered during an investigation and many factors influence their physical and chemical composition.[73] One *"drawback"* of using natural marks without a preliminary assessment of the artificially created marks is that give their enormous variability, a much higher number from a much higher number of donors should be investigated.

These points mentioned require a detailed consideration; the following methodology was created to obtain natural fingermarks which best represent those found in operational work (vide infra).

4.1.1 Multiple donor study

To assess variability in Phase 1 studies, a sample size of 3 - 5 fingermark donors is recommended.[63] This study used 5 participants all of whom provided informed consent.

4.1.2 Deposition pressure

Deposition pressure and contact time need to be accurately controlled within fingermark studies. For new methods, a compromise between the reproducibility of fingermark deposition procedures or sampling and producing a more accurate representation of the range of fingermarks encountered in actual casework. In this instance, no quantitative collection measures are necessary; however, clear instructions to '*touch the surface with light pressure using one finger for 1-2 seconds'* is a suitable means of ensuring relatively consistent deposition between donors and within fingermark sets for individual donors.[74]

4.1.3 Depletion series

Depletion series are used to determine the relative sensitivity of a fingermark technique. A series of fingermarks are deposited by successive contacts using the same fingertip.[73] In theory, with each additional contact, less residue is present to be deposited onto the next substrate. Each fingermark in the succession is developed and the sensitivity of the developer is assessed.[75] This can be performed on different substrates using different fingers to investigate the effect of material and fingermark quality. This procedure can also be used on the same surfaces but kept in different conditions.

4.1.4 Split fingerprints

Because of the inherent variability in fingermark composition between donors and for fingermarks from the same donor, whenever possible, efforts should be made to minimise the potential impact of this variability on the interpretation of the results. One of the ways of achieving this is using split fingermarks, where a depletion series of fingermarks is deposited and physically divided in two along the centre line. Each half of the depletion series is then processed with a different development technique and then recombined for an assessment of the number and quality of the developed marks. Wherever possible this should be the test method of choice, as this method allows for a comparison of marks from the same depletion series.[73]

4.1.5 Surface

It is highly unlikely that a fingermark enhancement technique would only apply to a single, clearly defined surface type.[73] Therefore, a range of surfaces that are representative of those that may be encountered in operational work should be investigated. Statistical data acquired through the Home Office UK identified the most common powdered surfaces at scenes of crime to be glass, painted metal, ceramic and gloss painted wood.[55]

4.1.6 Age of mark

The initial composition of fingermarks after deposition changes with time, due to the evaporation of both moisture content and volatile compounds and chemical reactions between residues and the environment (e.g. oxidation and photodegradation).[76,13] The extent to which this occurs is influenced by several factors, including the surface type and condition, level of exposure to direct sunlight, ambient temperature, humidity, and airflow across the surface.[76] It is therefore not valid to test enhancement techniques on freshly deposited fingermarks alone, and the experimental programme should include fingermarks across the range of ages that are likely to be encountered in a forensic context.

The time of access to crime scenes means fingermarks are developed within hours, weeks or even months after initially being generated. In practice, the most significant compositional changes occur within the first few days, and therefore a typical experiment may include fingermarks aged by 1 day, 7 days and 28 days.[73]

4.1.7 Environment

The methods used to simulate the required environment can be defined by the researcher but should try to replicate the conditions most commonly encountered in operational work wherever possible.[73]

4.2 Fingermark Collection Procedure

Natural fingermarks were obtained from a range of five donors who agreed to participate in this study. Donors variability included three males and two females, with an age range of 20-49 years old. The donors were asked to not wash their hands, use hand sanitiser, or wear gloves, for at least one-hour preceding their participation in this study. Each of the donors contributed forty-five natural fingermarks from nine fingers, five fingermarks for each depletion on three sets of identical substrates.

A range of substrates were selected with a variation in porosity and surface treatment, including; glass (Thermo Scientific Frosted Microscope Slides, Ground 90°, fishersci.co.uk), plastic (Homyl 5pcs ABS Styrene Plastic Flat Sheet, amazon.co.uk), and painted wood (Crown Quick Dry Gloss 750 mL Pure Brilliant White, amazon.co.uk) Smooth Planed Square Edge Whitewood spruce Timber (1.8 m x 34 mm x 18 mm, diy.com).

Before fingermark deposition, each surface was cleaned using soapy water, followed by ethanol to ensure complete removal of any pre-existing contaminants. These were then left to dry at room temperature for 24 hours before use in the study.

The split depletion consisted of 5 natural fingermarks deposited as depletions across the divide of two identical substrates. The surfaces are connected and using light pressure, donors were instructed to touch between the surfaces where the two materials connect for 1-2 seconds. Then using the same finger, they were asked to repeat this in a succession to produce a split depletion series, generating a succession of five fingermarks in total (**Figure 4.1**).
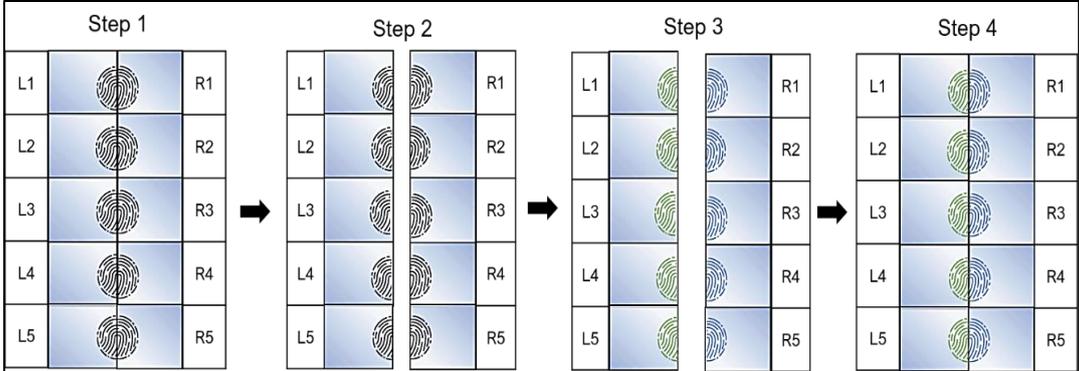
Figure 4.1: *Schematic diagram demonstrating the split depletion methodology used to assess the compatibility of emerging fingermark visualisation techniques. Two identical materials are connected. With the same finger, a series of fingermarks is deposited across the middle divide of the two connected surfaces. This enables both halves to be developed using different techniques, to limit factors that would arise from using two different fingers.*

Once fingermarks had been deposited, the three different sets were divided into separate groups according to date of collection, one group had been aged for 1 day between initial deposition and development, the second group had been aged for 7 days between initial deposition and development, and the third set had been aged for 28 days between initial deposition and development. The aged fingermarks were stored in ventilated containers under ambient light in a room maintained at 25 °C and average relative humidity of 75% for Canterbury, Kent, United Kingdom.

Meanwhile, the doped materials were prepared as powders (described in Chapter 2) and once the appropriate fingermark ageing period had elapsed, the substrates were retrieved and the depletions were separated, to enable one half to be developed with TPP:DMA and the other half to be developed using 4-TPT:DMA. Both powders were applied using separate squirrel hair zephyr brushes (www.csiequipment.com) and any excess powder was removed using separate marabou feather brushes (www.csiequipment.com). The developed fingermarks were graded using the grading system recommended by the Centre for Applied Science & Technology (CAST) displayed in **Table 4.1**.[73]

Table 4.1: *CAST grading scheme for the assessment of developed fingermarks.*[63]

Grade	Detail Visualised
0	No evidence of a fingermark
1	Some evidence of a fingermark
2	Less than 1/3 clear ridge detail
3	Between 1/3 and 2/3 clear ridge detail
4	Over 2/3 clear ridge detail

This study has endeavoured to follow recommendations of the International Fingerprint Research Group for Phase 1/2 research.[63] The preliminary nature of this research recommends caution when judging these findings, given that further validation studies are required to optimise and benchmark this methodology before implementation in an operational capacity. The results are specific to the parameters used in this study. Multiple trials of this type are required to build an overview of the performance.[73]

4.3 Analysis of developed fingermarks

All the CAST scores assigned to each fingermark developed in this research are displayed in the appendices, for TPP:DMA (Appendix H) and 4-TPT:DMA (Appendix I). Standard deviations have not been included owing to expected variation in the quality of fingermarks between donors, which is consistent with other studies of this type.[77] **Figure 4.2** displays a latent fingermark developed with both powders investigated in this study (TPP:DMA and 4-TPT:DMA). Both powders provide an excellent contrast to visualise the latent fingermark detail.
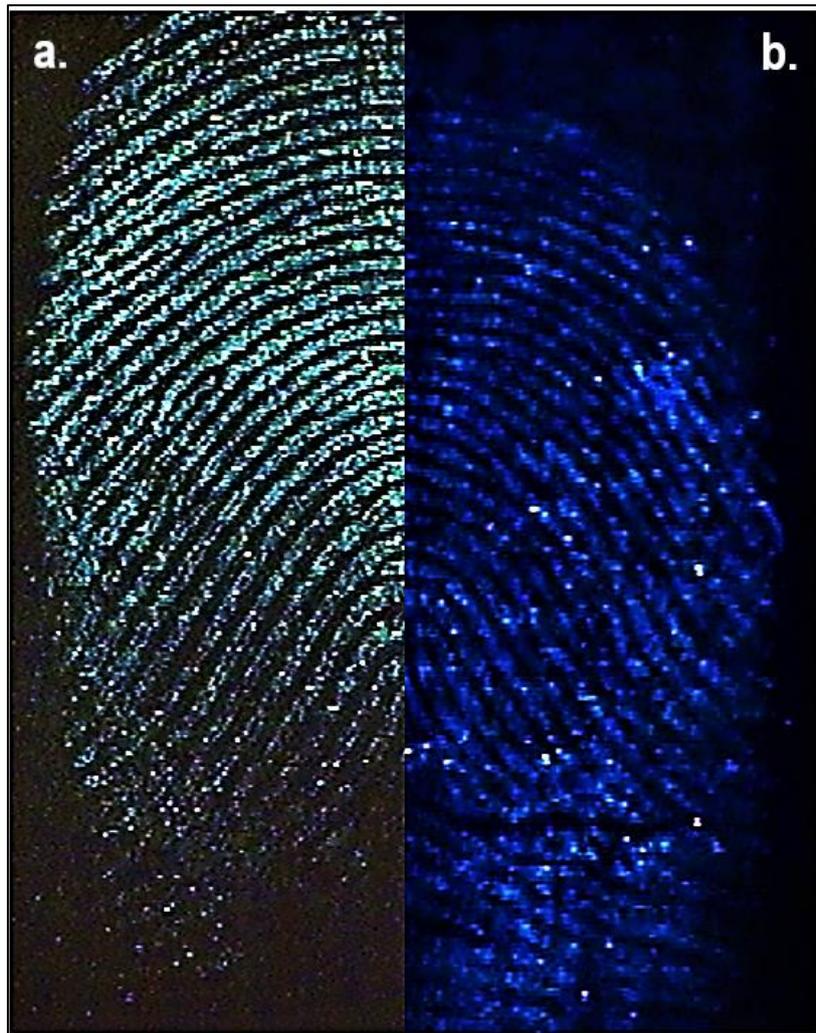
*Figure 4.2: Naturally obtained fingermarks on glass surfaces which had been aged for 1 day and developed using **TPP**:DMA (a), and **4-TPT**:DMA (b), visualised by 313 nm UV radiation. These fingermarks are not included in the participant's CAST grading scores*

Figure 4.3 - **Figure 4.8** contains six histograms of the CAST grades assigned to participant fingermarks, including, the depletion of fingermarks on a particular surface, with the specified ageing period, developed either by TPP:DMA or 4-TPT:DMA. CAST scores assigned to the fingermarks have been grouped as followed; developed fingermarks graded with CAST scores 3-4 are shown in green and represent developed marks where more than ⅓ of *minutiae* is visible. Developed fingermarks graded with CAST scores 1-2 are shown in orange and represent developed marks where less than ⅓ of *minutiae* is visible. Fingermarks graded with CAST score 0 are shown in red represent those marks where development had occurred but displayed no evidence of a fingermark.

Figure 4.3: *Schematic representation of the CAST scores for fingermarks deposited by all donors on* **plastic** *surfaces, across all ageing periods, developed using* **TPP**:*DMA. The depletions are grouped within their representative ageing period (1, 7 or 28 days). The three colours represent the CAST score for the fingermarks. CAST scores 3-4, shown in green, represent developed fingermarks that display between ⅓ and full visualisation of the fingermark ridge characteristics. CAST scores 1-2, shown in yellow, represent developed fingermarks that display some evidence of a fingermark; however, less than ⅓ of ridge detail is visible. CAST score 0, shown in red, represent grades where development was attempted, however, no evidence of a fingermark was displayed.*

97

Figure 4.4: *Schematic representation of the CAST scores for fingermarks deposited by all donors on **plastic** surfaces, across all ageing periods, developed using **4-TPT**:DMA. The depletions are grouped within their representative ageing period (1, 7 or 28 days). The three colours represent the CAST score for the fingermarks. CAST scores 3-4, shown in green, represent developed fingermarks that display between ⅓ and full visualisation of the fingermark ridge characteristics. CAST scores 1-2, shown in yellow, represent developed fingermarks that display some evidence of a fingermark; however, less than ⅓ of ridge detail is visible. CAST score 0, shown in red, represent grades where development was attempted, however, no evidence of a fingermark was displayed.*

Figure 4.5: *Schematic representation of the CAST scores for fingermarks deposited by all donors on **painted wood**, across all ageing periods, developed using **TPP**:DMA. The depletions are grouped within their representative ageing period (1, 7 or 28 days). No fingermarks were detected on this surface type, therefore, the CAST score 0, shown in red, represent grades where development was attempted, however, no evidence of a fingermark was displayed.*
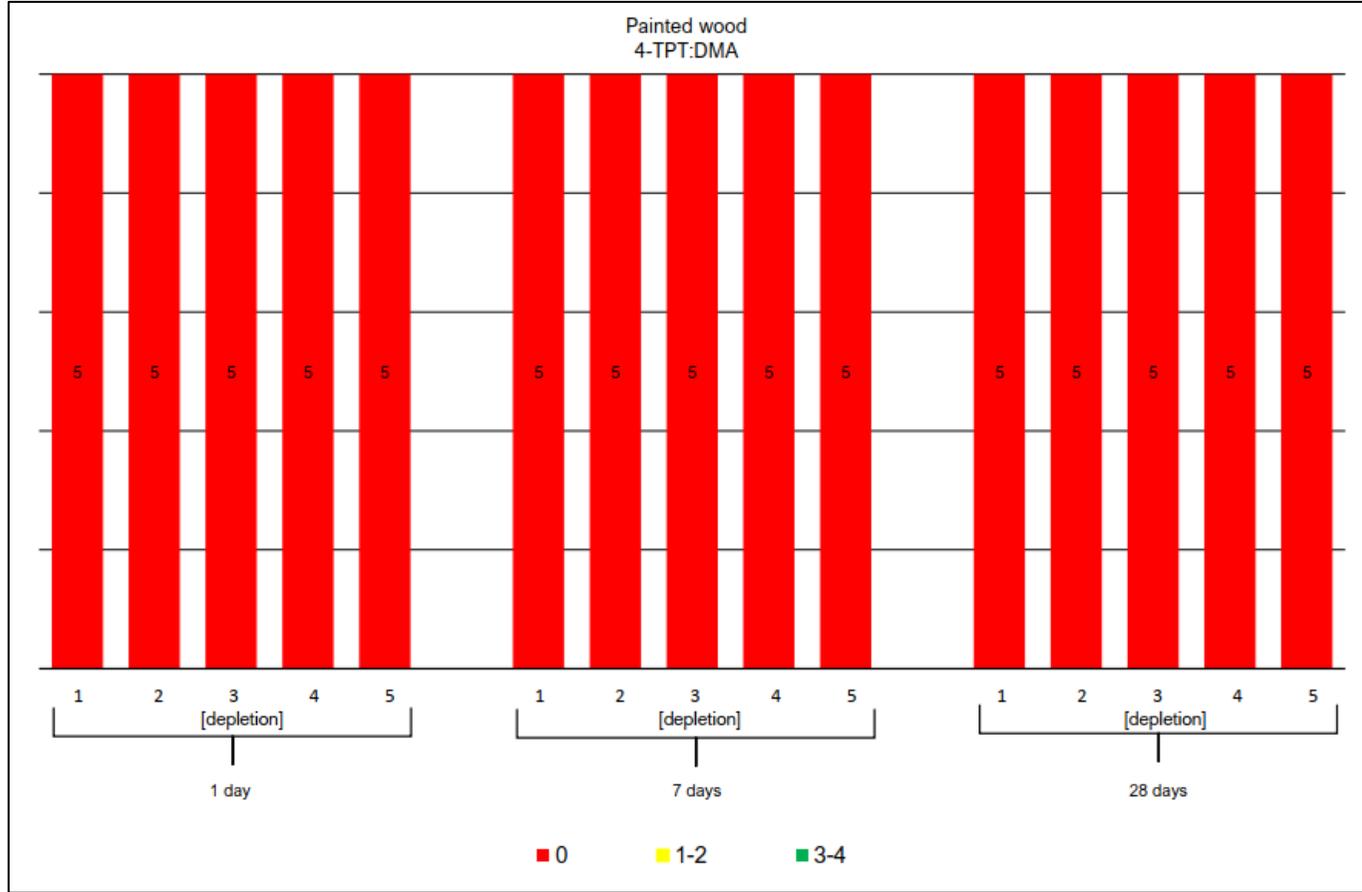
Figure 4.6: *Schematic representation of the CAST scores for fingermarks deposited by all donors on **painted wood**, across all ageing periods, developed using **4-TPT**:DMA. The depletions are grouped within their representative ageing period (1, 7 or 28 days). No fingermarks were detected on this surface type, therefore, the CAST score 0, shown in red, represent grades where development was attempted, however, no evidence of a fingermark was displayed.*
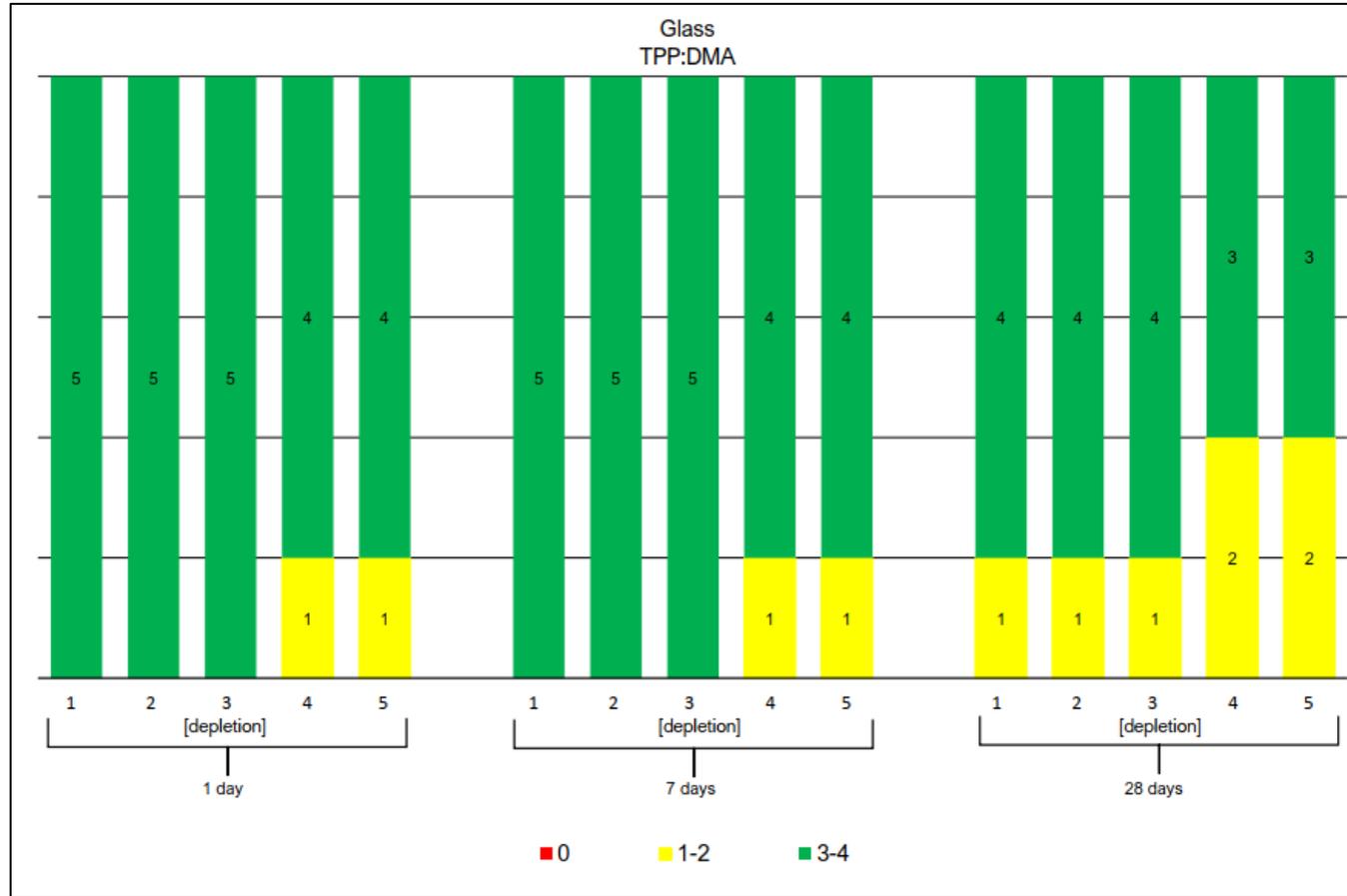
Figure 4.7: *Schematic representation of the CAST scores for fingermarks deposited by all donors on **glass** surfaces, across all ageing periods, developed using **TPP**:DMA. The depletions are grouped within their representative ageing period (1, 7 or 28 days). The two colours represent the CAST score for the fingermarks. CAST scores 3-4, shown in green, represent developed fingermarks that display between ⅓ and full visualisation of the fingermark ridge characteristics. CAST scores 1-2, shown in yellow, represent developed fingermarks that display some evidence of a fingermark; however, less than ⅓ of ridge detail is visible. CAST score 0 was not applied to any of the fingermarks on glass surfaces.*
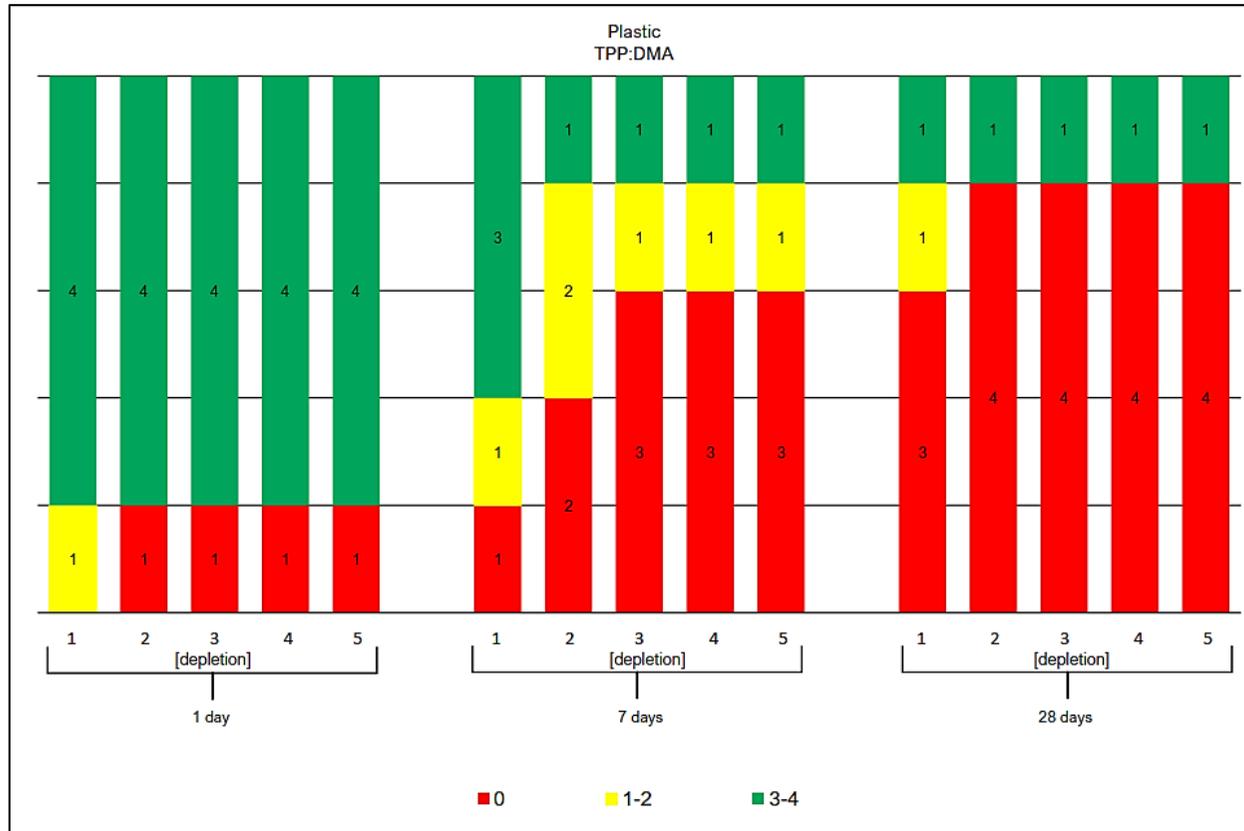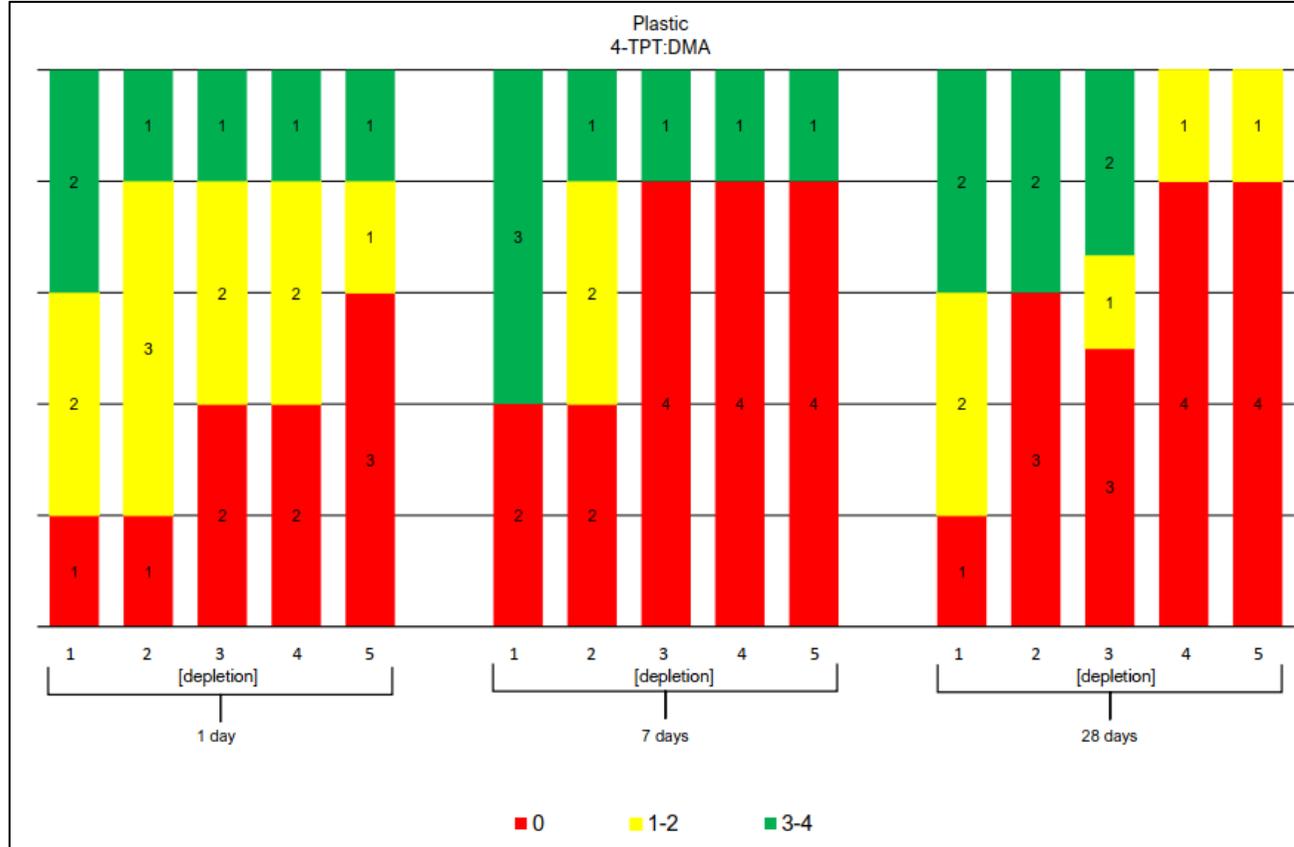
Figure 4.8: *Schematic representation of the CAST scores for fingermarks deposited by all donors on **glass** surfaces, across all ageing periods, developed using **4-TPT**:DMA. The depletions are grouped within their representative ageing period (1, 7 or 28 days). The two colours represent the CAST score for the fingermarks. CAST scores 3-4, shown in green, represent developed fingermarks that display between ⅓ and full visualisation of the fingermark ridge characteristics. CAST scores 1-2, shown in yellow, represent developed fingermarks that display some evidence of a fingermark; however, less than ⅓ of ridge detail is visible. CAST score 0 was not applied to any of the fingermarks on glass surfaces*

TPP:DMA and 4-TPT:DMA were both unsuccessful at developing any of the fingermarks deposited onto painted wood surfaces. This can only be ascribed to the porosity of painted wood because the development of fingermarks on plastic and glass surfaces had been successful.

Figure 4.9 displays a comparison of CAST scores for fingermarks development with TPP:DMA and 4-TPT:DMA in terms of number and quality of visualisations on plastic and glass surfaces across all donors, inclusive of all ageing periods. These results show that TPP:DMA was more effective out of the two developers; however, both were highly effective for fingermarks deposited on to glass surfaces. These results show that 85% of the 75 fingermarks on glass surfaces developed using TPP:DMA classed in the range of 3-4 according to the CAST scale, and 75% of the 75 fingermarks on glass surfaces developed using 4-TPT:DMA classed in the range of 3-4 according to the CAST scale. Both developers displayed a consistent detection of the fingermarks deposited onto glass surfaces.
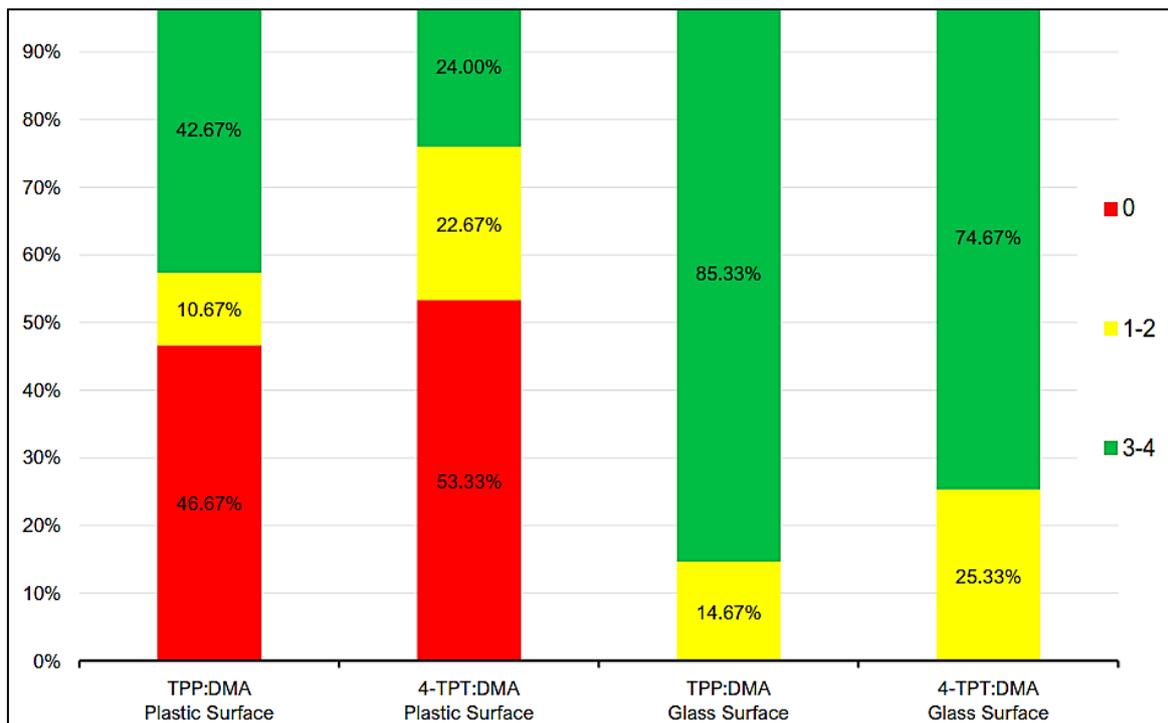
Figure 4.9: *Schematic diagram that compares the CAST grades of fingermarks, inclusive of all ageing periods and depletions on **plastic** and **glass** surfaces, developed using **TPP**:DMA or **4-TPT**:DMA. The three colours represent the CAST score for the fingermarks. CAST scores 3-4, shown in green, represent developed fingermarks that display between ⅓ and full visualisation of the fingermark ridge characteristics. CAST scores 1-2, shown in yellow, represent developed fingermarks that display some evidence of a fingermark; however, less than ⅓ of ridge detail is visible. CAST score 0, shown in red, represent grades where development was attempted, however, no evidence of a fingermark was displayed.*

Inclusive of all ageing periods, the percentage class for CAST scores 3-4 applied to fingermarks developed using **TPP**:DMA on plastic surfaces and glass surfaces were 42.67% and 85.33% respectively. Comparing these two percentages show that **TPP**:DMA was twice as effective at visualising fingermarks on glass surfaces than plastic surfaces.

The high percentage obtained for visualising fingermark detail on glass surfaces resulted in 0% of the fingermarks on glass surfaces being graded with the CAST score 0. In contrast, 46.67% of the fingermarks developed using **TPP**:DMA on plastic surfaces was graded with the CAST score 0.

Inclusive of all ageing periods, the percentage class for CAST scores 3-4 applied to fingermarks developed using **4-TPP**:DMA on plastic surfaces and glass surfaces were 24% and 74.67% respectively. Comparing these two percentages show that **4-TPP**:DMA was three times more effective at visualising fingermarks on glass surfaces than plastic surfaces.

The high percentage obtained for visualising fingermark detail on glass surfaces resulted in 0% of the fingermarks on glass surfaces being graded with the CAST score 0. In contrast, 53.33% of the fingermarks developed using **4-TPP**:DMA on plastic surfaces was graded with the CAST score 0. Compared to **TPP**:DMA, 10.66% more fingermarks on glass surfaces were graded with the CAST score 1-2 when developed with **4-TPT**:DMA.

Figure 4.10 expands on the analysis of average CAST scores including depletion series, separated by data for fingermarks aged for 1, 7 and 28 days before development. Each category is derived from 25 fingermarks per developer method, sourced from 5 donors. Painted wood has not been included as no fingermarks were visualised.
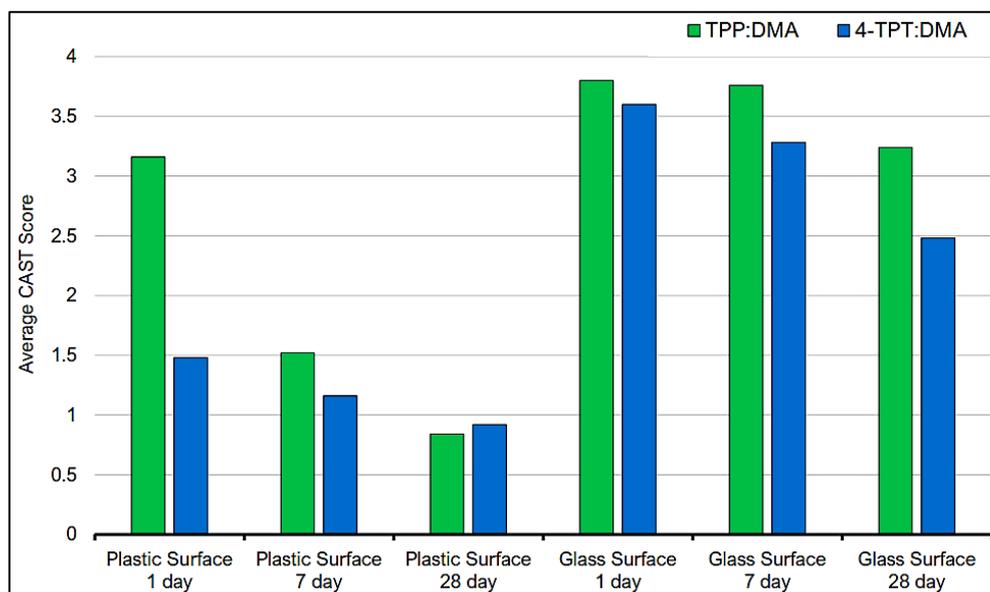
Figure 4.10: *Schematic diagram that compares the averaged CAST scores, for fingermarks deposited onto **plastic** and **glass** surfaces, developed with **TPP**:DMA (green) and **4-TPT**:DMA (blue), at the specified ageing period (1, 7 or 28 days).*

TPP:DMA slightly outperformed **4-TPT**:DMA, when used to develop fingermarks on plastic and glass surfaces, with the exception to plastic surfaces aged for 28 days. The results of this study show a promise of these materials for the development of fingermarks on plastic and glass surfaces, however, further work is required to fully validate these results.

4.4 Conclusion

The results display consistent fingermark visualisation for those developed using TPP:DMA and 4-TPT:DMA, on both plastic and glass surfaces, with TPP:DMA being the better powder for visualising fingermarks.

TPP:DMA and 4-TPT:DMA was unsuccessful at developing fingermarks of any quality for painted wood surfaces. As fingermarks could be visualised on the other types of surfaces, it can be assumed that the porosity of painted wood, prevented the development of latent fingermarks. Both materials were found to perform best when used on glass surfaces and achieved almost similar scores across the ageing periods and depletions for fingermarks on glass surfaces.

Whilst both powders achieved similar CAST scores, on average; TPP:DMA scores exceeded those of 4-TPT:DMA. This is largely believed to be due to the physical properties of the material. SEM-EDX images (shown in chapter 3) confirmed TPP:DMA to have a relatively similar/even distribution of particle size and shape, compared to 4-TPT:DMA, which was identified to be uneven, with greater variability of particle shapes and sizes. Visual observation identified TPP:DMA to form '*softer*' particles, compared to 4-TPT:DMA which appeared to clump together when ground. The regular and uniform distribution of TPP:DMA particles have a large *'flatter'* surface area, increasing contact and adhering better to latent fingermark residue, thus, identifying TPP:DMA to be the better powder to use for the development of latent fingermarks, on glass and plastic surfaces.

CHAPTER 5.   CONCLUSIONS

In this research, two organic persistent luminescent materials have been synthesised, optimised, prepared as powders, and applied to latent fingermarks under guidelines published by the international fingerprint research group.

The first persistent luminescent material, (3-Bromopropyl)triphenylphosphonium bromide, was synthesised by refluxing triphenylphosphine with 1,3-dibromopropane in acetonitrile. The persistent luminescence was obtained through organic doping with an electron donor, N,N-dimethylaniline, during the recrystallisation method, double-layered diffusion. The optimal doping ratio of TPP to DMA was identified to be 1:20.

The second persistent luminescent material, 2,4,6-tri(4-pyridyl)-1,3,5-triazine, was synthesised through the catalytic trimerization of 4-cyanopyridine. The persistent luminescence was obtained by adding electron donor, N,N-dimethylaniline, to the synthesis. To this synthesis, it was found that by using ten times less amount of DMA moles to 4-cyanopyridine moles, resulted in the formation of the optimised product.

Few studies have used organic persistent luminescent materials to visualise latent fingermarks. Mostly, as they have only been discovered within the last decade and refined regarding the ease of accessibility and reproducibility. This study has identified a potential for the use of such powders on the operational benefit level. However, considerably more work is required to establish how effective these materials truly would be for use in practice. Ideally, future work would focus on using a larger number of participants in the fingermark study, as well as investigating alternate surface types to understand, how versatile organic persistent luminescent materials may be.

The theory surrounding organic persistent luminescence, suggests that incorporation of dopant into the lattices of the host material forms charge carriers during UV excitation. The charge carries result in an extended and increased photoluminescent intensity which is observed. This theory is still relatively new, and investigations continue to identify new explanations and a better understanding of the mechanisms

involved with organic persistent luminescence. The parameters concerning ideal variables to consider for effective doping of the material during the recrystallisation are yet to be established. Factors such as temperature, time, route of recrystallisation, effects of different solvents and so on need to be investigated, to establish an optimal and effective method for obtaining the doped material.

It has been claimed that DMA is doped inside the forming TPP lattices during crystallisation. However, our work suggests otherwise as DMA could not be identified in the TPP:DMA material, by ^{1}H-NMR spectroscopy, single crystal XRD or LCMS. Instead, it is believed that DMA removes residual acid from the crystallisation, eliminating a means of quenching within the luminescent material. Using higher doping ratios removed an increased amount of residual acid, reaching a maximum at 1:20.

The length of time that governs the type of luminescence, known to be 'persistent' is subjective, as observable photoluminescent emissions are currently considered to be either due to a material being fluorescent or phosphorescent. The actual emission time to distinguish if the material is phosphorescent, or persistent luminescent, is currently undetermined and yet to be established.

Although the associated benefits of a particular method differ between each study, there is still not one powder that can be used to develop fingermarks of optimal quality on all types of surface. Despite this recognised performance variation, there is very little reported evidence of large-scale comparative studies to demonstrate the relative effectiveness of powders other than the experiments carried out by the Home Office Scientific Development branch.[55]

Although TPP:DMA was identified to perform better as a fingermark developer, there is no denying that 4-TPT:DMA was also successful at developing latent fingermarks on the same surfaces at the same ageing periods. However, TPP:DMA has the advantage, due to its physical properties being better suited to developing latent fingermarks. Between August 2016 and June 2019, 365 articles were published concerning fingermark detection and imaging/recording,[78] with articles on powder dusting making up 35% (129) of all the reports on fingermark detection and imaging/recording.

Considering that a substantial amount of work has focused on fingermarks visualisation by the powder dusting method, it is recommended that future investigations should study the effects of physical properties on the development of latent fingermarks, as surprisingly, little research has focused on these types of interactions. This would help to identify stronger powders to use for the development of latent fingermarks.

REFERENCES

1 Forensic Science Regulator, *Codes of Practice and Conduct. Fingerprint Examination – Terminology, Definitions and Acronyms*, Home Office, United Kingdom, 2017.

2 B. Fisher, W. Tilstone, and C. Woytowicz, *Introduction to Criminalistics: The Foundation of Forensic Science*, Academic Press, United States, 2009.

3 L.H. Adamu and M.G. Taura, *IJHA*, 2017, **1**, 1–8.

4 A.R.W. Jackson, J.M. Jackson, H. Mountain, and D. Brearley, *Forensic Science*, Pearson Higher Ed, United Kingdom, 4th edn., 2016.

5 D. Maltoni, D. Maio, A.K. Jain, and S. Prabhakar, *Handbook of Fingerprint Recognition*, Springer London, United Kingdom, 2nd edn., 2009.

6 H. Faulds, *Nature*, 1880, **22**, 605–605.

7 R. Williams, *Handbook of Forensic Science*, Taylor & Francis, United Kingdom, 1st edn., 2013.

8 S. Cadd, M. Islam, P. Manson, and S.M. Bleay, *Sci. Justice*, 2015, **55**, 219–238.

9 S.M. Bleay, V. Sears, R. Downham, H. Bandey, A. Gibson, V. Bowman, L. Fitzgerald, T. Ciuksza, J. Ramadani, and C. Selway, *Fingerprint Source Book v2.0*, Home Office Centre for Applied Science and Technology (CAST), United Kingdom, 2nd edn., 2017.

10 G. Sodhi and J. Kaur, *Forensic Science Int.*, 2001, **120**, 172–176.

11 H.L. Bandey, S.M. Bleay, V.J. Bowman, R.P. Downham, and V.G. Sears, *Fingermark Visualisation Manual*, Home Office Centre for Applied Science and Technology (CAST), United Kingdom, 1st edn., 2014.

12 A. Gaw, *Lee and Gaensslen's Advances in Fingerprint Technology*, CRC Press, United States, 3rd edn., 2012.

13 A. Girod, R. Ramotowski, and C. Weyermann, *Forensic Science Int.*, 2012, **223**, 10–24.

14 The Forensic Science Regulator, *Fingermark Visualisation and Imaging*, Home Office Centre for Applied Science and Technology (CAST), United Kingdom, 2017.

15 M. Wang, Y. Zhu, and C. Mao, *Langmuir*, 2015, **31**, 7084–7090.

16 R. Mukamal, How Humans See in Color, https://www.aao.org/eye-health/tips-prevention/how-humans-see-in-color, (accessed 7 September 2020).

17   S. Arshad-Hussain, PhD Thesis, Tripura University, 2009.

18   The Electromagnetic Spectrum, https://chem.libretexts.org/Bookshelves/Introductory_Chemistry/Map%3A_Introductory_Chemistry_(Tro)/09%3A_Electrons_in_Atoms_and_the_Periodic_Table/9.02%3A_The_Electromagnetic_Spectrum, (accessed 19 April 2020).

19   G. Tranter and D. Koppenaal, in *Encyclopedia of Spectroscopy and Spectrometry*, eds. D. Koppenaal, G. E. Tranter and J. C. Lindon, Academic Press, United Kingdom, 3rd edn., 2016, pp. 636–653.

20   D. Harvey, *Modern Analytical Chemistry*, McGraw-Hill Education, United States, 1st edn., 1999.

21   M. Wang, M. Li, A. Yu, Y. Zhu, M. Yang, and C. Mao, *Adv. Funct. Mater.*, 2017, **27**, 1606243.

22   R. Ma, R. Shimmon, A. McDonagh, P. Maynard, C. Lennard, and C. Roux, *Forensic Science Int.*, 2012, **217**, e23–e26.

23   K-V. Eeckhout, P. Smet, and D. Poelman, *Materials*, 2010, **3**, 2536–2566.

24   Z. Lin, R. Kabe, K. Wang, and C. Adachi, *Nat Commun*, 2020, **11**, 191.

25   J. Xu and S. Tanabe, *J Lumin.*, 2019, **205**, 581–620.

26   H. A. Klasens, *J. Electrochem. Soc.*, 1953, **100**, 366–375.

27   T. Matsuzawa, Y. Aoki, N. Takeuchi, and Y. Murayama, *J. Electrochem. Soc.*, 1996, **143**, 2670–2673.

28   X. Yang and D. Yan, *J. Mater. Chem. C*, 2017, **5**, 7898–7903.

29   Y. Yang, K-Z. Wang, and D. Yan, *Chem. Commun.*, 2017, **53**, 7752–7755.

30   X. Yang and D. Yan, *Chem. Sci.*, 2016, **7**, 4519–4526.

31   X. Yang and D. Yan, *Adv. Optical Mater.*, 2016, **4**, 897–905.

32   H. Mieno, R. Kabe, N. Notsuka, M.D. Allendorf, and C. Adachi, *Adv. Optical Mater.*, 2016, **4**, 1015–1021.

33   D. Wang, Q. Yin, Y. Li, and M. Wang, *J Lumin.*, 2002, **97**, 1–6.

34   C. Zhao and D. Chen, *Mater. Lett*, 2007, **61**, 3673–3675.

35   Y. Lin, Z. Tang, and Z. Zhang, *Mater. Lett*, 2001, **51**, 14–18.

36   L. Jiang, C. Chang, D. Mao, and C. Feng, *Opt. Mater.*, 2004, **27**, 51–55.
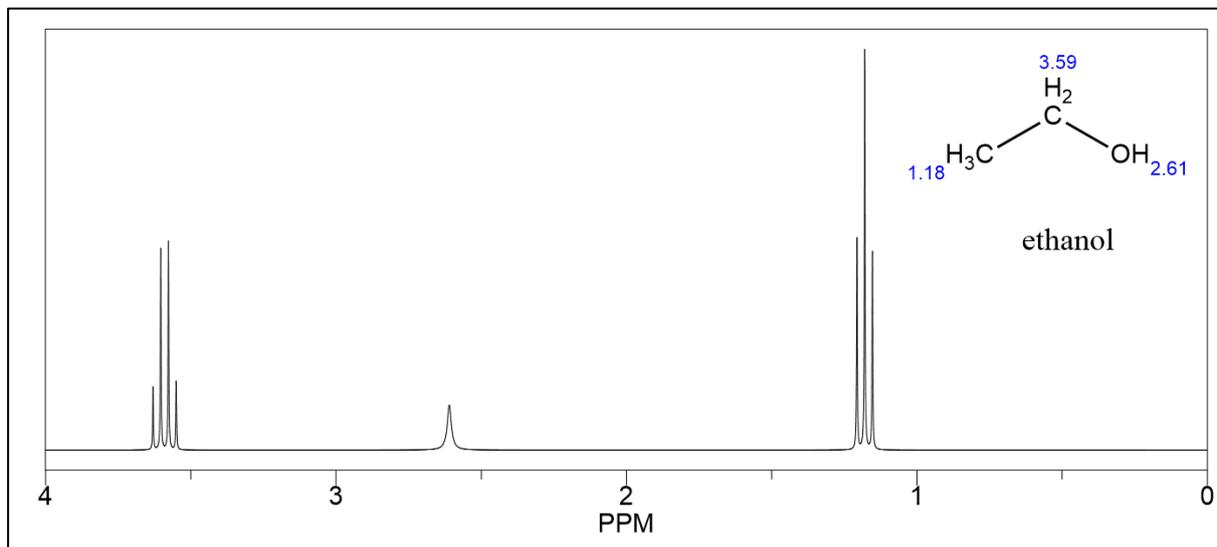
37   Z. Lin, R. Kabe, N. Nishimura, K. Jinnai, and C. Adachi, *Adv. Mater.*, 2018, **30**, 1803713.

38   M.P. Anesh, S.K.H. Gulrez, A. Anis, H. Shaikh, M.E.A. Mohsin, and S.M. AL-Zahrani, *Adv. Polym. Technol.*, 2014, **33**, 1–9.

39   H. Tan, T. Wang, Y. Shao, C. Yu, and L. Hu, *Front. Chem.*, 2019, **7**, 387.

40   W-H Zhang, X-X Hu, and X-B. Zhang, *Nanomaterials (Basel)*, 2016, **6**, 81.

41   R. Kabe and C. Adachi, *Nature*, 2017, **550**, 384–387.

42   Z. An, C. Zheng, Y. Tao, R. Chen, H. Shi, T. Chen, Z. Wang, H. Li, R. Deng, X. Liu, and W. Huang, *Nat. Mater*, 2015, **14**, 685–690.

43   L. Gu, H. Shi, M. Gu, K. Ling, H. Ma, S. Cai, L. Song, C. Ma, H. Li, G. Xing, X. Hang, J. Li, Y. Gao, W. Yao, Z. Shuai, Z. An, X. Liu, and W. Huang, *ANGEW CHEM INT EDIT*, 2018, **57**, 8425–8431.

44   T. Főrster, *Discuss. Faraday Soc.*, 1959, **27**, 7–17.

45   D.L. Dexter, *J. Chem. Phys.*, 1953, **21**, 836–850.

46   K. Jinnai, R. Kabe, and C. Adachi, *Adv. Mater.*, 2018, **30**, 1800365.

47   Z. Lin, R. Kabe, and C. Adachi, *Chem. Lett.*, 2019, **49**, 203–206.

48   P. Alam, N.L.C. Leung, J. Liu, T-S. Cheung, X Zhang, Z He, R.T.K. Kwok, J.W.Y. Lam, H.H.Y. Sung, I.D. Williams, C.C.S. Chan, K.S. Wong, Q. Peng, and B.Z. Tang, *Adv. Mater.*, 2020, **32**, 2001026.

49   A. Gaw, in *Lee and Gaensslen's Advances in Fingerprint Technology*, ed. R. Ramotowski, CRC Press, United States, 3rd edn., 2012, pp. 307–180.

50   F.K. Kanodarwala, S. Moret, X. Spindler, C. Lennard, and C. Roux, *WIREs. Forensic sci.*, 2019, **1**, e1341.

51   M-J. Choi, A.M. McDonagh, P. Maynard, and C. Roux, *Forensic Science Int.*, 2008, **179**, 87–97.

52   S. Rag, S. Jose, U. S. Sumod, and M. Sabitha, *J Pharm Bioallied Sci*, 2012, **4**, 186–193.

53   G. Oberdörster, E. Oberdörster, and J. Oberdörster, *EHP*, 2005, **113**, 823–839.

54   X. Yuan, X. Zhang, L. Sun, Y. Wei, and X. Wei, *Part. Fibre Toxicol.*, 2019, **16**, 18.

55   S.M. Bleay, G. Bradshaw, and J.E. Moore, *Fingerprint Development and Imaging Newsletter: Special Edition*, Home Office, United Kingdom, 2006.

56   S.J. McCook, D.P. Tate, and J. Beller, *JFI*, 2016, **66**, 577–590.

57   S. Gürbüz, B.O. Monkul, T. İpeksaç, M.G. Seden, and M. Erol, *J. Forensic Sci.*, 2015, **60**, 727–736.

58   B.J. Theaker, K.E. Hudson and F.J. Rowell, *Forensic Science Int.*, 2008, **174**, 26–34.

59   J.D. James, C.A. Pounds, and B. Wilshire, *J Forensic Sci.*, 1991, **36**, 1368–1375.

60   J. D. James, C.A. Pounds, and B. Wilshire, *Powder Metall.*, 1991, **34**, 39–44.

61   N-N. Zhang, Y-F. Han, M-X. Du, R-J. Sa, M-S. Wang, and G-C. Guo, *Chem. Eur. J.*, 2019, **25**, 13972–13976.

62   M-X. Li, Z-X. Miao, M. Shao, S-W. Liang, and S-R. Zhu, *Inorg. Chem.*, 2008, **47**, 4481–4489.

63   J. Almog, A. Cantu, C. Champod, T. Kent, and C. Lennard, *J. Forensic Identif*, 2014, **64**, 174–197.

64   V. Viswanathan, *Inventions*, , DOI:10.3390/inventions4010013.

65   S.D. Sarker, Z. Latiff, and A.I. Gray, Eds., *Natural Products Isolation*, Humana Press, United States, 2nd edn., 2006.

66   A. Sharma and N.S.M. Quantrill, *Spectrochim Acta A Mol Biomol Spectrosc*, 1994, **50**, 1161–1177.

67   P. Atkins, J. Paula, and J. Keeler, *Atkins' Physical Chemistry*, OUP Oxford, United Kingdom, 11th edn., 2017.

68   J. Janczak, M. Śledź, and R. Kubiak, *Journal of Molecular Structure*, 2003, **659**, 71–79.

69   Arrowhead Forensics Latent Print Development - Latent Print Reference Pad, https://www.arrowheadforensics.com/arrowhead-by-discipline/latent-print-examiners/fingerprint-processing-chemicals-discipline/latent-print-reference-pad.html, (accessed 7 September 2020).

70   T. Kent, *JFI*, 2010, **60**, 371–379.

71   M. Wood, *Angew. Chem-Ger. Int. Edit*, 2012, **51**, 12272–12274.

72   R.S. Croxton, M.G. Baron, D. Butler, T. Kent, and V.G. Sears, *Forensic Sci Int*, 2010, **199**, 93–102.

73   V.G. Sears, S.M. Bleay, H.L. Bandey, and V.J. Bowman, *Sci. Justice*, 2012, **52**, 145–160.

74   C. Lennard, *Aust. J. Forensic Sci.*, 2020, **52**, 125–145.

75   S. Fieldhouse, *Forensic Sci Int*, 2011, **207**, 96–100.

76   N.E. Archer, Y. Charles, J.A. Elliott, and S. Jickells, *Forensic Science Int.*, 2005, **154**, 224–239.

77   S. Chadwick, M. Neskoski, X. Spindler, C. Lennard, and C. Roux, *Forensic Science Int.*, 2017, **273**, 153–160.

78   A. Bécue, H. Eldridge, and C. Champod, *Forensic Science International: Synergy*, 2020, **2**, 442–480.

79   (3-Bromopropyl)triphenylphosphonium bromide, https://www.sigmaaldrich.com/spectra/fnmr/FNMR001000.PDF, (accessed 23 September 2020).

80   N,N-Dimethylaniline, https://www.sigmaaldrich.com/spectra/fnmr/FNMR009993.PDF.

APPENDICES

APPENDIX A

Appendix A: *Example ¹H-NMR spectrum of ethanol. There are three different types of environments the hydrogens (H) are experiencing, one for the CH₃ group, one for the CH₂ group and one for the OH group. The H on the -OH group is not coupling with the other H atoms and appears on the spectrum as a singlet. The CH₃ and the CH₂ hydrogens are coupling with each other, resulting in a triplet and quartet, respectively.*

APPENDIX B
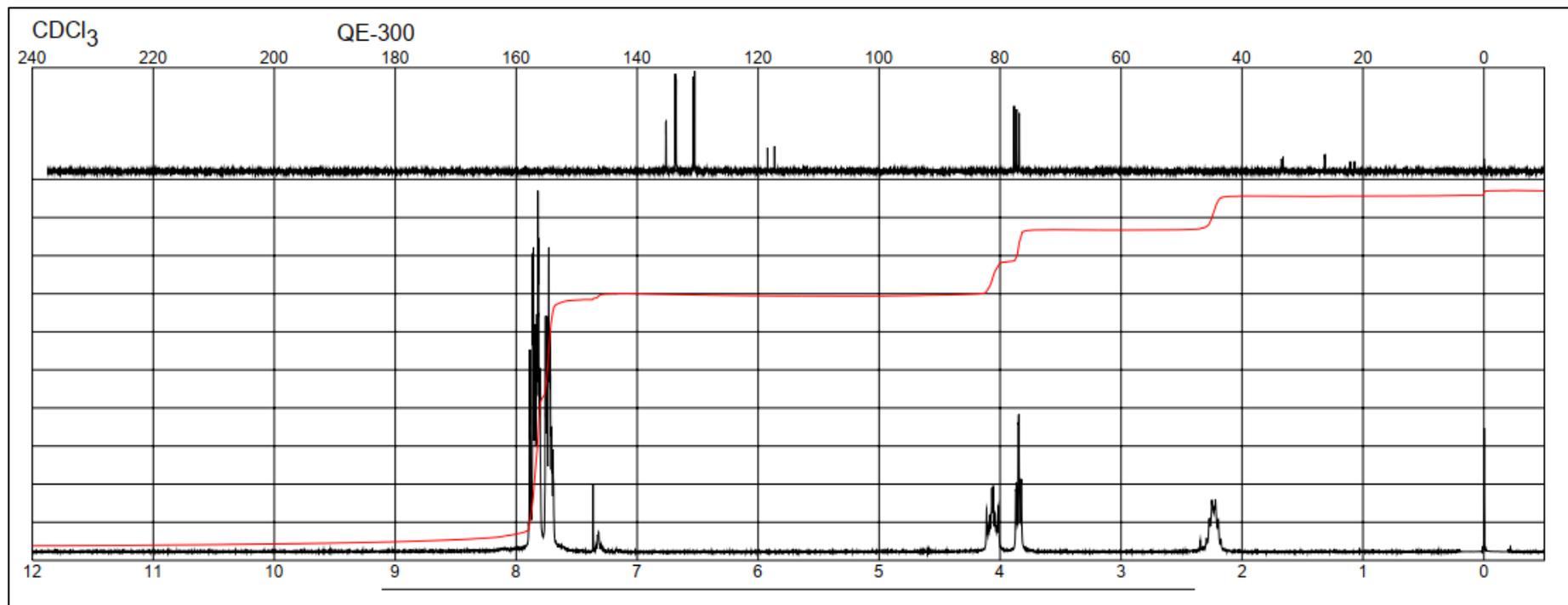
Appendix B: ^{1}H-NMR spectrum of (3-Bromopropyl)triphenylphosphonium bromide in CDCl3.[79]

APPENDIX C

CDCl$_3$ QE-300
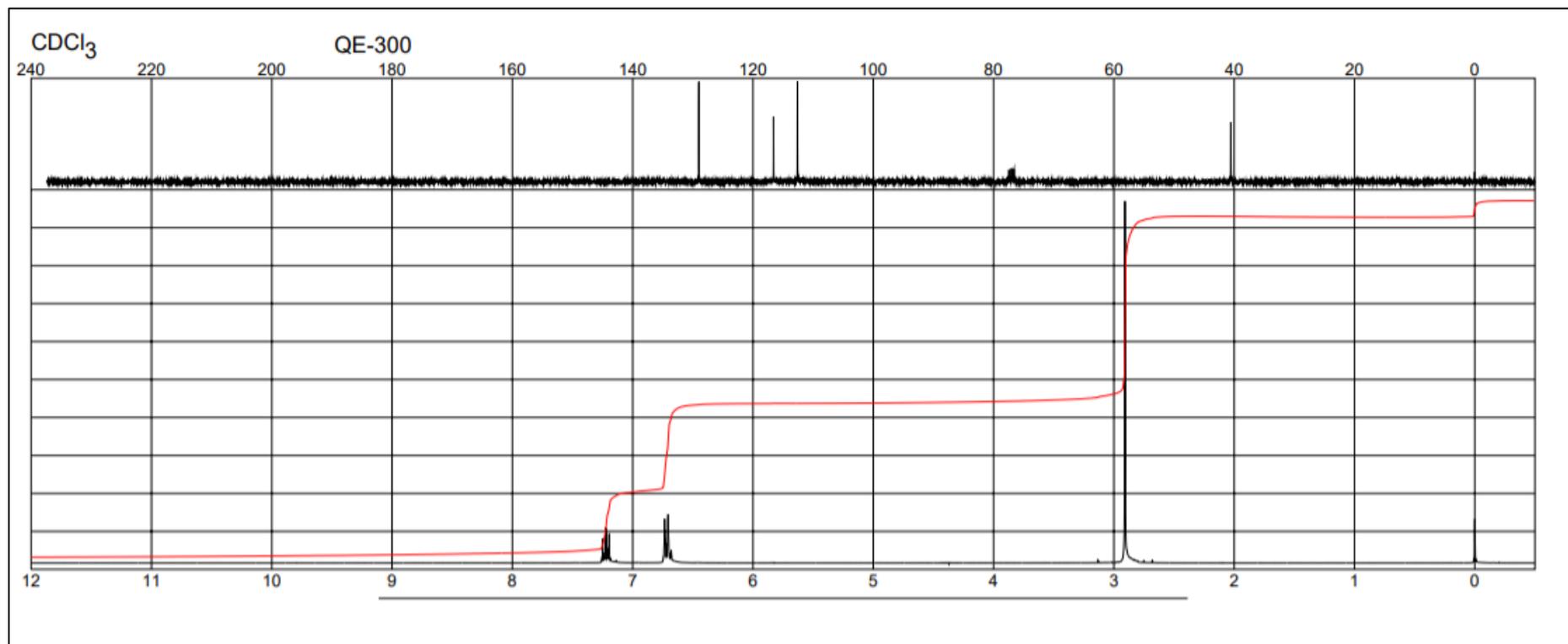
Appendix C: ^{1}H-NMR spectrum of N,N-dimethylaniline in CDCl$_3$.[80]

APPENDIX D

TPP-DMA.mp4

Appendix D: A video recording showing the persistent luminescence of TPP:DMA:R. The material was exposed to a handheld UV LED (370 nm) in dark conditions.

APPENDIX E

4-TPT-DMA.mp4

Appendix E: A video recording showing the persistent luminescence of 4-TPT. The material was exposed to a handheld UV LED (370 nm) in dark conditions.

APPENDIX F

Phosphorescent Parameters	
Total decay time (s)	3.00
No. of flashes	5.00
Delay time (ms)	0.10
Gate time (ms)	100.00
Scan mode	5.00
Start (nm)	400.00
Stop (nm)	750.00
Ex. Wavelength (nm)	390.00

Appendix F: Fluorometer instrument settings used to record the phosphorescent emission and excitation spectral measurements for 4-TPT:DMA.

APPENDIX G
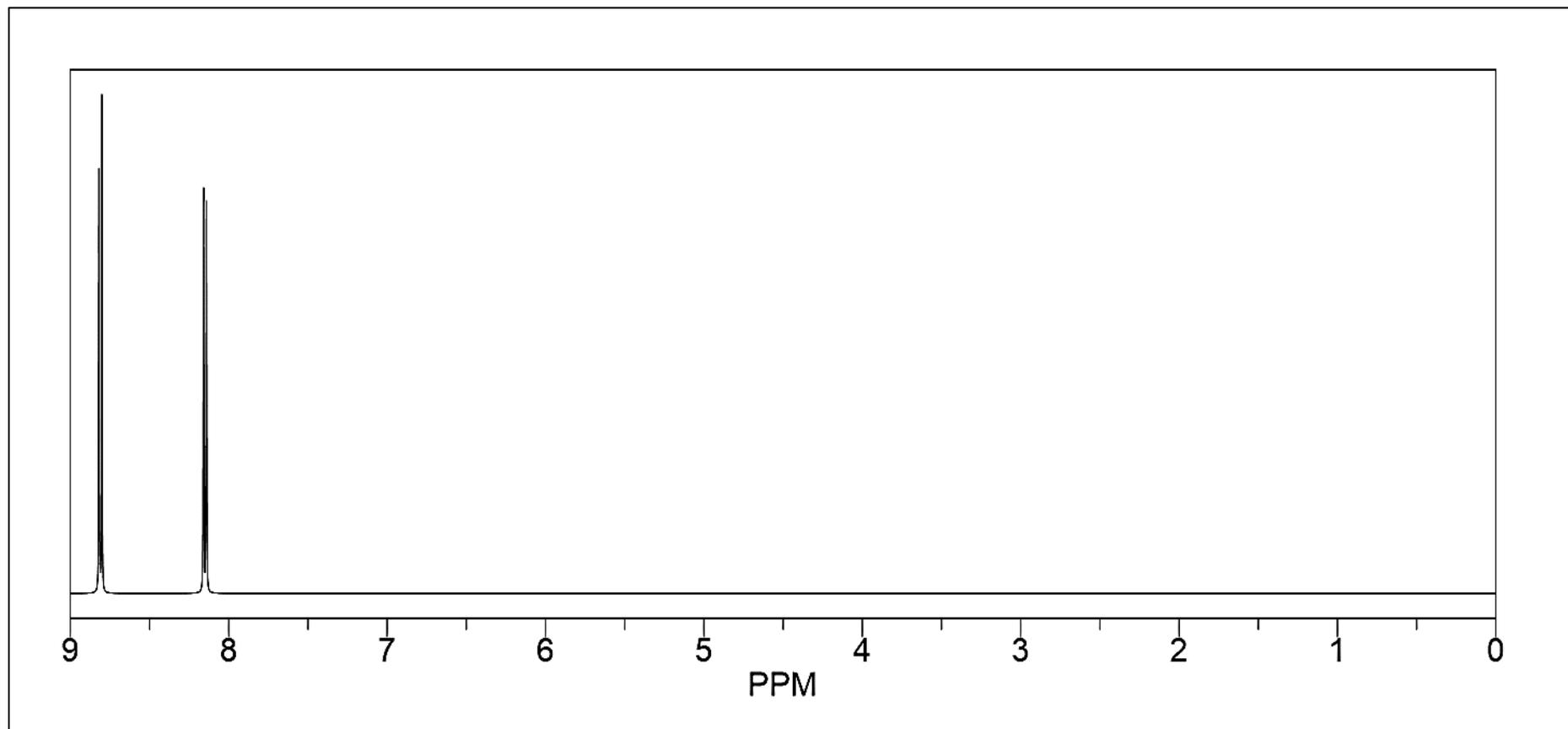
Appendix G: *ChemNMR ^{1}H-NMR Estimation of 2,4,6-tri(4-pyridyl)-1,3,5-triazine in CDCl$_3$.*

APPENDIX H

(3-bromopropyl)triphenylphosphonium bromide														
1 Day					7 day					28 day				
Participant No.														
1	**2**	**3**	**4**	**5**	**1**	**2**	**3**	**4**	**5**	**1**	**2**	**3**	**4**	**5**
[Depletion] Plastic														
[1] 1	4	4	4	4	0	4	4	4	1	0	4	0	0	1
[2] 0	4	4	4	4	0	4	1	2	0	0	4	0	0	0
[3] 0	4	4	4	4	0	4	0	2	0	0	4	0	0	0
[4] 0	4	4	3	4	0	4	0	2	0	0	4	0	0	0
[5] 0	4	4	3	4	0	4	0	2	0	0	4	0	0	0
[Depletion] Painted Wood														
[1] 0	0	0	0	0	0	0	0	0	0	0	0	0	0	0
[2] 0	0	0	0	0	0	0	0	0	0	0	0	0	0	0
[3] 0	0	0	0	0	0	0	0	0	0	0	0	0	0	0
[4] 0	0	0	0	0	0	0	0	0	0	0	0	0	0	0
[5] 0	0	0	0	0	0	0	0	0	0	0	0	0	0	0
[Depletion] Glass														
[1] 4	4	4	4	4	4	4	4	3	4	4	4	4	2	4
[2] 4	4	4	4	4	4	4	4	3	4	4	4	4	2	4
[3] 4	4	4	3	4	4	4	4	3	4	4	4	3	2	3
[4] 4	4	4	2	4	4	4	4	3	4	4	4	2	2	3
[5] 4	4	4	2	4	4	4	4	2	4	3	4	2	2	3

Appendix H: The CAST grade assigned to each fingermark developed across all donors, ageing periods and surfaces investigated in this study using TPP:DMA. The ageing period includes 1, 7, and 28 days. The surface is listed and the CAST grades for the depletions for an ageing period are listed beneath.

2,4,6-tri(4-pyridyl)triazine-1,3,5														
1 Day					7 day					28 day				
Participant No.														
1	2	3	4	5	1	2	3	4	5	1	2	3	4	5
[Depletion] Plastic														
[1] 1	4	2	3	0	0	4	4	3	0	0	3	1	3	1
[2] 1	4	2	2	0	0	4	1	1	0	0	3	0	3	0
[3] 0	4	2	1	0	0	4	0	0	0	0	2	0	3	0
[4] 0	4	1	1	0	0	4	0	0	0	0	2	0	0	0
[5] 0	4	1	0	0	0	4	0	0	0	0	2	0	0	0
[Depletion] Painted Wood														
[1] 0	0	0	0	0	0	0	0	0	0	0	0	0	0	0
[2] 0	0	0	0	0	0	0	0	0	0	0	0	0	0	0
[3] 0	0	0	0	0	0	0	0	0	0	0	0	0	0	0
[4] 0	0	0	0	0	0	0	0	0	0	0	0	0	0	0
[5] 0	0	0	0	0	0	0	0	0	0	0	0	0	0	0
[Depletion] Glass														
[1] 4	4	4	4	4	4	4	4	2	4	3	3	3	2	4
[2] 4	4	4	4	4	4	4	4	2	4	3	3	3	2	3
[3] 4	4	4	3	4	3	3	4	2	4	2	3	3	2	2
[4] 4	3	4	2	4	3	3	4	1	4	2	3	3	1	2
[5] 3	2	4	1	4	3	3	4	1	4	2	3	3	1	1

Appendix I: *The CAST grade assigned to each fingermark developed across all donors, ageing periods and surfaces investigated in this study using 4-TPT:DMA. The ageing period includes 1, 7, and 28 days. The surface is listed and the CAST grades for the depletions for an ageing period are listed beneath.*

APPENDIX J

Appendix J: *Restrictions caused by the COVID-19 pandemic affected the way donors could participate in this study, which had to follow official regulations which limited the number of people allowed in one room, as well as, in the building at any time. No close contact was allowed, and the participants could only be in the room by themselves, therefore, this study was changed to suit and meet the regulations arising from COVID-19. Participants were contacted via email and those who agreed to provide fingermarks for this study were supplied with the following document. The substrates which donors were required to deposit their finger marks on had been set up in a room, three days before their participation. Upon entry, they were directed to their station and provided with the following instructions and images*

**Participant Information and Study Guidelines for the Assessment of
Fingermark Detection Techniques**

Aims

The research associated with this study aims to produce a latent fingermark developer using newly discovered organic persistent luminescent materials.

All research investigating new materials as latent fingermark developers must undergo a validation study to assess the material(s) compatibility as a fingermark developer. As these materials would be used by the Forensic Science community, strict guidelines and procedures must be followed to ensure that accurate results are obtained. For results to be valid, a range of donors are required to deposit natural fingermarks on various surfaces of similar and dissimilar types.

The initial composition of fingermarks once deposited change with time. To assess the effect time has on the quality of development, fingermarks will be deposited onto surfaces of the same nature, stored, and developed at different intervals (1,7,28 days). Surfaces with different properties are used to assess the material(s) suitability, by identifying whether the material is limited to a particular surface type or a can be applied to a range of surfaces.

The same finger can be used to generate more than one fingermark. In theory, with each additional contact, less fingermark residue will be deposited onto the surface of the material. A succession of fingermarks are deposited using the same finger, thereafter, developed to assess the sensitivity of the material being investigated.

To limit pressure variability between deposited fingermarks, two identical substrates are placed together and a fingermark is deposited where the two materials connect. This creates a 'split' fingermark which enables one half to be developed using a new method and the other half by an industry standard method. These are joined together and directly compared/graded to assess the quality of the new method against established method.

Please ensure the following

- Do not wash your hands for at least one hour prior to participating in this study.
- Do not handle chemicals for at least one hour prior to this study.
- Do not wear gloves for at least one hour prior to this study.
- Do not touch any of the items to move them.

Summary

This study will require you to deposit a latent fingermark onto a substrate. This 'natural' latent fingermark needs to be evenly placed between two identical materials.
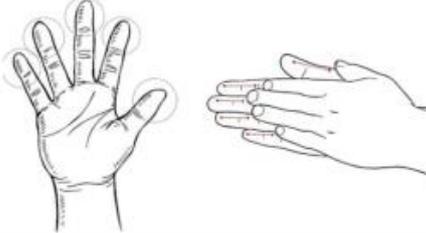
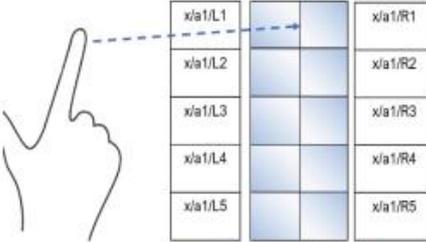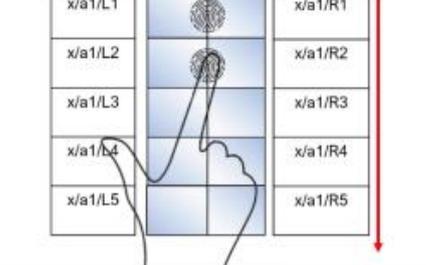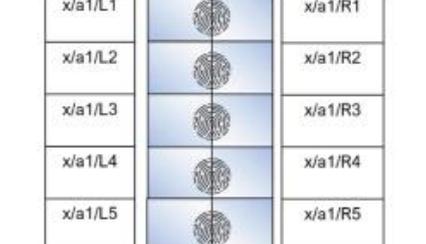After the first fingermark has been deposited, subsequent deposits are made using the same finger, producing a succession of ten fingermarks in total.

There are three different stations.

The first station contains three split columns of material A: Plastic.
The second station contains three split columns of material B: Painted Wood.
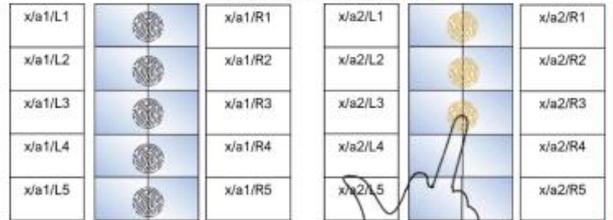The third station contains three split columns of material C: Glass.

Do not touch anything on these benches unless instructed to do so.

If you are happy to participate in this study and are ready to do so, please continue to read the instructions detailed below.

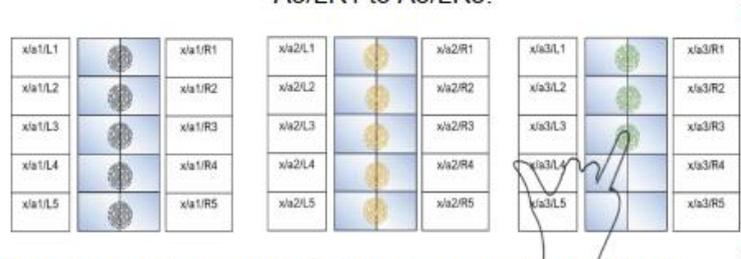| Step	Instructions and Image
1	**Go to station A.** At the station are three columns of identical materials. Each column contains a row of identical articles. Each row contains two identical items joined together.
2	Rub each finger pad with another to homogenise the residues on your fingertips.
3	Using one finger, apply a light pressure to material A1/LR1 in the space where the two surfaces are connected for 1-2 seconds and lift your finger.
4	Using the <u>same</u> finger, apply a light pressure to material A1/LR2 in the space where the two surfaces are connected for 1-2 seconds and lift your finger.
5	Using the <u>same</u> finger, repeat this process for remainder of materials within that row. Remember to continue to article A1/LR3 and end at A1/LR5.

	Now you have finished the first column, you will need to repeat these instructions for the two remaining columns, ensuring, you use a different finger for each separate column, as followed:
6	Using a finger **different** to previous, repeat these steps for A2/LR1 to A2/LR5.
7	Using a **different** finger than previous, repeat these steps for A3/LR1 to A3/LR5.
	Without touching any of the items, proceed to station B.
8	Repeat steps 1-7 for the three columns of materials at workbench B. Remembering to use a **different** finger for <u>each</u> column than a finger already used. Repeat steps 1-7 for the three columns of materials at workbench C. Remembering to use a **different** finger for <u>each</u> column than a finger already used.